Transmit Antenna Selection and User Selection in Multiuser MIMO Downlink Systems

By: Mohammed Al-Shuraifi

A Thesis Submitted in Fulfilment of the Requirements
for the Degree of Doctor of Philosophy (PhD)
in
Communications

Department of Electronic and Computer Engineering,
College of Engineering, Design and Physical Sciences
Brunel University London
London, United Kingdom

Supervised By: Professor Hamed Al-Raweshidy

May 2016

Deticated to my parents,
my wife,
my children,
my brothers and sister.

Abstract

Multiuser multiple input multiple output (MU-MIMO) systems play essential role in improving throughput performance and link reliability in wireless communications. This improvement can be achieved by exploiting the spatial domain and without the need of additional power and bandwidth. In this thesis, three main issues which are of importance to the data rate transmission have been investigated.

Firstly, antenna selection in MU-MIMO downlink systems has been considered, where this technique can be efficiently used to reduce the complexity and cost caused by radio frequency chains, associated with antennas, while keeping most of the diversity advantages of the system. We proposed a transmit antenna selection algorithm which can select an optimal set of antennas for transmission in descending order depending on the product of eigenvalues of users' effective channels. The capacity achieved by the proposed algorithm is about 99.6% of the capacity of the optimum search method, with much lower complexity.

Secondly, user selection technology in MU-MIMO downlink systems has been studied. Based on the QR decomposition, we proposed a greedy suboptimal user selection algorithm which adopts the product of singular values of users' effective channels as a selection metric. The performance achieved by the proposed algorithm is identical to that of the capacity-based algorithm, with significant reduction in complexity.

Finally, a proportional fairness scheduling algorithm for MU-MIMO downlink systems has been proposed. By utilising the upper triangular matrix obtained by applying the QRD on the users' effective channel matrices, two selection metrics have been proposed to achieve the scheduling process. The first metric is based on the maximum entry of the upper triangular matrix, while the second metric is designed using the ratio between the maximum and minimum entries of the triangular matrix multiplied by the product of singular values of effective channels. The two metric provide significant degrees of fairness.

For each of these three issues, a different precoding method has been used in order to cancel the interuser interference before starting the selection process. This allows to investigate each precoding design separately and to evaluate the computational burden required for each design.

Acknowledgements

First of all, I would like to express my appreciation and gratefulness to the Ministry of Higher Education-Iraq for funding my PhD study.

I would like to thank my supervisor Professor Hamed Al-Raweshidy for his valuable advices and guidance during the PhD period. He has been very helpful and supportive for all these years.

I am thankful to my second supervisor Professor John Cosmas for his encouragement and support. My gratitude goes to my colleagues in the Wireless Networks and Communications Centre (WNCC), who have been supportive throughout this period.

I would like to acknowledge the great attitude of all the staff members that I have interacted with at Brunel University and specially in the department of Electronic and Computer Engineering.

Finally, to my mother, wife, brothers and sister: thank you for being beside me as a source of care, love, motivation and encouragement, which travel the distance that separates us, and fill me with patience and commitment.

Table of Contents

List of Figures

List of Tables

List of Abbreviations

Abbreviation	Definition
ADC	analog-to-digital converter
AS	antenna selection
AWGN	additive white Gaussian noise
BC	broadcast channel
BD	block diagonalization
BER	bit error rate
BF	beamforming
BS	base station
CSI	channel state information
DG	diversity gain
DMT	diversity-multiplexing tradeoff
DoF	degrees of freedom
GSO	Gram-Schmidt orthogonalization
ICI	intercell interference
i.i.d	independent and identically distributed
IUI	interuser interference
LTE	long term evolution
MIMO	multiple-input multiple-output
MMSE	minimum mean square error
MU-MIMO	multiuser multiple input multiple output

PF	proportional fairness
QRD	QR decomposition
RF	radio frequency
SISO	single input single output
SNR	signal-to-noise ratio
SVD	singular value decomposition
TAS	transmit antenna selection
US	user selection
ZF	zero-forcing
ZFBF	zero-forcing beamforming
3G	third generation
4G	fourth generation
5G	fifth generation

List of Symbols

Notation	Definition
γ	received SNR
$\log(.)$	logarithmic function
P_e	probability of error
$\mathbf{a}$	a vector
$\mathbf{A}$	A matrix
$\mathbb{C}^{n\times m}$	the space of $n \times m$ complex matrix
$\log_2(.)$	logarithm to base 2
$(.)^H$	Hermitian of a matrix
$(.)^T$	transpose of a matrix
$(.)^\dagger$	pseudoinverse of a matrix
$\det(.)$	determinant of a matrix
λ	eigenvalue of a matrix
$\otimes$	Kronecker product
$\|.\|$	norm on a vector
$\|.\|_F$	Frobenius norm
$\mathcal{N}(.)$	null space of a matrix
$\mathcal{R}(.)$	row space of a matrix
$\text{null}(.)$	orthonormal basis of a null space matrix
$\mathbb{E}\{.\}$	expectation
$\sum$	sum
$\prod$	product
$\arg\max f(x)$	the point for which the function $f(x)$ has maximum value
$\arg\min f(x)$	the point for which the function $f(x)$ has minimum value
$\|\mathcal{A}\|$	cardinality of set $\mathcal{A}$
$\mathbf{I}_n$	identity matrix with $n \times n$ dimension
$\text{rank}(.)$	rank of matrix

Chapter 1

Introduction

1.1 Problem Statement

Wireless communication plays an essential role in everyday life. Its applications can be clearly seen in devices like mobile phones, tablets, computers, and so on. Moreover, it becomes indispensable when, for instance, two air planes communicate with each other or with the ground. However, the main aspects of life are in continuous change and evolution. In the past few decades, one can see that wireline devises, such as telephones or faxes, were considered main means in performing business processes. Conversely, we see the end of these devises is in sight today and they are replaced by more advanced and reliable means like Emails. Furthermore, the internet has progressed from wireline to wireless, and from delivering simple data and text mails to sophisticated web sites for interactive use. The demand for high speed and robust internet with better access has steadily grown and the appetite for powerful laptops, smart phones and tablets that have the ability to support multimedia services is increasingly requested by people. This huge growth in the internet and wireless devises has led to explosion in data traffic worldwide. For example, the number of smartphone users in the UK has reached more than 39 millions in 2015 and expected to reach 45 millions in 2017. Further, the average mobile broadband download speed

delivered by mobile communications standard has significantly risen from about 6 Mb/s (migabit per second) on the third generation (3G) to 15 Mb/s on the fourth generation (4G) and is expected to reach several gegabits on 5G. As a result, the traditional tools and methodologies used for quality evaluation and traffic management have to be revisited. In addition, searching for new models and algorithms have become a matter of importance in order to characterise that big amount of data in terms of velocity, volume, and variability, while keeping the complexity and cost as low as possible.

1.2 Motivation

Providing faster and reliable data transmission has drawn big attention in recent wireless technologies with taking into account the cost and complexity which may limit of solutions presented in this field. Conducting researches found that the data bit rate and spectral efficiency is an increasing function with the number of antennas. Subsequently, multiple antenna or multiple-input multiple-output (MIMO) technology was proposed to increase data bit rate in wireless communication. Many significant researches have been done on MIMO architecture since mid 1990's. These researches have focused on several aspects of wireless communication such as increasing data rate, improving reliability, reducing complexity and cost and so on. Basically, multiple antenna system means equipping the transmitter and/or the receiver with multiple antenna elements. These antennas have to be connected with another devices which are the radio frequency components in order to achieve the transmission process. That means if the transmitter is equipped with M antennas, the number of complete RF chains must be the same, including M devises of Analog-to-Digital (A/D) converters which are involved in the design of these chains. Compared to antenna elements, RF chains are considerably expensive. Moreover, deploying more RF components will increase the power consumption in the system. Scaling up the number of antennas in MIMO system to improve the performance of wireless transmission must be accompanied with increasing the number of RF switches, and leading to more

expenses and power consumption in the system. To cope with this problem, antenna selection technology comes to reduce the cost and complexity of MIMO architecture, while keeping most of its benefits. Considerable algorithms based on technical and mathematical concepts have been proposed to achieve either transmit or receive antenna selection or joint transmit/receive antenna selection. Our research concerns with transmit antenna selection (TAS) for MIMO systems.

Another important issue in MIMO systems is the number of simultaneous users that can be served by BS. In this correspondence, It has been found that the number of transmit antennas, the number of receive antennas, and the scattering of the channel play a crucial role in determining the number of users that can be simultaneously supported in multiple antenna or multiuser MIMO systems (MU-MIMO) [30]. For example, with a fixed number of transmit antennas at BS, increasing the number of simultaneous users beyond a particular limit leads to reduce the achievable data rate in the network. Consequently, the concept of user selection has emerged as a pioneering technology to improve the average sum rate for MIMO systems with the existence of a large number of simultaneously supportable users. More specifically, with the availability of partial or complete knowledge of the channel, the base station can select the best set of users to communicate with. Based on matrix theory and linear algebra concepts, several prominent algorithms have been designed to select optimal set of users under block diagonalization (BD) approach, whereby data streams are cleared of interference and sent to the terminal users.

Most user selection algorithms are not capable of providing fairness during selection process. In other words, users with good channel conditions are chosen for communication, while the other users with poor channel conditions will not have the opportunity to be served. Here lies the importance of proportional fairness (PF) scheduling as an approach which takes into account fairness among users through selection process. Each selected set is updated with time according to the instantaneous channel information at BS. In summary, Combining TAS and US technologies as well as taking into consideration PF scheduling can substantially improve performance and reduce bit error rate for MU-MIMO systems under BD scheme.

1.3 Contributions

The thesis contains the following contributions:

- **Designing a greedy transmit antenna selection algorithm**

  We investigate the antenna selection in MU-MIMO downlink systems. We propose a greedy transmit antenna selection algorithm which aims at reaching the performance obtained by the exhaustive-search algorithm (optimum method) but with lower complexity. At each step, the algorithm finds the antenna that contributes least to the product of eigenvalues of users' effective channels and deactivate it. In a descending order, the algorithm repeats until the required number of antennas is reached. The proposed algorithm uses the iterative precoding design to precancel the inter user interference. The performance, link reliability, and complexity of the proposed algorithm have been validated and compared to two other algorithms; the exhaustive search algorithm and the norm-based algorithm.

- **Designing a suboptimal greedy user selection algorithm**

  We study the user selection for MU-MIMO downlink systems. For high signal-to-noise (SNR) regime, a suboptimal greedy user selection algorithm has been proposed. The objective of the proposed algorithm is to achieve the performance obtained by the capacity-based algorithm with lower complexity. At each iteration, the algorithm selects a user that maximizes the product of singular values of users' effective channels. The algorithm repeats until the required number of users is reached. The product of singular values can be obtained from the upper triangular matrix after applying the QR decomposition (QRD) operation on the user's effective channel. The algorithm designs its precoders using the Gram-Schmidt Orthogonalization (GSO) operation in order to nullify the interuser interference. The performance and complexity order of the proposed algorithm have been analysed and compared to the performance and complexity

of other suboptimal user selection algorithms and for uncorrelated and highly correlated channels.

- **Designing a proportional fairness scheduling algorithm**

  We study the proportional fairness (PF) scheduling for MU-MIMO downlink systems and propose a greedy algorithm for this purpose. With an aim to achieve a considerable degree of fairness, two selection metrics have been proposed depending on the upper triangular matrix obtained by applying GSO on the users' effective channels. The first metric is designed using the maximum entry of the upper triangular matrix, while the second metric is designed using the ratio between the maximum and minimum entries of the triangular matrix multiplied by the product of singular values of effective channels. The proposed algorithm utilizes the block diagonalization (BD) method to precancel the interuser interference. The performance of the proposed selection metrics has been validated and compared to other greedy algorithms.

1.4 Publications

Published

1. M. Al-Shuraifi and H. Al-Raweshidy, " Optimizing antenna selection using limited CSI for massive MIMO systems," in *Proc. IEEE Fourth International Conference on Innovative Computing Technology (INTECH)*, Luton, UK, Aug. 2014.

2. M. Al-Shuraifi and H. Al-Raweshidy, " Fast antenna selection algorithm for multiuser MIMO systems under block diagonalization," in *Proc. IEEE Fourth International Conference on Future Generation Communication Technology (FGCT),* Luton, UK, July 2015.

submitted

1. M. Al-Shuraifi and H. Al-Raweshidy, " Near-optimum transmit antenna selection algorithm for multiuser MIMO downlink systems," *IEEE Commun. Lett.* , submitted for publication.

2. M. Al-Shuraifi and H. Al-Raweshidy, " A user selection algorithm for downlink MU-MIMO systems using product of singular values," *Elseveir journal*, submitted for publication.

1.5 Thesis Organization

The remainder of this thesis is organized as follows:

Chapter 2 gives a brief introductory background of the research work presented in this thesis. It begins by providing an overview of MIMO system and its main techniques used to transmit data streams from transmitter to receiver. Next, it discusses the MIMO channel capacity and Shannon equation. The two strategies of power allocation are presented; the equal power allocation and water filling strategy. Also, in this context the relation between MIMO channel capacity and the condition number of its channel is investigated. Then, some linear signal detection methods for spatial multiplexing MIMO systems are studied. After that, it discusses MU-MIMO communication and opportunistic beamforming which is an example of exploiting multiuser diversity to increase the whole system throughput. Finally, it studies linear transmission in MU-MIMO broadcast channels by providing a brief discussion of three important precoding methods, by which interuser interference can be perfectly cancelled.

Chapter 3 studies the transmit antenna selection for MU-MIMO downlink systems. It begins by providing a brief introduction about the advantages of antenna selection and the approaches used in this technology. The system model of MU-MIMO downlink is

presented, followed by explaining the iterative precoding design used to precancel IUI. Then, two main concepts used to design the proposed TAS algorithm are described; angle between two subspaces and intersection of null spaces. After that, the proposed algorithm is explained, followed by outlining the main operations of the proposed algorithm. Finally simulation results, which evaluate the performance, reliability and complexity of the proposed algorithm compared to other algorithms, are provided.

Chapter 4 investigates user selection for MU-MIMO downlink systems. It begins by providing an essential background and literature review on user selection techniques and precoding methods. Next, it presents the system model of MU-MIMO downlink system, followed by explaining the method used in designing the precoders, which is based on GSO operation. Then, the proposed user selection algorithm is presented with explanation of the proposed performance metric. This is followed by outlining the main operations of the proposed algorithm. After that, the chapter analyzes the computational complexity of the proposed algorithm and compares it to the complexity order of other user selection algorithms. Finally, simulation results, which evaluate the performance and run time of the proposed algorithm compared to other algorithms, are plotted.

Chapter 5 studies the proportional fairness scheduling for MU-MIMO downlink systems. It begins by reviewing the concepts of fair scheduling technique and the main constraints of multiuser diversity. Next, it presents the system model, followed by explaining the block diagonalization precoding method used to precancel the IUI. Then, the proposed PF scheduling algorithm is presented, where two performance metrics have been proposed in order to achieve the the required degree of fairness. After that, the chapter provides the outlines of the proposed algorithm. Finally, simulation results, which evaluate the performance of the proposed algorithm compared to other algorithm are shown.

Lastly, chapter 6 concludes the thesis and suggests possible future work.

Chapter 2

Background

2.1 Overview of MIMO Systems

In the past few decades, wireless communication has rapidly grown due to several advantages it offers compared to wireline communication. For instance, mobility and easy deployment are main features which make wireless communication increasingly applied in modern life. However, data rates of wireless systems are still less than that provided by wireline competitors, which lead to limited spectrum, signal fluctuation, and low transmit power in wireless environment. Hence, novel techniques for increasing data rates and improving link reliability are highly significant.

Multiple Input Multiple Output (MIMO) technology can effectively improve capacity and link reliability of wireless communication. A MIMO system is built by using multiple antennas at both the transmitter and receiver ends. These antennas are separated by a specific distance and are deployed in vertical and horizontal arrays. The physical separation between these antennas is exploited to add more degrees of freedom in the spatial dimension which we don't find in single antenna communication systems. The spatial degrees of freedom can be used to significantly enhance the spectral efficiency, combat fading in wireless communication channel, and suppress interference. This is achieved by intelligently designing transceivers and algorithms

for signal processing. There are two main advantages of MIMO with respect to the technique used to transmit data across the propagation channel; spatial diversity techniques or spatial multiplexing techniques. Spatial multiplexing aims at increasing achievable data rate [48]-[49] [60]. On the other hand, spatial diversity intends to increase the robustness and quality of transmitted signal [45]-[47]. Further, the fundamental ideas of diversity and multiplexing tradeoff(DMT) have been investigated in [50]-[51], while novel signaling algorithm to switch between diversity and multiplexing are proposed in [52]-[53].

Hence, It can be seen that the capability of MIMO to improve the performance in wireless communication systems comes at no additional power and bandwidth. Due to this precious property, MIMO has played crucial role in many standards of wireless communication such as WiMAX, 3GPP (3rd Generation Partnership Project), 4G long term evolution (LTE) and so on.

2.2 MIMO Techniques

As mentioned above, MIMO techniques (or MIMO coding) are classified into two main categories:diversity techniques or spatial multiplexing techniques. To investigate the advantage of each technique, let us consider a MIMO system with N_t transmit antennas at the base station, and N_R receive antennas at the receiver. The channel between two ends is denoted by $\mathbf{H}$ and given as $\mathbf{H} \in \mathbb{C}^{N_R \times N_t}$.

2.2.1 Spatial Diversity

Spatial diversity intends to increase the robustness and quality of signal by sending multiple encoded copies of the signal across different antenna elements. These replicas are sent over the propagation channel $\mathbf{H}$ such that they are statistically independent. As a result, the probability of fading all signal replicas simultaneously is very low, i.e., if one of these copies has higher probability to fade, the probability of fading the

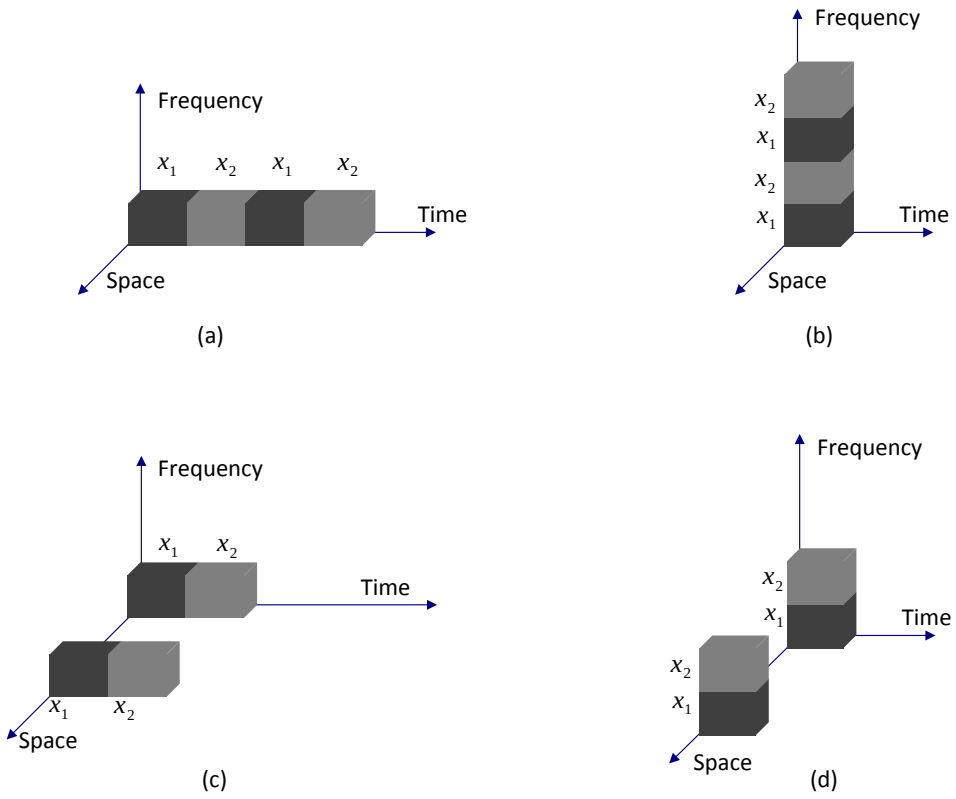

Figure 2.1: Spatial diversity techniques (extracted from [20]) (a) Time diversity (b) Frequency diversity (c) Space-time diversity (d) Space-frequency diversity.

remaining copies is low. Hence, we have better chance to receive the transmitted signal. The diversity gain (DG), which is a performance criterion of diversity techniques, is defined as follows [62] [63]

$$d_{Div} = -\lim_{\gamma \to \infty} \frac{\log P_e}{\log \gamma} \tag{2.1}$$

where P_e is the error probability and γ is the SNR. d_{Div} denotes the diversity gain, also known as *diversity order*. The maximum diversity gain that can be obtained by

using spatial diversity technique is

$$(d_{Div})_{max} = N_t \times N_R \tag{2.2}$$

which represents the total number of diversity paths (or channel paths) available in MIMO channel $\mathbf{H}$. Figure 2.1 shows some techniques used in spatial diversity [46].

2.2.2 Spatial Multiplexing

Spatial multiplexing aims at increasing achievable data rate. To do this, data stream is divided into multiple independent substreams; the substreams are transmitted simultaneously through spatial channels. At the receiver, appropriate techniques can be used to separate these substreams. The spatial multiplexing gain can be defined as [62] [63]

$$d_{Mul} = \lim_{\gamma \to \infty} \frac{R}{\log \gamma} \tag{2.3}$$

where R denotes the rate measured in (bits/s/Hz) and is a function of the SNR, i.e., $R = f\,(\text{SNR})$. The maximum spatial multiplexing gain achieved by MIMO channel $\mathbf{H}$ is

$$(d_{Mul})_{max} = \min\,(N_t, N_R) \tag{2.4}$$

which means the minimum of N_t and N_R. d_{Mul} is also known as the *number of degrees of freedom* that can be available by MIMO system with channel $\mathbf{H}$.

2.2.3 The Diversity-Multiplexing Tradeoff

For a given MIMO channel, it is possible to obtain both diversity and multiplexing gain simultaneously, i.e., a tradeoff between the probability of error of this MIMO system and its data rate. Under high SNR regime, an optimal scheme for diversity-multiplexing tradeoff (DMT) is proposed by [61], which assumes an i.i.d. Raleigh flat fading channel. In this scheme, the authors describe the fundamental tradeoff of

the gain that each MIMO coding technique can extract(e.g.,maximum multiplexing gain can be obtained at the cost of no diversity gain). To be more specific, consider a scheme with multiplexing gain c and diversity gain d. Hence, one can sacrifice of all the benefit of MIMO spatial multiplexing channel in order to maximize the system reliability. To retrieve part of that benefit, the rate of the proposed scheme is formulated as

$$R^{\star} = c \ \log \mathrm{SNR} \tag{2.5}$$

In addition, the average error probability of the proposed scheme decays like $1/\mathrm{SNR}^{d}$. Hence, the optimal diversity advantage $d_{opt}(c)$ as a function of the multiplexing gain c can be written as [61]

$$d_{opt}(c) = (N_t - c)\,(N_r - c) \tag{2.6}$$

where $c = 0, 1, ..., \min(N_t, N_r)$. Equation 2.6 is applied whenever the block length of the word $l \geq N_t + N_r - 1$. In Figure 2.2, the optimal diversity advantage d_{opt} is plotted against each multiplexing gain c. As seen in the Figure, the maximum value of c doesn't exceed the maximum degrees of freedom $\min(N_t, N_r)$ provided by MIMO channel, while d_{opt} doesn't exceed the maximum level of diversity gain $N_t N_r$ given by the channel. Hence, we can evaluate the performance of any scheme by comparing it to the optimal tradeoff curve shown in Figure 2.2.

2.3 MIMO Channel Capacity

Consider a MIMO system with N_t transmit antennas and N_R receive antennas. The MIMO channel $\mathbf{H}$ can be represented by $N_R \times N_t$ matrix $\mathbf{H} \in \mathbb{C}^{N_R \times N_t}$ and the received signal $\mathbf{y} \in \mathbb{C}^{N_R \times 1}$ as

$$\mathbf{y} = \mathbf{H}\mathbf{x} + \mathbf{n} \tag{2.7}$$

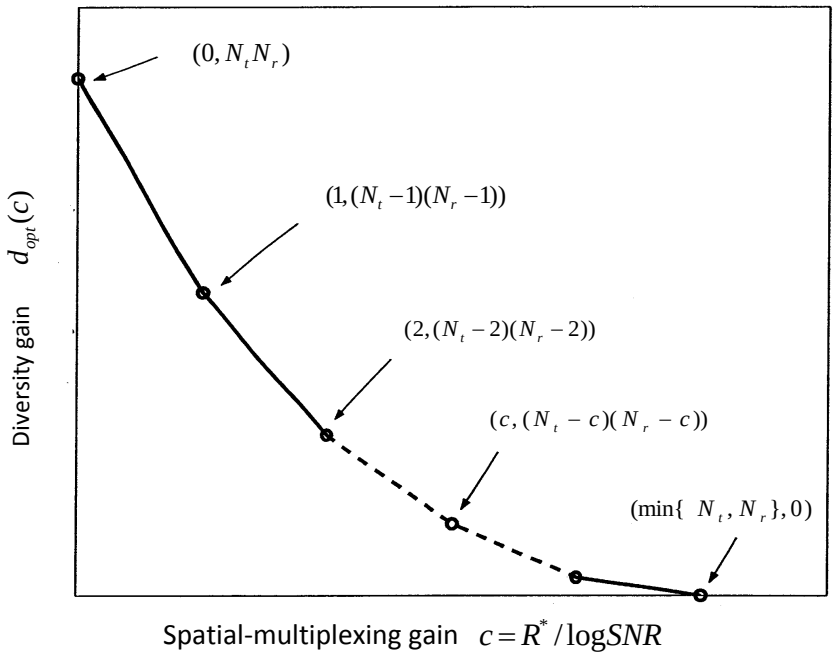

Figure 2.2: Optimal diversity-multiplexing tradeoff. (Figure extracted from [61])

where $\mathbf{x} \in \mathbb{C}^{N_t \times 1}$ is the transmitted signal. The vector $\mathbf{n} \in \mathbb{C}^{N_R \times 1}$ denotes the additive white Gaussian noise with covariance matrix as

$$\mathbb{E}\left\{\mathbf{n}\mathbf{n}^H\right\} = N_o \mathbf{I}_{N_R} \tag{2.8}$$

where N_o, $\mathbf{I}_n$ are the variance of $\mathbf{n}$ and $N_R \times N_R$ identity matrix, respectively. In addition, we assume the average power across all transmit antennas is P, i.e.

$$\mathbb{E}[\mathbf{x}^H \mathbf{x}] \leq P \tag{2.9}$$

2.3.1 Shannon Capacity and MIMO channel

Claude Shannon had defined the capacity of a channel as the maximum rate of reliable communication or *mutual information* between the channel input and output and denoted as C. This means that the possible rate of information R doesn't go greater than C, i.e.

$$R \leq C \tag{2.10}$$

According to Shannon's definition, the channel capacity can be written as [59]

$$C = B \log_2(1+\gamma), \qquad \text{[bps]} \tag{2.11}$$

where B and γ denote the channel bandwidth and received SNR, respectively.

When there is a perfect channel knowledge at the receiver and the transmitter, the capacity of MIMO channel is [54]

$$C = \max_{\mathbf{Q}:\mathbf{tr}(\mathbf{Q})=P} \log_2 \det\left(\mathbf{I}_{N_{r,k}} + \frac{1}{N_o}\mathbf{H}\mathbf{Q}\mathbf{H}^H\right), \qquad \text{[bits/sec/Hz]} \tag{2.12}$$

where $\mathbf{Q}$ denotes the covariance matrix of the transmit signal such that

$$\mathbf{Q} = \mathbb{E}[\mathbf{x}\mathbf{x}^H] \tag{2.13}$$

and N_o is the noise power. The MIMO channel $\mathbf{H}$ can be converted into parallel, free of interference single-input/single-output (SISO) channels by using singular value decomposition of matrix $\mathbf{H}$ as

$$\mathbf{H}=\mathbf{U}\mathbf{\Sigma}\mathbf{V}^H \tag{2.14}$$

where $\mathbf{U}$ is $N_R \times N_R$ unitary matrix, $\mathbf{V}$ is $N_t \times N_t$ unitary matrix, and $\mathbf{\Sigma}$ is $N_R \times N_t$ diagonal matrix with non-negative entries. The diagonal elements of matrix $\mathbf{\Sigma}$ are known as the singular values of $\mathbf{H}$ and denoted by σ_i, which are arranged in descending order, i.e.

$$\sigma_1 \geq \sigma_2 \geq ... \geq \sigma_{\min(N_t,N_R)} \tag{2.15}$$

Moreover the rank of $\mathbf{H}$ is given as

$$\tau_H = \min(N_t, N_R) \tag{2.16}$$

The precoding and postcoding process of the MIMO channel can be simply described as shown in Fig. 2.1, where the input signal is multiplied by matrix $\mathbf{V}$ before transmission, i.e.

$$\mathbf{x} = \mathbf{V}\tilde{\mathbf{x}} \tag{2.17}$$

At the receiver, the received signal is multiplied by $\mathbf{U}^H$. Hence, using (2.7), the output signal is given as

$$\begin{aligned} \tilde{\mathbf{y}} &= \mathbf{U}^H(\mathbf{H}\mathbf{x} + \mathbf{n}) \\ &= \mathbf{U}^H(\mathbf{U}\mathbf{\Sigma}\mathbf{V}^H(\mathbf{V}\tilde{\mathbf{x}}) + \mathbf{n}) \\ &= \mathbf{\Sigma}\tilde{\mathbf{x}} + \tilde{\mathbf{n}} \end{aligned} \tag{2.18}$$

where

$$\tilde{\mathbf{n}} = \mathbf{U}^H\mathbf{n} \tag{2.19}$$

Since $\mathbf{\Sigma}$ is diagonal matrix, we get

$$\tilde{y}_i = \sigma_i\tilde{x}_i + \tilde{n}_i \ , \quad i = 1, 2, ..., \min(N_t, N_R) \tag{2.20}$$

As a result, we obtain τ_H parallel and non-interfering channels, which are usually referred to as the channel *eigenmodes*. The sum rate capacity can be written as

$$C = \sum_{i=1}^{\tau_H} \log_2\left(1 + \frac{P_i\lambda_i}{N_o}\right), \quad \text{bits/s/Hz} \tag{2.21}$$

where λ_i's denote the eigenvalues of $\mathbf{H}\mathbf{H}^H$, i.e.

$$\lambda_i = \sigma_i^2 \tag{2.22}$$

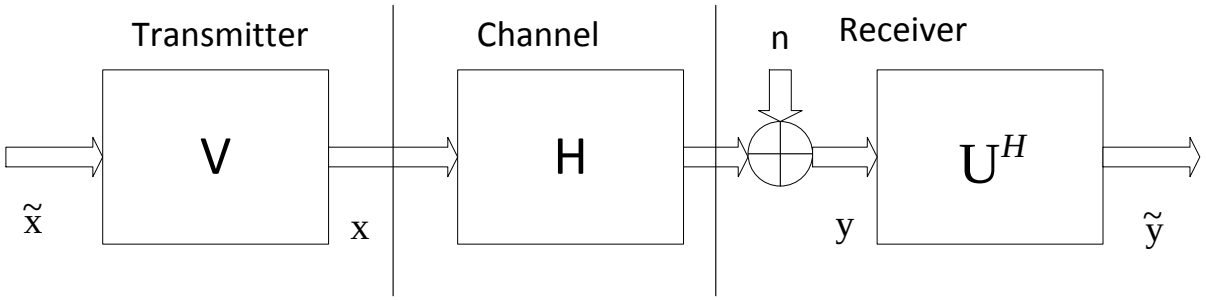

Figure 2.3: SVD decomposition when channel information is available at the transmitter (Figure extracted from [20])

and τ_H denotes the total number of λ_i, i.e., the rank of matrix $\mathbf{H}$. Here, P_i denotes the power allocated to the ith eigenmode using water filling strategy and as shown in the next subsection.

2.3.2 Water-Filling model

The parallel channels, explained in previous subsection, have different qualities according to the difference in singular values. This is paving the way for the use of water-filling strategy, whereby power is optimally distributed over the parallel channels by using the following form [55]

$$P_i = \left(\varepsilon - \frac{N_o}{\sigma_i^2}\right)^+ \tag{2.23}$$

where,

$$(a)^+ = \begin{cases} a, & \text{if } a > 0. \\ 0, & \text{if } a \leq 0. \end{cases} \tag{2.24}$$

P_i is the power of $\tilde{\mathbf{x}}_i$, and ε is the waterfill level which satisfies the total power

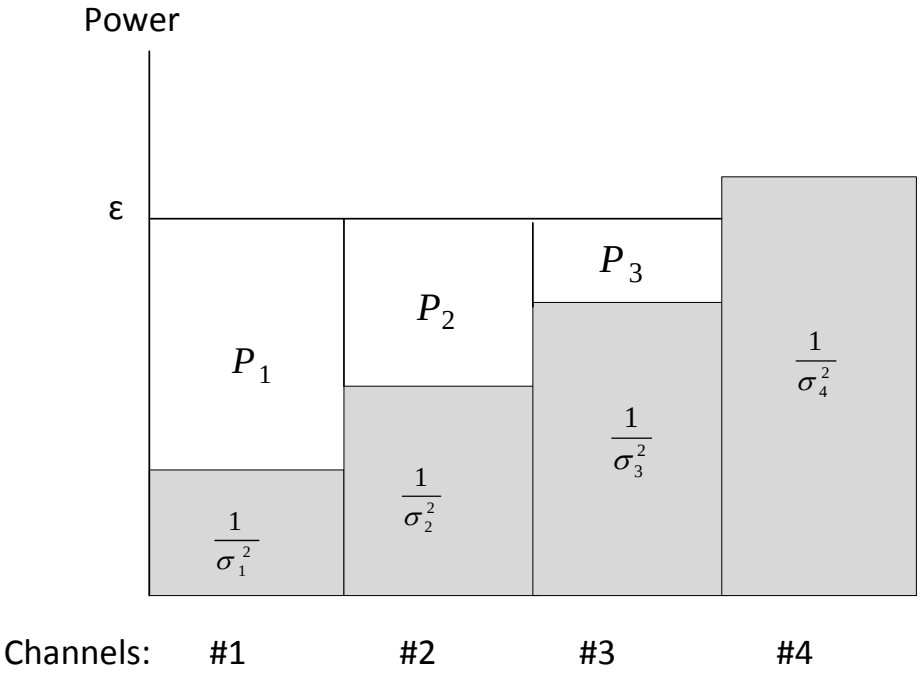

Figure 2.4: Power allocation using water-filling algorithm. (Figure extracted from [55])

constraint as

$$\sum_{i=1}^{\tau_H} P_i = P \tag{2.25}$$

The maximum in Equation 2.12 is achieved when the covariance matrix $\mathbf{Q}$ is optimally chosen such that

$$\mathbf{Q}=\mathbf{V}\mathbf{P}\mathbf{V}^H \tag{2.26}$$

where $\mathbf{P}$ is $N_t \times N_t$ diagonal matrix whose diagonal entries are defined as

$$\mathbf{P} = \text{diag}(P_1, ..., P_{\tau_H}, 0, ..., 0) \tag{2.27}$$

At low SNR, the water-filling strategy allocates more power to those channels with high singular values, and allocates less or no power to the channels with less or zero singular values. More specifically, channels with good conditions are allocated power more than those with worse conditions, as shown in Fig.2.4.

At high SNR, power allocated through water-filling is approximately equal across all parallel channels. This is expected, since the increase in power has recovered the poor channels [55].

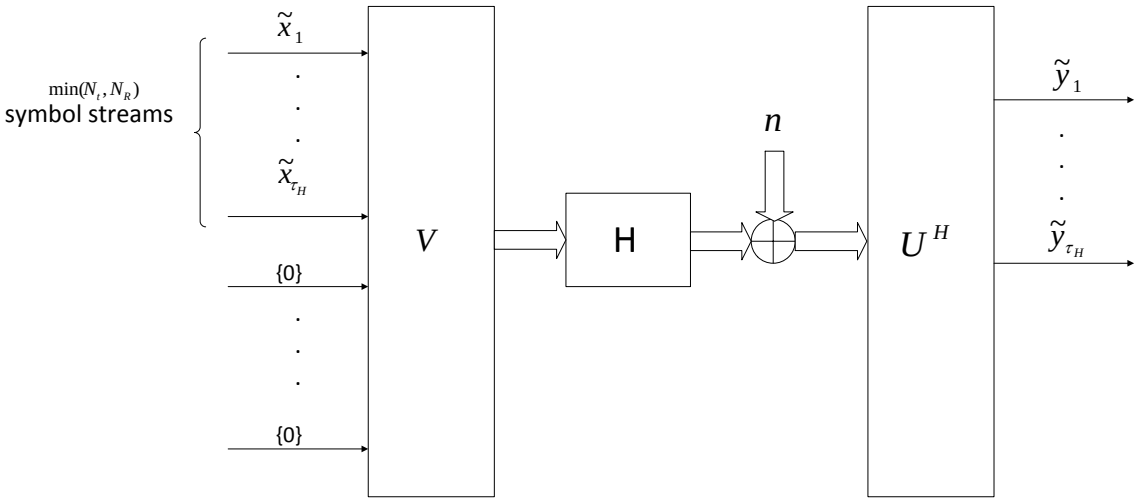

Figure 2.5: SVD model for MIMO channel: we allocate equal amounts of power over the non-zero eigenmodes in the high SNR regime. (Figure extracted from [59])

At high SNR, the optimal strategy is to allocate equal amounts of power on the transmit antennas. In this case, the transmit covariance matrix is given as

$$\mathbf{Q} = \frac{P}{N_t}\mathbf{I} \tag{2.28}$$

Thus, Equation 2.12 can be written as [54] [73]-[77]

$$C = \log_2 \det\left(\mathbf{I}_{N_{r,k}} + \frac{P}{N_t N_o}\mathbf{H}\mathbf{H}^H\right), \quad \text{bits/s/Hz} \tag{2.29}$$

Equal power allocation is also considered for all parallel directions when there is no channel knowledge in the transmitter.

2.3.3 Rank and Condition Number in Spatial Multiplexing

To determine the key parameters of performance in spatial multiplexing technique, we focus on each of the two scenarios; high SNR and low SNR regimes. In the high SNR, the scenario of equal power allocation on each of the non-zero eigenmodes can be considered asymptotically optimal because the water level is deep [59]:

$$C \approx \sum_{i=1}^{f} \log\left(1 + \frac{P\lambda_i}{fN_o}\right) \approx f \log \mathrm{SNR} + \sum_{i=1}^{f} \log\left(\frac{\lambda_i}{f}\right), \quad \text{bits/s/Hz} \tag{2.30}$$

where f denotes the number of non-zero λ_i, i.e., $f = \tau_H$, and $\mathrm{SNR} = P/N_o$. *The parameter f represents the number of spatial degrees of freedom provided by MIMO channel.* Hence, the dimension of the transmitted signal becomes equal to f due to the modification caused by MIMO channel as shown in Figure 2.5. This means that the number of spatial degrees of freedom provided by MIMO channel is equal to $\min(N_t, N_R)$.

The rank represents a coarse measure of the capacity of MIMO channel. To obtain a finer form, we need to investigate the non-zero eigenvalues themselves. Using Jensen's inequality,

$$\frac{1}{f}\sum_{i=1}^{f} \log\left(1 + \frac{P}{fN_o}\lambda_i\right) \leq \log\left(1 + \frac{P}{fN_o}\left(\frac{1}{f}\sum_{i=1}^{f}\lambda_i\right)\right) \tag{2.31}$$

Now,

$$\sum_{i=1}^{f} \lambda_i = \mathrm{trace}\left[\mathbf{H}\mathbf{H}^H\right] = \sum_{i,j} |h_{ij}|^2, \tag{2.32}$$

which expresses the total power gain of matrix $\mathbf{H}$ when energy is divided equally

over all transmit antennas. Clearly, Equations 2.31 and 2.32 show that among the channels whose total power gain is the same, the highest capacity is achieved by the one that has equal eigenvalues. In general, in the high SNR regime, the capacity of MIMO channel is maximized if its singular values are less spread out. This is referred to as the *condition number* of matrix **H** and is defined as [78]

$$\text{condition number} = \max_i \lambda_i / \min_i \lambda_i \tag{2.33}$$

which represents the ratio between the maximum and minimum eigenvalues of the channel matrix **H**. If the condition number of a matrix approaches 1, we say that matrix is *well-conditioned*. As a result, we conclude:

Well-conditioned MIMO channel matrices can facilitate communication in the high SNR regime

At low SNR, allocating power to the strongest eigenmodes and leaving the weak eigenmodes with no power allocation would be considered optimal policy. The achieved capacity is [59]

$$C \approx \frac{P}{N_o} \left(\max_i \lambda_i \right) \log_2 e, \quad \text{bits/s/Hz} \tag{2.34}$$

The *power gain* provided by MIMO channel is $\max_i \lambda_i$. Hence, in the Low SNR, the effect of the rank or condition number of MIMO channel matrix is vanished.

2.4 Linear Signal Detection of Spatial Multiplexing MIMO Systems

When channel state information (CSI) is available at the transmitter, SVD is exploited to attain the full degrees of freedom (DoF) of MIMO channel as seen in previous section. However, if only the receiver has CSI, this procedure is not possible since the transmitted data symbols all arrive cross-coupled at the receiver. Consequently, the receiver is not capable of separating these symbols efficiently in order

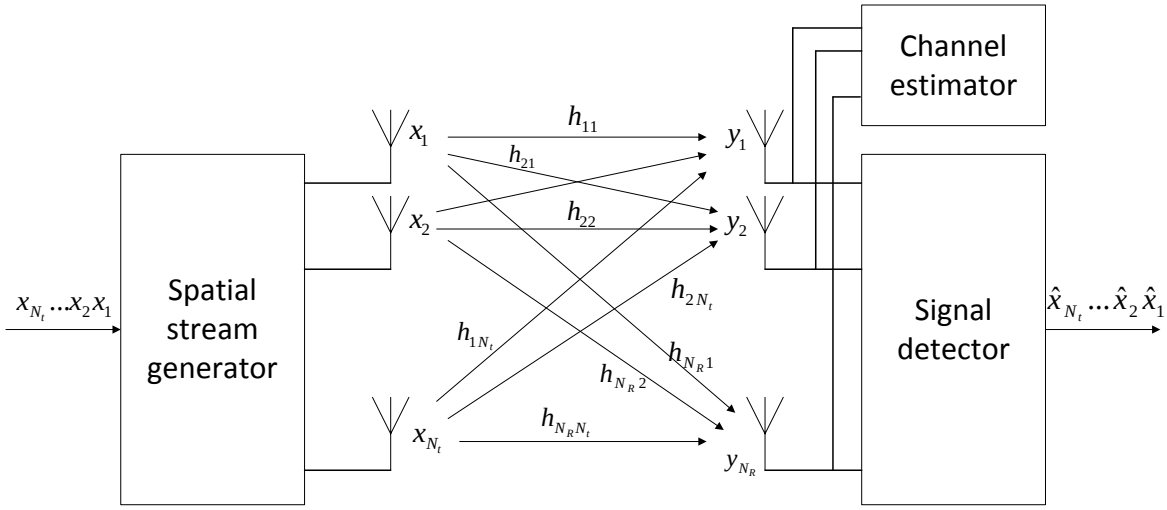

Figure 2.6: Spatial multiplexing and linear detection in MIMO systems. (Figure extracted from [20]

that the obtained performance has full DoF. An alternative solution for this problem is to use linear receivers (detectors) as shown in Fig.2.6. If we assume the case where the channel is invariant with time, the received signal can be written as

$$\begin{aligned} \mathbf{y} &= \mathbf{H}\mathbf{x} + \mathbf{n} \\ &= \sum_{i=1}^{N_t} \mathbf{h}_i x_i + \mathbf{n} \end{aligned} \tag{2.35}$$

where $\mathbf{h}_1, ..., \mathbf{h}_{N_t}$ denote the columns of matrix $\mathbf{H}$ and x_i's are the independent data symbols sent by transmit antennas, as shown in Figure 2.6. $\mathbf{n}$ denotes the noise vector with zero mean and variance N_o. In linear receivers, all transmitted signals are treated as interferences except the one sent from the target antenna. Hence, If the desired data stream for detection at the receiver is m, Equation 2.35 is written as

$$\mathbf{y} = \mathbf{h}_m x_m + \sum_{i \neq m} \mathbf{h}_i x_i + \mathbf{n} \tag{2.36}$$

where x_m is the data symbol sent from transmit antenna m through channels $h_{1m}, h_{2,m}, ..., h_{N_R,m}$ and the second term in the equation represents the interferences which can be minimized or removed by the use of linear receiver (or detector) [59].

2.4.1 ZF Signal Detection

One idea to suppress the interferences in (2.36) is to project the received signal $\mathbf{y}$ onto the subspace $\mathbf{V}_m$, where $\mathbf{V}_m$ is an orthogonal matrix to the subspace spanned by the vectors $\mathbf{h}_1, ..., \mathbf{h}_{m-1}, \mathbf{h}_{m+1}, ..., \mathbf{h}_{N_t}$. This process repeats till all data streams sent by transmit antennas are decorrelated. In general, zero-forcing detector uses the pseudoinverse of matrix $\mathbf{H}$ to decorrelate the signal $\mathbf{y}$ at the receiver as follows

$$\mathbf{W}_{ZF} = \left(\mathbf{H}^H \mathbf{H}\right)^{-1} \mathbf{H}^H \tag{2.37}$$

where $\mathbf{W}_{ZF}$ is the pseudoinverse of matrix $\mathbf{H}$, i.e.

$$\mathbf{W}_{ZF} = \mathbf{H}^\dagger \tag{2.38}$$

and $(.)^H$ denotes the Hermitian transpose operation. After multiplying $\mathbf{y}$, i.e. Equation 2.35, by the weight matrix $\mathbf{W}_{ZF}$, the effect of channel is inverted as

$$\begin{aligned} \hat{\mathbf{x}}_{ZF} &= \mathbf{W}_{ZF} \ \ \mathbf{y} \\ &= \mathbf{x} + \left(\mathbf{H}^H \mathbf{H}\right)^{-1} \mathbf{H}^H \ \mathbf{n} \\ &= \mathbf{x} + \hat{\mathbf{n}}_{ZF} \end{aligned} \tag{2.39}$$

where

$$\begin{aligned}\hat{\mathbf{n}}_{ZF} &= \mathbf{W}_{ZF}\mathbf{n} \\ &= \left(\mathbf{H}^H\mathbf{H}\right)^{-1}\mathbf{H}^H\mathbf{n}\end{aligned} \tag{2.40}$$

and $\hat{\mathbf{x}}_{ZF}$ denotes the vector of detected data symbols. According to (2.21), the error covariance matrix is given as [56]-[58]

$$\begin{aligned}\mathbf{\Omega}_{ZF} &= \mathbb{E}\left\{(\hat{\mathbf{x}}_{ZF}-\mathbf{x})(\hat{\mathbf{x}}_{ZF}-\mathbf{x})^H\right\} \\ &= N_o\left(\mathbf{H}^H\mathbf{H}\right)^{-1} \\ &= \sum_{i=1}^{N_t}\frac{N_o}{\sigma_i^2}\end{aligned} \tag{2.41}$$

which also represents the noise power after zero-forcing detector. Clearly, Equation 2.41 shows that small singular values of $\mathbf{H}$ result in large errors in detected signal due to noise amplification.

2.4.2 MMSE Signal Detection

Linear MMSE (minimum mean square error) receiver minimizes the mean squared error between the transmitted symbols, $\mathbf{x}$, and the output of the detector, $\hat{\mathbf{x}}$, as shown in Fig.2.6. The weight matrix of MMSE linear receiver is given as

$$\mathbf{W}_{MMSE} = \left(\mathbf{H}^H\mathbf{H} + N_o\mathbf{I}_{N_t}\right)^{-1}\mathbf{H}^H \tag{2.42}$$

After post-processing of the received signal, we obtain the following

$$\begin{aligned}\hat{\mathbf{x}}_{MMSE} &= \mathbf{W}_{MMSE}\mathbf{y} \\ &= \left(\mathbf{H}^H\mathbf{H} + N_o\mathbf{I}_{N_t}\right)^{-1}\mathbf{H}^H\mathbf{y} \\ &= \mathbf{x} + \left(\mathbf{H}^H\mathbf{H} + N_o\mathbf{I}_{N_t}\right)^{-1}\mathbf{H}^H\mathbf{n} \\ &= \mathbf{x} + \hat{\mathbf{n}}_{MMSE}\end{aligned} \tag{2.43}$$

where

$$\hat{\mathbf{n}}_{MMSE} = \left(\mathbf{H}^H\mathbf{H} + N_o\mathbf{I}_{N_t}\right)^{-1}\mathbf{H}^H\mathbf{n} \tag{2.44}$$

and $\hat{\mathbf{x}}_{MMSE}$ denotes the vector of post-detected data symbols. Hence, the resulting noise power after MMSE detector can be written as [20]

$$\begin{aligned}\mathbf{\Omega}_{MMSE} &= \mathbb{E}\left\{\left(\hat{\mathbf{x}}_{MMSE} - \mathbf{x}\right)\left(\hat{\mathbf{x}}_{MMSE} - \mathbf{x}\right)^H\right\} \\ &= \mathbb{E}\left\{\left\|\left(\mathbf{H}^H\mathbf{H} + \sigma_n^2\mathbf{I}_{N_t}\right)^{-1}\mathbf{H}^H\mathbf{n}\right\|^2\right\} \\ &= \sum_{i=1}^{N_t}\frac{N_o\sigma_i^2}{(N_o + \sigma_i^2)}\end{aligned} \tag{2.45}$$

By focusing on (2.41) and (2.45), we notice the difference in noise enhancement between ZF and MMSE receivers. More specifically, if we assume

$$\sigma_{min}^2 = \min\left\{\sigma_1^2, \sigma_2^2, ..., \sigma_{N_t}^2\right\} \tag{2.46}$$

Then, the effects of noise enhancement due to these linear detectors can be written as

$$\mathbf{\Omega}_{ZF} = \sum_{i=1}^{N_t}\frac{N_o}{\sigma_i^2} \approx \frac{N_o}{\sigma_{min}^2} \tag{2.47}$$

$$\mathbf{\Omega}_{MMSE} = \sum_{i=1}^{N_t} \frac{N_o \sigma_i^2}{(N_o + \sigma_i^2)} \approx \frac{N_o \sigma_{min}^2}{(N_o + \sigma_{min}^2)} \tag{2.48}$$

From (2.47) and (2.48), it is obvious that MMSE detector has less noise amplification than ZF detector. Moreover, if

$$\sigma_{min}^2 \gg \sigma_n^2 \tag{2.49}$$

and thus,

$$\sigma_n^2 + \sigma_{min}^2 \approx \sigma_{min}^2 \tag{2.50}$$

then both filters will have the same noise enhancement effect. Note that ZF receiver nullifies the interferences sent from all transmit antennas except for the desired one at the cost of reducing the energy of the stream of interest. In contrast, MMSE preserves the energy of the desired stream to the possible extent without regard to inter-stream interference. Hence, ZF receiver is considered in high SNR scenario, while MMSE performs better in cases when inter-stream interference is low (or in low SNR regime).

2.5 MIMO Channel Correlation

Correlation in channel occurs due to either insufficient place between antennas or lack of scattering. As a result, the data rate of the system is reduced because the various paths of the MIMO channel will become more dependent and correlated to each other. To study the impact of correlation, consider a narrowband flat-fading MIMO channel $\mathbf{H}$ with N_t transmit antennas and N_R receive antennas such that $\mathbf{H} \in \mathbb{C}^{N_R \times N_t}$. The Kronecker model can be used to approximately describe the channel covariance matrix as

$$\Theta_H = \Theta_{Tx} \otimes \Theta_{Rx} \tag{2.51}$$

where Θ_H denotes the channel covariance matrix and $\otimes$ is the Kronecker product. Θ_{Tx}, Θ_{Rx} are the correlation matrices corresponding to the transmit antennas and

receive antennas, respectively. Assuming complex Gaussian channel coefficients and from Equation 2.51, as in [64]-[67], the channel matrix $\mathbf{H}$ can be expressed as

$$\mathbf{H} = \Theta_{Rx}^{1/2}\ \mathbf{J}_{iid}\ \Theta_{Tx}^{1/2} \tag{2.52}$$

where $\mathbf{J}_{iid}$ represents $N_R \times N_t$ independent and identically distributed (i.i.d.) complex Gaussian random variables channel with zero mean and unit variance. Here $(.)^{1/2}$ is the matrix square root, i.e.

$$\Theta^{1/2}(\Theta^{1/2})^H = \Theta \tag{2.53}$$

2.6 Multiuser MIMO Communication

In Multiuser MIMO (MU-MIMO) technique, a base station communicates wirelessly with multiple users and data is transmitted in either downlink or uplink direction. In MIMO downlink channel (broadcast channel), a base station transmits data streams to the users. On the other hand, uplink takes place when the base station receives various information from the users. In fact, MIMO capacity can be scaled using the minimum number of antennas at the base station and the number of total antennas used by users. For this reason, our research concerns with the downlink transmission.

2.6.1 Multiuser Diversity

With the availability of full CSI at the transmitter, increasing the number of simultaneous users, which have independent faded paths with BS, will increase the probability to find one user with good channel condition at any time. By allocating most of the shared channel resource to that user, the total throughput of the system is significantly maximized [59] [68]-[72]. Hence, multiuser diversity gain is increased due to increase in system throughput.

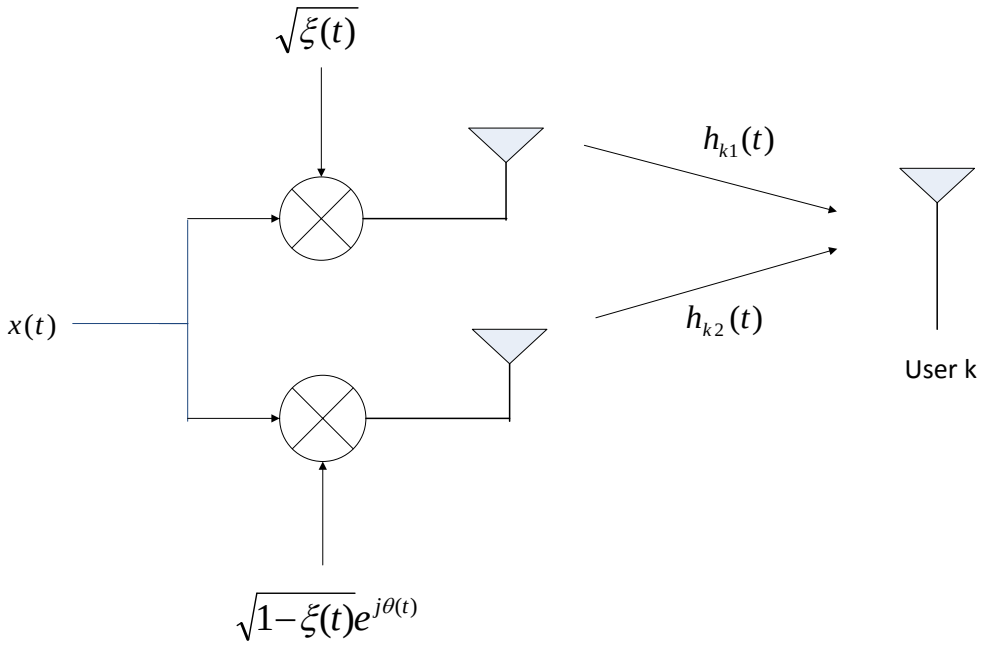

Figure 2.7: Opportunistic beamforming. (Figure extracted from [59])

Comparison between diversity techniques and multiuser diversity leads to the following:

- while diversity techniques aims at increasing the reliability of the system over slow fading channels, the main objective of multiuser diversity is to increase the system throughput in fast fading channels.
- the main objective of diversity techniques is to combat fading in channel; on the other hand, multiuser diversity exploits channel fading to increase system

performance.

Hence, the key factors that affect the multiuser diversity are the dynamic range and the rate of channel fluctuations.

2.6.1.1 Opportunistic Beamforming

In environments with flat fade (or small fluctuations) channels, it is possible to increase the multiuser diversity advantage by making the variations of the channel faster and larger. Concentrating on the downlink direction, this scenario can be achieved by the use of *opportunistic beamforming* technique [59] [68], as shown in Figure 2.7.

Consider a BS with N_t transmit antennas and communicates with a user k in time t. Let $h_{kl}(t)$ denote the complex channel from transmit antenna l to user k in time t. In time t, each antenna transmits the same symbol $x(t)$ except that we multiply each symbol by a complex number $\sqrt{\xi_l(t)}e^{j\theta_l(t)}$ at antenna l, for $l = 1, ..., N_t$, such that

$$\sum_{l=1}^{N_t} \xi_l(t) = 1 \tag{2.54}$$

This is to preserve the total transmit power. At user k, the received signal is written as

$$y_k(t) = \left(\sum_{l=1}^{N_t} \sqrt{\xi_l(t)} e^{j\theta_l(t)} h_{kl}(t) \right) x(t) + n_k(t) \tag{2.55}$$

In other words, at time t, the transmitted signal can be expressed in vector form as $\mathbf{w}(t)x(t)$, where

$$\mathbf{w}(t) = \begin{bmatrix} \sqrt{\xi_1(t)} e^{j\theta_1(t)} \\ \vdots \\ \sqrt{\xi_{N_t}(t)} e^{j\theta_{N_t}(t)} \end{bmatrix} \tag{2.56}$$

is a unit vector. Hence, the received signal at user k becomes

$$y_k(t) = \left(\mathbf{h}_k(t)\mathbf{w}(t) \right) x(t) + n_k(t) \tag{2.57}$$

where $\mathbf{h}_k(t)$ represents the channel gain vector from the transmit antennas to user k and is given as

$$\mathbf{h}_k(t) = [h_{k,1}(t), ..., h_{k,N_t}(t)] \tag{2.58}$$

At user k, the total channel gain can be new written as

$$\mathbf{h}_k(t)\mathbf{w}(t) = \sum_{l=1}^{N_t} \sqrt{\xi_l(t)} e^{j\theta_l(t)} h_{kl}(t) \tag{2.59}$$

As seen from Equation 2.59 that each transmit antenna is allocated a fraction of power denoted as $\xi_l(t)$, while $\theta_l(t)$ denotes the phase shift applied at transmit antenna l to the signal. By varying the values of $\xi_l(t)$, $\theta_l(t)$ over time ($\xi_l(t)$ from 0 to 1 and $\theta_l(t)$ from 0 to 2π), we obtain signals which are transmitted in a time-varying direction. In other words, the overall channel is induced to fluctuate over time even if the channel gains $\{h_{kl}(t)\}$ are physically flat faded (fluctuating very little). Then, the overall SNR received by each user is fed back to the base station (e.g., user k feeds back $|\mathbf{h}_k(t)\mathbf{q}(t)|^2/N_o$ to the base station). According to these SNR values, the base station will schedule transmission to users.

The variation rate of $\{\xi_l(t)\}$ and $\{\theta_l(t)\}$ with time is considered as a system design parameter. Adapting the values of these parameters is equivalent to changing the transmit direction, i.e., $\mathbf{w}(t)$. Hence, in *opportunistic beamforming* technique, we vary the values of powers and phases allocated to each transmit antenna in order to obtain a beam which is randomly swept over time; base station schedules transmission to the user which is currently as close to the beam as any other user. At any time, the probability of finding a user with very close distance to the beam increases by increasing the number of users in the system, and this leads to significantly maximize the system data rate.

2.6.2 MU-MIMO Broadcast Channel

Figure 2.8 shows the downlink channel, also known as broadcast channel (BC), of a MU-MIMO system. The basestation has an array of N_t transmit antennas and transmits the signal vector $\mathbf{x} \in \mathbb{C}^{N_t \times 1}$ simultaneously to K users, each user has $N_{r,k}$ receive antennas, $k = 1, 2, ..., K$. Let $\mathbf{H}_k \in \mathbb{C}^{N_{r,k} \times N_t}$ denotes the downlink channel gain matrix from BS to the kth user. Hence, the received signal $\mathbf{y}_k \in \mathbb{C}^{N_{r,k} \times 1}$ at the kth user is given as

$$\mathbf{y}_k = \mathbf{H}_k \mathbf{x} + \mathbf{n}_k \tag{2.60}$$

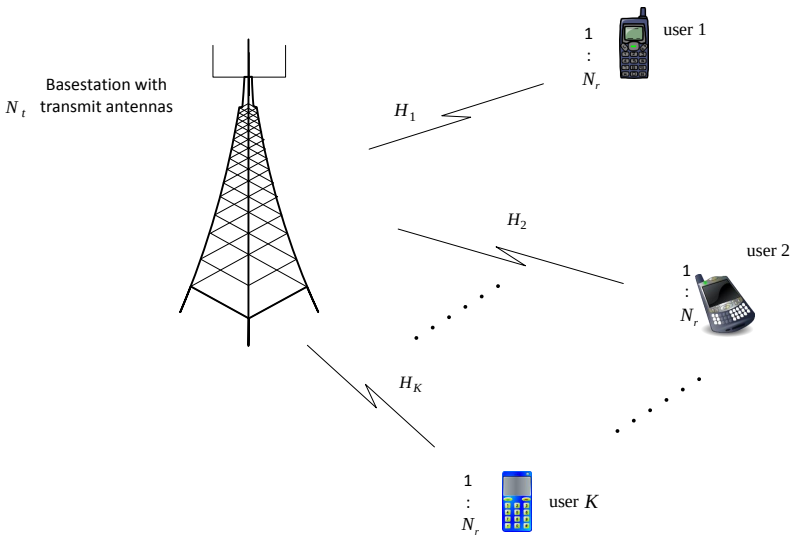

Figure 2.8: MU-MIMO downlink channel: broadcast channel.

where $\mathbf{n}_k \in \mathbb{C}^{N_{r,k} \times 1}$ is circularly symmetric complex Gaussian noise with zero mean and covariance matrix as

$$\mathbb{E}\left\{\mathbf{n}_k \mathbf{n}_k^H\right\} = N_o \mathbf{I}_{N_{r,k}} \tag{2.61}$$

Hence, all users can be expressed by a single vector equation as follows

$$\underbrace{\begin{bmatrix} \mathbf{y}_1 \\ \mathbf{y}_2 \\ \vdots \\ \mathbf{y}_K \end{bmatrix}}_{\mathbf{y}} = \underbrace{\begin{bmatrix} \mathbf{H}_1 \\ \mathbf{H}_2 \\ \vdots \\ \mathbf{H}_K \end{bmatrix}}_{\mathbf{H}} \mathbf{x} + \underbrace{\begin{bmatrix} \mathbf{n}_1 \\ \mathbf{n}_2 \\ \vdots \\ \mathbf{n}_K \end{bmatrix}}_{\mathbf{n}} \tag{2.62}$$

2.7 Linear Transmission in MU-MIMO BC

The main advantage of linear transmission in downlink MU-MIMO systems is to precancel the interuser interference (IUI) at the transmitter. This is achieved by multiplying the transmitted data symbols with a precoding matrix before transmission. Channel knowledge must be available at the transmitter in order to design the precoders. Consider the MUMIMO model shown in Figure 2.8 in which the base station is equipped with N_t transmit antennas and communicates with K users, each user has $N_{r,k}$ antennas, $k = 1, 2, ..., K$. Let $\tilde{\mathbf{x}}_k \in \mathbb{C}^{N_{r,k} \times 1}$, $\mathbf{W}_k \in \mathbb{C}^{N_t \times N_{r,k}}$ denote the transmit signal and precoding matrix for the kth user. Hence, the actual transmit signal for the kth user can be expressed as

$$\mathbf{x}_k = \mathbf{W}_k \tilde{\mathbf{x}}_k \tag{2.63}$$

The received signal $\mathbf{y}_k \in \mathbb{C}^{N_{r,k} \times 1}$ at user k is given as

$$\mathbf{y}_k = \mathbf{H}_k \mathbf{W}_k \tilde{\mathbf{x}}_k + \underbrace{\sum_{j=1, j \neq k}^{K} \mathbf{H}_k \mathbf{W}_j \tilde{\mathbf{x}}_j}_{IUI} + \mathbf{n}_k \tag{2.64}$$

where $\mathbf{H}_k \in \mathbb{C}^{N_{r,k} \times N_t}$ is the channel from BS to user k and $\mathbf{n}_k$ is the additive white Gaussian noise vector.

2.7.1 Zero-Forcing Beamforming

In *beamforming* (BF), the data streams are passed through a beamformer before being transmitted over different antennas. The beamformer is a weight vector designed with a specific amplitudes and phases in order to steer the transmitted beam in the direction of intended users and, at the same time, cancel the interference caused by the others [79]. More specifically, the beamformer will act to constructively accumulate the components in desired directions and destructively in non-desired directions. This will enhance the received SNR at the terminal users and cancel interuser interference.

Consider a MIMO downlink system with one base station which communicates with K users; each user has one receive antenna. The base station is equipped with N_t transmit antennas and the channel model is assumed to be zero-mean circularly symmetric complex Gaussian random variable . At user k, the received signal is written as

$$y_k = \mathbf{h}_k \mathbf{x} + n_k \tag{2.65}$$

where $\mathbf{x} \in \mathbb{C}^{N_t \times 1}$ is the transmitted symbol, $\mathbf{h}_k \in \mathbb{C}^{1 \times N_t}$ is the channel vector from the base station to the kth user, and y_k is the signal received by user k. n_k denotes the noise described as AWGN with zero mean and variance $N_o = 1$. The transmitted signal has a power constraint averaged as

$$\mathbb{E}\left\{\mathbf{x}\mathbf{x}^H\right\} \leq P \tag{2.66}$$

and perfect knowledge of CSI is assumed at the base station.

In BF, each user stream is separated by a different beamforming direction. The

transmitted signal is given as

$$\mathbf{x} = \sum_{k=1}^{K} \sqrt{P_k}\mathbf{w}_k\tilde{x}_k \tag{2.67}$$

where $\tilde{x}_k$, $\mathbf{w}_k$ are the data symbol and the beamforming vector, respectively, and define

$$\mathbf{W} = [\mathbf{w}_1, ..., \mathbf{w}_K] \tag{2.68}$$

The transmit power for user k is denoted as P_k such that

$$\mathbf{P} = \text{diag}\{P_1, ..., P_k\} \tag{2.69}$$

Hence, the received signal at user k can be written as

$$y_k = \sqrt{P_k}\mathbf{h}_k\mathbf{w}_k\tilde{x}_k + \sum_{j\neq k} \sqrt{P_j}\mathbf{h}_k\mathbf{w}_j\tilde{x}_j + n_k \tag{2.70}$$

The sum rate which can be obtained using this scheme is [82]

$$R_{BF} = \max_{\mathbf{w}_k, P_k} \sum_{k=1}^{K} \log\left(\frac{1 + \sum_{j=1}^{K} P_j|\mathbf{h}_k\mathbf{w}_j|^2}{1 + \sum_{j=1, j\neq k}^{K} P_j|\mathbf{h}_k\mathbf{w}_j|^2}\right) \tag{2.71}$$

where Equation 2.71 is subject to

$$\sum_{k=1}^{K} ||\mathbf{w}_k||^2 P_k \leq P \tag{2.72}$$

In *zero-forcing beamforming* (ZFBF) [82], the beamformers have to satisfy

$$\mathbf{h}_k\mathbf{w}_j = 0 \ , \quad j \neq k \tag{2.73}$$

Now, let

$$\mathbf{H} = [\mathbf{h}_1^T \ \ldots \ \mathbf{h}_K^T]^T \tag{2.74}$$

then the matrix $\mathbf{W}$ can be selected to be the pseudo-inverse of the channel matrix $\mathbf{H}$ as

$$\begin{aligned}\mathbf{W} &= \mathbf{H}^{\dagger} \\ &= \mathbf{H}^{H}\left(\mathbf{H}\mathbf{H}^{H}\right)^{-1}\end{aligned} \tag{2.75}$$

Hence, Equation 2.71 becomes

$$R_{ZFBF} = \sum_{k=1}^{K} \log\left(1 + P_k\right) \tag{2.76}$$

and it is subject to

$$\sum_{k=1}^{K} \varrho_k^{-1} P_k \leq P \tag{2.77}$$

where

$$\varrho_k = \frac{1}{||\mathbf{w}_k||^2} = \frac{1}{\left[\left(\mathbf{H}\mathbf{H}^{H}\right)^{-1}\right]_{k,k}} \tag{2.78}$$

denotes the effective channel gain specified to user k [81]-[83]. The amount of power P_k can be optimally allocated by the use of waterfilling strategy explained previously in section 3.

2.7.2 Block Diagonalization

As seen in Equation 2.64, user k receives IUI from other transmit antennas other than the target one. This interference can be efficiently removed by the use of block diagonalization (BD) precoding technique, which is proposed by [30]. BD imposes the following constraint

$$\mathbf{H}_k \mathbf{W}_j = 0, \quad \text{for } k \neq j \tag{2.79}$$

where $\mathbf{W}_k$ must be a unitary matrix to meet the total transmit power constraint of the system, i.e.

$$\mathbf{W}_j \in \mathbb{U}\left(N_t, N_{r,k}\right) \tag{2.80}$$

After eliminating all multi-user interference, Equation 2.35 can be written as

$$\mathbf{y}_k = \mathbf{H}_k \mathbf{W}_k \tilde{\mathbf{x}}_k + \mathbf{n}_k \tag{2.81}$$

At this stage, all received signals are cleared of interference. Next, we can apply one of the detection methods explained in the previous section in order to estimate $\tilde{\mathbf{x}}_k$.

Now, we explain how to design the precoders $\{\mathbf{W}\}_{k=1}^{K}$. Consider $\tilde{\mathbf{H}}_k$ which can be defined as

$$\tilde{\mathbf{H}}_k = \left[\mathbf{H}_1^H, ..., \mathbf{H}_{k-1}^H \;\; \mathbf{H}_{k+1}^T, ..., \mathbf{H}_K^H\right]^H \tag{2.82}$$

Note that $\tilde{\mathbf{H}}_k$ contains all users' channels except for the intended one, which is user k. To satisfy the condition in Equation 2.36, $\mathbf{W}_j$ must lie in the null space of $\tilde{\mathbf{H}}_k$. This is possible if

$$N_t > \sum_{k=1}^{K} N_{r,k} \tag{2.83}$$

This implies that the total sum of all active users' receive antennas is not more than the total transmit antennas at the base station. This is to ensure that the null space is not empty matrix and the IUI can be perfectly removed by BD precoding. We define the singular value decomposition of $\tilde{\mathbf{H}}_k$ as

$$\tilde{\mathbf{H}}_k = \tilde{\mathbf{U}}_k \left[\tilde{\mathbf{\Sigma}}_k, \mathbf{0}_{\tilde{\tau}_k \times (N_t - \tilde{\tau}_k)}\right] \left[\tilde{\mathbf{V}}_k^{(1)}, \tilde{\mathbf{V}}_k^{(0)}\right]^H \tag{2.84}$$

where $\tilde{\tau}_k$ is the rank of $\tilde{\mathbf{H}}$ and is given as

$$\tilde{\tau}_k = \min\left(\sum_{j=1, j\neq k}^{K} N_{r,j}, N_t\right) \tag{2.85}$$

and $\tilde{\mathbf{\Sigma}}_k$ is a diagonal matrix which contains the singular values with dimension of $\tilde{\tau}_k \times \tilde{\tau}_k$, i.e.

$$\tilde{\mathbf{\Sigma}}_k = \mathrm{diag}\left(\sigma_{1,k}, ..., \sigma_{\tilde{\tau}_k,k}\right) \tag{2.86}$$

The matrices $\tilde{\mathbf{V}}_k^{(1)}$, $\tilde{\mathbf{V}}_k^{(0)}$ contain the first $\tilde{\tau}_k$ and the last $N_t - \tilde{\tau}_k$ columns of the right singular vectors, respectively. Multiplying $\tilde{\mathbf{H}}_k$ with $\tilde{\mathbf{V}}_k^{(0)}$, we obtain the following

relationship

$$\begin{aligned}\tilde{\mathbf{H}}_k\tilde{\mathbf{V}}_k^{(0)} &= \tilde{\mathbf{U}}_k\left[\tilde{\mathbf{\Sigma}}_k, \mathbf{0}\right]\begin{bmatrix}\left(\tilde{\mathbf{V}}_k^{(1)}\right)^H \\ \left(\tilde{\mathbf{V}}_k^{(0)}\right)^H\end{bmatrix}\tilde{\mathbf{V}}_k^{(0)} \\ &= \tilde{\mathbf{U}}_k\tilde{\mathbf{\Sigma}}_k\left(\tilde{\mathbf{V}}_k^{(1)}\right)^H\tilde{\mathbf{V}}_k^{(0)} \\ &= \tilde{\mathbf{U}}_k\tilde{\mathbf{\Sigma}}_k\ \mathbf{0} \\ &= \mathbf{0}\end{aligned} \tag{2.87}$$

As seen in Equation 2.45, the matrix $\tilde{\mathbf{V}}_k^{(0)}$ contains the null space vectors of $\tilde{\mathbf{H}}_k$. Hence, the precoding matrix for the kth user can be expressed as

$$\mathbf{W}_k = \tilde{\mathbf{V}}_k^{(0)} \tag{2.88}$$

where $\tilde{\mathbf{V}}_k^{(0)}$ has the dimension $\tilde{\tau}_k \times (N_t - \tilde{\tau}_k)$. The precoders for the remaining users can be obtained by following the same procedure. After precoding, the received signals are given as

$$\begin{bmatrix}\mathbf{y}_1 \\ \vdots \\ \mathbf{y}_K\end{bmatrix} = \begin{bmatrix}\mathbf{H}_1\tilde{\mathbf{V}}_1^{(0)} & & 0 \\ & \ddots & \\ 0 & & \mathbf{H}_K\tilde{\mathbf{V}}_K^{(0)}\end{bmatrix}\begin{bmatrix}\tilde{\mathbf{x}_1} \\ \vdots \\ \tilde{\mathbf{x}_K}\end{bmatrix} + \begin{bmatrix}\mathbf{n}_1 \\ \vdots \\ \mathbf{n}_K\end{bmatrix} \tag{2.89}$$

which is equivalent to Equation 2.37. The sum rate capacity of the system can be written as [71]

$$\begin{aligned}C &= \sum_{i=1}^{K}\log_2\det\left(\mathbf{I}_{N_{r,k}} + \frac{P}{N_tN_o}\mathbf{H}_k\mathbf{W}_k\mathbf{W}_k^H\mathbf{H}_k^H\right) \\ &= \sum_{i=1}^{K}\log_2\det\left(\mathbf{I}_{N_{r,k}} + \frac{P}{N_tN_o}\mathbf{H}_{eff}\mathbf{H}_{eff}^H\right), \quad \text{bits/s/Hz}\end{aligned} \tag{2.90}$$

where

$$\mathbf{H}_{eff} = \mathbf{H}_k \mathbf{W}_k \tag{2.91}$$

denotes the effective (equivalent) channel of user k after precoding process. If N_o is assumed unity, then Equation 2.90 can be expressed as

$$C = \sum_{i=1}^{K} \log_2 \det \left(\mathbf{I}_{N_{r,k}} + \frac{P}{N_t} \mathbf{H}_{eff} \mathbf{H}_{eff}^H \right), \quad \text{bits/s/Hz} \tag{2.92}$$

2.7.3 Iterative Precoder Design

The iterative precoder design is proposed by [31] as an alternative to the BD. Unlike BD which uses the SVD, the iterative precoding method is based on QR decomposition (QRD) to obtain the precoders for the MU-MIMO systems. As a result, this method can be preferred to transmit data in MU-MIMO systems rather than BD because QRD has lower complexity than SVD. Consider matrix $\mathbf{A} \in \mathbb{C}^{p \times q}$ with $p < q$, then $\mathbf{A}^H$ can be written as

$$\mathbf{A}^H = \left[\mathbf{Q}_{1_{q \times p}} \mathbf{Q}_{2_{q \times (q-p)}} \right] \begin{bmatrix} \mathbf{R}_{1_{p \times p}} \\ \mathbf{0}_{(q-p) \times p} \end{bmatrix} \tag{2.93}$$

where $\mathbf{R}_1 \in \mathbb{C}^{(p \times p)}$ is an upper triangular matrix and $\mathbf{Q}_2 \in \mathbb{C}^{q \times (q-p)}$ contains an orthonormal basis vectors of the null space of matrix $\mathbf{A}$, i.e.

$$\mathbf{A}\mathbf{Q}_2 = 0 \tag{2.94}$$

and

$$\mathbf{Q}_2^H \mathbf{Q}_2 = \mathbf{I} \tag{2.95}$$

Note that the same conditions illustrated in Equations 2.79, 2.82, and 2.83 must be satisfied in this method as well. To illustrate this precoding method, let us consider finding the precoding matrix for user 1, which is denoted by $\mathbf{F}_1^{(n)}$ at the ith iteration. Initially, we set

$$\mathbf{F}_1^{(1)} = \mathbf{I}_{N_t} \tag{2.96}$$

At step two, we have

$$\begin{aligned} \mathbf{F}_1^{(2)} &= \mathbf{F}_1^{(1)} \times \text{null}(\mathbf{H}_2\mathbf{F}_1^{(1)}) \\ &= \text{null}(\mathbf{H}_2) \end{aligned} \tag{2.97}$$

After the ith iteration, we obtain $\mathbf{F}_1^{(i)}$ such that

$$\mathbf{H}_k\mathbf{F}_1^{(i)} = 0 \ , \quad \forall 1 < k \leq i \tag{2.98}$$

In each step, $\mathbf{F}_1^{(i)}$ can be found from $\mathbf{F}_1^{(i-1)}$ in a recursive way, as follows

$$\mathbf{F}_1^{(i)} = \mathbf{F}_1^{(i-1)}\mathbf{G}_1^{(i)} \tag{2.99}$$

where $\mathbf{G}_1^{(i)}$ lies in $\mathcal{N}(\mathbf{H}_n\mathbf{F}_1^{(i-1)})$, where $\mathcal{N}(.)$ denotes the null space matrix. We can obtain $\mathbf{G}_1^{(i)}$ as follows

$$\mathbf{G}_1^{(i)} = \text{null}\left(\mathbf{H}_i\mathbf{F}_1^{(i-1)}\right) \tag{2.100}$$

where $\text{null}\left(\mathbf{H}_i\mathbf{F}_1^{(i-1)}\right)$ denotes an orthonormal basis of $\mathcal{N}(\mathbf{H}_i\mathbf{F}_1^{(i-1)})$ and can be obtained using Gram-Schmidt orthogonalization (GSO). In the same way, we can obtain other users' precoder matrices recursively. Figure 2.9 describes the iterative precoder design. Note that at the end of the iterations, we obtain the precoders for all users. These precoders are obtained from those in previous iterations, i.e., in horizontal line. Also note that the precoder of the last user (or diagonal line) is obtained from the precoder of the last user in previous iteration, i.e., the gray colour in Figure 2.9. The sum rate capacity of the system after precoding is given as [71]

$$C = \sum_{i=1}^{K} \log_2 \det \left(\mathbf{I}_{N_{r,k}} + \frac{P}{N_t N_o} \mathbf{H}_k \mathbf{F}_k^{(n)} \mathbf{F}_k^{(n)H} \mathbf{H}_k^H \right)$$
$$= \sum_{i=1}^{K} \log_2 \det \left(\mathbf{I}_{N_{r,k}} + \frac{P}{N_t N_o} \mathbf{H}_{eff} \mathbf{H}_{eff}^H \right), \quad \text{bits/s/Hz} \tag{2.101}$$

where,

$$\mathbf{H}_{eff} = \mathbf{H}_k \mathbf{F}_k^{(n)} \tag{2.102}$$

denotes the effective channel of user k after precoding process. Note that $\mathbf{F}_k^{(n)}$ is the final precoding matrix of user k at $n = K$ iterations as shown in Figure 2.9.

2.8 Summary

In this chapter, some issues which underlie the research work in this thesis have been briefly explained. We firstly provided a simple introduction of MIMO techniques and their advantages. Next, we studied the capacity of MIMO channel and the different ways of power allocation used in the transmitter side. Then, we studied two common methods used to linearly detect data at the receiver side in spatial multiplexing MIMO systems. After that, we briefly studied MIMO channel correlation for narrowband flat-fading channels. Finally, we moved to MU-MIMO systems and in this context we investigated three different methods used for linear transmission.

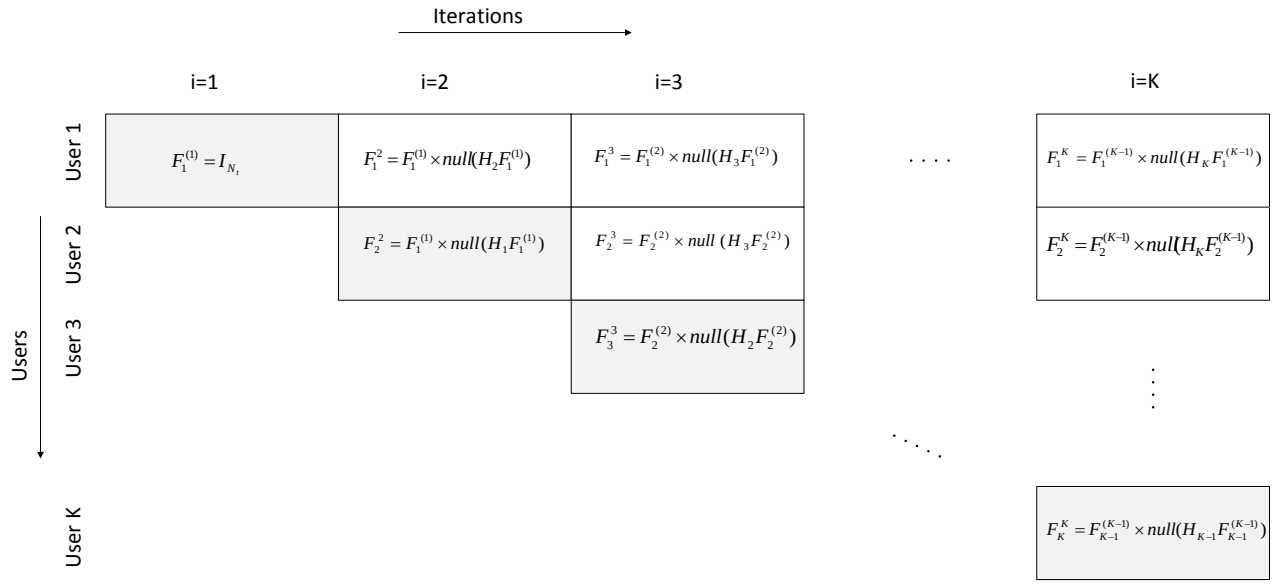

Figure 2.9: Iterative precoder design.

Chapter 3

Transmit Antenna Selection for Downlink MU-MIMO Systems

In this chapter, a greedy suboptimal transmit antenna seleciton algorithm for downlink multiuser MIMO systems is proposed. The proposed algorithm selects an optimal subset of antennas among the total antennas available in the base station for transmission in a descending order. Moreover, the proposed selection metric of the algorithm is the product of eigenvalues of effective channels. The eigenvalues of each user's effective channel can be obtained from that of the prior iteration repeatedly by the use of relationship between the principal angles of a specific subspace and its eigenvalues. Simulation results show that the proposed algorithm achieves almost identical performance as the exhaustive search algorithm with significant reduction in complexity.

3.1 Introduction

One main issue with scaling up multiple-input multiple-output (MIMO) systems relates to the cost and complexity of radio frequency (RF) components that are de-

ployed with antenna elements [1]. To override this problem, antenna selection (AS) technique comes to reduce the number of analog components required, likewise preserves most of the advantages of MIMO systems such as diversity to improve the reliability of the system, or spatial multiplexing to increase the sum data rate of the system. The principal idea of AS scheme is to connect a limited number of RF chains to a subset of antennas optimally selected among all available antennas in transmitter and/or receiver. However, equipping MIMO with more antennas leads to increase the complexity of the system due to the high number of computations required to achieve optimal antenna selection.

Many algorithms of AS have been introduced to alleviate the computation process, yet to keep the advantages of MIMO systems to a considerable extent, and researches conducted with either transmit antenna selection (TAS), receive antenna selection (RAS), or joint transmit/receive antenna selection [2]-[4]. Moreover, these studies varied according to the purpose for which MIMO was designed, i.e. diversity or spatial multiplexing. In the context of diversity with TAS or RAS, antennas with the highest SNR have to be chosen [2] [3] [5] [6] . For TAS, this strategy corresponds to beamforming and is also known as hybrid maximum ratio transmission, while in joint transmit/receive AS the selection process is equivalent to choose a channel submatrix that can maximize the sum of the squared magnitudes of joint transmit/receive channel SNR [3], [7]. On the other hand, antenna selection with SM involves various criteria such as channel capacity [8]-[12], squared Frobenius-norm of effective channels [13], channel's minimum singular value [14], post processing SNR for the decesion-feedback detector (DFD) [15] and so on. Furthermore, big interest has emerged recently to analyse the performance of using antenna selection in large scale MIMO systems. The problem of the maximum-SNR joint beamforming transmit antenna selection for MIMO systems with a large number of transmit antennas has been considered and solved polynomially based on the maximum principal singular value as a selection metric in [16]. The method exhibits a good performance for mobile users with two receive antennas but it tends to be more challenging when the number of receive antennas is increased. A suboptimal algorithm of AS based on the distribution of the mutual information to improve the energy efficiency of large scale MIMO

systems is proposed in [17] where authors found that AS can be efficiently applied only if the circuit power consumption of MIMO system is quite close or greater than the transmit power.

Since optimum method of AS requires exhaustive search over all possible combinations of antenna subsets which makes it impractical to use when there is a large number of antennas, any algorithm of AS should be designed to reduce the complexity of selection process as well as achieve the required level of efficiency. Motivated by the idea of selecting users depending on the product of eigenvalues of their effective channels which is introduced in [35], we propose a suboptimal TAS algorithm for MU-MIMO downlink systems. At each iteration, the antenna which maximizes the product of eigenvalues of effective channels obtained by a set of transmit antennas is selected and deactivated. The selection process repeats till we reach the required subset of antennas. The iterative precoding method introduced by [31] is applied to cancel the interuser interference (IUI) in the precoding stage of the selection process. This precoding method is used instead of the traditional block diagonalization (BD) method which applies SVD to cancel IUI because the iterative method requires small concatenated matrix size to generate the null space matrix. Moreover, to obtain the null space matrix, the proposed algorithm applies the QR decomposition (QRD) rather than SVD operation in order to reduce the computational burden through selection process.

3.2 MU-MIMO Block Diagonalization System

3.2.1 System Model

Consider a single-cell downlink MU-MIMO system that has a base station (BS) equipped with N_t, N_s transmit antennas and radio frequency chains, respectively. The BS communicates simultaneously with K mobile users , each user is equipped with N_r receive antennas. Under the assumption of perfect channel state information in the

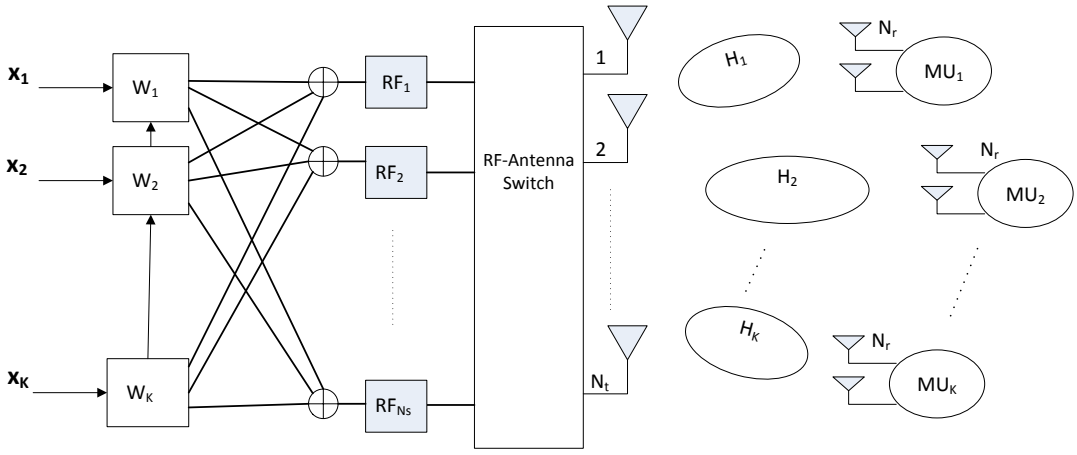

Figure 3.1: Proposed model for multiuser MIMO system with BD precoding technique. (Figure extracted from [97])

transmitter side, the channel propagation from BS to the kth user, $k = 1, 2, ..., K$, is given as $\mathbf{H_k} \in \mathbb{C}^{\boldsymbol{N_r} \times \boldsymbol{N_t}}$. Each user's channel $\mathbf{H_k}$ is assumed to be independent from other users' channels and has full rank,

$$\text{rank}(\mathbf{H_k}) = \min(\boldsymbol{N_r}, \boldsymbol{N_t}) \ , \quad \boldsymbol{N_t} > \boldsymbol{N_r} \tag{3.1}$$

Therefore, the overall system channel ascertains full rank matrix, i.e.,

$$\mathbf{H} = [\mathbf{H_1^H H_2^H ... H_K^H}]^{\boldsymbol{H}} \tag{3.2}$$

For the $\boldsymbol{k}$th user, a symbol vector $\mathbf{x_k} \in \mathbb{C}^{\boldsymbol{N_r} \times \mathbf{1}}$ is transmitted with an input covariance matrix given as

$$\mathbf{Q_k} = \mathbb{E}\{\mathbf{x_k x_k^H}\} \tag{3.3}$$

and a total transmit power as

$$\boldsymbol{P} = \sum_{\boldsymbol{k=1}}^{\boldsymbol{K}} \text{trace}(\mathbf{Q_k}) \tag{3.4}$$

The transmitted signal is multiplied by a precoding matrix $\mathbf{W_k} \in \mathbb{C}^{\boldsymbol{N_t} \times \boldsymbol{N_r}}$ and

transmitted to users. Thus, the kth user receives [20]

$$\mathbf{y}_k = \mathbf{H}_k \mathbf{W}_k \mathbf{x}_k + \sum_{j=1, j\neq k}^{K} \mathbf{H}_k \mathbf{W}_j \mathbf{x}_j + \mathbf{z}_k \tag{3.5}$$

where $z_k \in \mathbb{C}^{N_r \times 1}$ denotes the Additive White Gaussian Noise (AWGN) with $(0, N_o)$.

3.2.2 Iterative Precoder Design method

Block diagonalization intends to cancel IUI of MU MIMO channel and decompose it into parallel lines of single user MIMO (SU MIMO) channels. For user k, the precoder matrix has to satisfy the condition

$$\mathbf{H}_k \mathbf{W}_j = 0, \quad \forall j \neq k \tag{3.6}$$

where $\mathbf{W}_k$ must be a unitary matrix to satisfy the total transmitted power, i.e.,

$$\mathbf{W}_k \in \mathbb{U}\,(N_t, N_r) \tag{3.7}$$

Moreover, $\mathbf{W}_k$ can be broken down into two matrices $\mathbf{F}$ and $\mathbf{\Lambda}$ that is

$$\mathbf{W}_k = \mathbf{F}_k \mathbf{\Lambda}_k \tag{3.8}$$

where $\mathbf{F}_k$ is designed to nullify the IUI and $\mathbf{\Lambda}_k$ is to optimize data rate. Therefore, $\mathbf{F}_k$ is designed to lie in the intersection of all other users' nullspaces except user k, i.e., $\mathcal{N}(\tilde{\mathbf{H}}_k)$, where

$$\tilde{\mathbf{H}}_k = \left[\mathbf{H}_1^T, ..., \mathbf{H}_{k-1}^T, \mathbf{H}_{k+1}^T, ..., \mathbf{H}_K^T\right]^T \tag{3.9}$$

where $\boldsymbol{\mathcal{N}(\tilde{H}_k)}$ denotes the null space matrix of $\tilde{\mathbf{H}}_{\boldsymbol{k}}$. An iterative method is proposed in [31] to design $\mathbf{F}_{\boldsymbol{k}}$. The method applies the QR decomposition instead of SVD to compute the nullspace matrix. Conceptually, let us describe the precoding matrix for user 1, which is denoted by $\mathbf{F}_{\mathbf{1}}^{(\boldsymbol{i})}$ at the $\boldsymbol{i}$th iteration. Initially, we set $\mathbf{F}_{\mathbf{1}}^{(\mathbf{1})} = \mathbf{I}_{\boldsymbol{N_t}}$. At step two, $\mathbf{F}_{\mathbf{1}}^{(\mathbf{2})} = \boldsymbol{\mathcal{N}(\mathbf{H_2})}$. After the $\boldsymbol{i}$th iteration, we obtain $\mathbf{F}_{\mathbf{1}}^{(\boldsymbol{i})}$ such that

$$\mathbf{H}_{\boldsymbol{k}}\mathbf{F}_{\mathbf{1}}^{(\boldsymbol{i})} = \mathbf{0}\ , \quad \text{for all } \mathbf{1} < \boldsymbol{k} \leq \boldsymbol{i} \tag{3.10}$$

In each step, $\mathbf{F}_{\mathbf{1}}^{(\boldsymbol{i})}$ can be found from $\mathbf{F}_{\mathbf{1}}^{(\boldsymbol{i-1})}$ in recursive way as follows:

$$\mathbf{F}_{\mathbf{1}}^{(\boldsymbol{i})} = \mathbf{F}_{\mathbf{1}}^{(\boldsymbol{i-1})}\mathbf{G}_{\mathbf{1}}^{(\boldsymbol{i})} \tag{3.11}$$

where $\mathbf{G}_{\mathbf{1}}^{(\boldsymbol{i})}$ is in $\boldsymbol{\mathcal{N}(\mathbf{H}_i\mathbf{F}_1^{(i-1)})}$. Hence, $\mathbf{G}_{\mathbf{1}}^{(\boldsymbol{i})}$ can be taken as

$$\mathbf{G}_{\mathbf{1}}^{(\boldsymbol{i})} = \text{null}\left(\mathbf{H}_{\boldsymbol{i}}\mathbf{F}_{\mathbf{1}}^{(\boldsymbol{i-1})}\right) \tag{3.12}$$

where $\text{null}\left(\mathbf{H}_{\boldsymbol{i}}\mathbf{F}_{\mathbf{1}}^{(\boldsymbol{i-1})}\right)$ denotes the matrix whose column vectors represent an orthonormal basis of $\boldsymbol{\mathcal{N}(\mathbf{H}_i\mathbf{F}_1^{(i-1)})}$. In the same way, we can obtain other users' precoder matrices recursively.

To ensure nullity of $\tilde{\mathbf{H}}_{\boldsymbol{k}}$, number of transmit antennas must be larger than the total number of receive antennas of users which are simultaneously communicating with BS, i.e.,

$$\boldsymbol{N_t} > \sum_{\boldsymbol{k=1}}^{\boldsymbol{K}} \boldsymbol{N_{r,k}} \tag{3.13}$$

where $\boldsymbol{N_{r,k}}$ denotes the number of receive antennas of user $\boldsymbol{k}$.

3.3 Multiuser Transmit Antenna Selection

Optimum transmit antenna selection is performed by exhaustively searching over all possible antenna combinations, i.e.,

$$\boldsymbol{S_{optimum}} = \boldsymbol{C_{N_t}^{N_s}} \tag{3.14}$$

where $\boldsymbol{S} \subset \boldsymbol{\{1, 2, ..., K\}}$ denotes a set of users which can be served simultaneously by the BS. Hence, exhaustive search makes antenna selection technique impractical to use when the number of transmit antennas is large. Many suboptimal AS algorithms are proposed to reduce the computation complexity, also to achieve as close as possible to the optimum method. In this section, we introduce two TAS algorithms that have been verified to perform very close to the exhaustive search method with much lower complexity.

To introduce the proposed algorithms, we begin by summarizing two definitions; the principle angle between two subspaces and the orthonormal basis for the intersection of two null spaces.

3.3.1 Angle Between Two Subspaces

Let $\boldsymbol{\mathcal{A}_1}$, $\boldsymbol{\mathcal{A}_2} \subset \mathbb{C}^n$ with $\boldsymbol{a_1 = dim(\mathcal{A}_1) \leq dim(\mathcal{A}_2) = a_2}$. The principal angles $\boldsymbol{\theta_1, ..., \theta_{a_1}} \in \boldsymbol{[0, \pi/2]}$ between $\boldsymbol{\mathcal{A}_1}$, $\boldsymbol{\mathcal{A}_2}$ are defined recursively by [19]

$$\begin{aligned} \boldsymbol{\cos\theta_j} &= \max_{\mathbf{u}\in\boldsymbol{\mathcal{A}_1}} \max_{\mathbf{v}\in\boldsymbol{\mathcal{A}_2}} \mathbf{u}^*\mathbf{v} \\ &= \mathbf{u_j^*v_j} \qquad\qquad \boldsymbol{j = 1, ..., a_1} \end{aligned} \tag{3.15}$$

subject to:

$$\begin{aligned} &||\mathbf{u}|| = ||\mathbf{v}|| = \mathbf{1} \\ &\mathbf{u}^{*}\mathbf{u_i} = \mathbf{0} \qquad\qquad \boldsymbol{i = 1, ..., j-1} \\ &\mathbf{v}^{*}\mathbf{v_i} = \mathbf{0} \qquad\qquad \boldsymbol{i = 1, ..., j-1} \end{aligned} \tag{3.16}$$

Let column vectors of matrices $\mathbf{L_1}$, $\mathbf{L_2}$, $\mathbf{X_1}$ and $\mathbf{X_2}$ be the orthonormal basis of the subspaces $\boldsymbol{\mathcal{A}_1}$, $\boldsymbol{\mathcal{A}_2}$, $\boldsymbol{\mathcal{A}_1^{\perp}}$ and $\boldsymbol{\mathcal{A}_2^{\perp}}$ respectively. The two matrices $\boldsymbol{\mathcal{A}_1^{\perp}}$ and $\boldsymbol{\mathcal{A}_2^{\perp}}$ denote the orthogonal complements of the subspaces $\boldsymbol{\mathcal{A}_1}$ and $\boldsymbol{\mathcal{A}_2}$, respectively. Then, the principal angles can be obtained as follows [21] [99] [23]

1. Apply the SVD operation on $\mathbf{L_1^H L_2}$ as

$$\text{SVD}\left(\mathbf{L_1^H L_2}\right) = \mathbf{U \Sigma V^H} \tag{3.17}$$

where $\boldsymbol{\Sigma = diag\left(\sigma_1, ..., \sigma_j\right)}$ are the singular values of $\mathbf{L_1^H L_2}$. Then, the principal angles between the two subspaces $\boldsymbol{\mathcal{A}_1}$ and $\boldsymbol{\mathcal{A}_2}$ are given as

$$\boldsymbol{\cos\theta_i = \sigma_i \ , \quad \forall\ i = 1, ..., j} \tag{3.18}$$

2. Or, alternatively, we calculate the SVD of $\mathbf{L_1^H X_2}$ as

$$\text{SVD}\left(\mathbf{L_1^H X_2}\right) = \check{\mathbf{U}}\check{\mathbf{\Sigma}}\check{\mathbf{V}}^{\boldsymbol{H}} \tag{3.19}$$

where $\check{\boldsymbol{\Sigma}} = \boldsymbol{diag\left(\check{\sigma}_1, ..., \check{\sigma}_j\right)}$.
The largest principal angle is obtained by either

$$\boldsymbol{\theta} = \arccos\left(\boldsymbol{\sigma_j}\right) \tag{3.20}$$

or,

$$\boldsymbol{\theta} = \arcsin\left(\boldsymbol{\check{\sigma}_j}\right) \tag{3.21}$$

where $\boldsymbol{\theta}$ is the angle between the two subspaces $\boldsymbol{\mathcal{A}_1}$ and $\boldsymbol{\mathcal{A}_2}$.

If we suppose $\boldsymbol{\lambda_i}$'s, $\boldsymbol{i = 1, ..., j}$, are the eigenvalues of matrix $\mathbf{L_1^H L_2 L_2^H L_1}$, it follows that

$$\boldsymbol{\lambda_i = \cos^2 \theta_i} \tag{3.22}$$

where $\boldsymbol{\theta_i}$'s represent the principal angles. From the relationship between eigenvalues and matrix determinant, equation (3.22) becomes

$$\begin{aligned} \prod_{i=1}^{a_1} \cos \theta_i &= \sqrt{\det\left(\mathbf{L}_1^H \mathbf{L}_2 \mathbf{L}_2^H \mathbf{L}_1\right)} \\ &= \cos \measuredangle \left(\boldsymbol{\mathcal{A}_1 \mathcal{A}_2}\right) \end{aligned} \tag{3.23}$$

where $\measuredangle \left(\boldsymbol{\mathcal{A}_1 \mathcal{A}_2}\right)$ refers to the product angle (or geometrical angel) between subspaces $\boldsymbol{\mathcal{A}_1}$ and $\boldsymbol{\mathcal{A}_2}$ [22]. Geometrically, $\boldsymbol{\cos^2 \measuredangle \left(\mathcal{A}_1 \mathcal{A}_2\right)}$ is the ratio between two volumes: The volume of the parallelepiped spanned by projecting the basis vectors of $\mathbf{L_1}$ onto $\mathbf{L_2}$, and the volume of the basis vectors of $\mathbf{L_1}$ [23].

3.3.2 Intersection of Null Spaces

Let $\boldsymbol{\mathcal{H}_1} \in \mathbb{C}^{m \times n}$ and $\boldsymbol{\mathcal{H}_2} \in \mathbb{C}^{p \times n}$ are two given subspaces, and the orthonormal basis for null$\left(\boldsymbol{\mathcal{H}_1}\right)$ is $\boldsymbol{\mathcal{U}}$. Also, consider $\boldsymbol{\mathcal{V}}$ is the orthonormal basis for matrix null$\left(\boldsymbol{\mathcal{H}_2 \mathcal{U}}\right)$. Hence, the orthonormal basis for null$\left(\boldsymbol{\mathcal{H}_1}\right) \bigcap$ null$\left(\boldsymbol{\mathcal{H}_2}\right)$ can be obtained as [19]

$$\begin{aligned} \text{null}\left(\boldsymbol{\mathcal{H}_1}\right) \bigcap \text{null}\left(\boldsymbol{\mathcal{H}_2}\right) &= \boldsymbol{\mathcal{U}}\ \text{null}\left(\boldsymbol{\mathcal{H}_2\ \mathcal{U}}\right) \\ &= \boldsymbol{\mathcal{U}\ \mathcal{V}} \end{aligned} \tag{3.24}$$

Equation (3.24) represents an economical method to calculate the orthonormal basis for the intersection of two null spaces.

Algorithm 1 Transmit antenna selection algorithm using product of eigenvalues of effective channels

Let $\boldsymbol{\Delta} = \{\boldsymbol{1, 2, ..., K}\}$. Collect $\mathbf{H}_{\boldsymbol{k}}$ $\forall \boldsymbol{k} \in \boldsymbol{\Delta}$
Let $\boldsymbol{\Gamma} = \{\boldsymbol{1, 2, ..., N_t}\}$, $\boldsymbol{\Upsilon} = \varnothing$
repeat (Main loop)
for $\boldsymbol{m} \in \boldsymbol{\Gamma}$ **do**
    Temporarily, Let $\tilde{\boldsymbol{\Gamma}} = \boldsymbol{\Gamma} - \{\boldsymbol{m}\}$, $\boldsymbol{N_t} = \boldsymbol{N_t} - \boldsymbol{1}$
    $\boldsymbol{i} = \boldsymbol{1}$, $\mathbf{F}_{\boldsymbol{1}}^{(\boldsymbol{1})} = \mathbf{I}_{\boldsymbol{N_t}}$
    Calculate $\boldsymbol{\delta}_{\boldsymbol{k}}^{(\boldsymbol{1})} = \det\left(\mathbf{H}_{\boldsymbol{k},\tilde{\boldsymbol{\Gamma}}}\mathbf{H}_{\boldsymbol{k},\tilde{\boldsymbol{\Gamma}}}^{*}\right)$ $\forall \boldsymbol{k} \in \boldsymbol{\Delta}$
    repeat
    $\mathbf{F}_{\boldsymbol{i+1}}^{(\boldsymbol{i+1})} = \mathbf{F}_{\boldsymbol{i}}^{(\boldsymbol{i})} \times \boldsymbol{\mathcal{N}}\left(\mathbf{H}_{\boldsymbol{i}}\mathbf{F}_{\boldsymbol{i}}^{(\boldsymbol{i})}\right)$
    $\bar{\mathbf{H}}_{\boldsymbol{i+1},\tilde{\boldsymbol{\Gamma}}}^{(\boldsymbol{i+1})} = \mathbf{H}_{\boldsymbol{i+1}}\mathbf{F}_{\boldsymbol{i+1}}^{(\boldsymbol{i+1})}$
    $\boldsymbol{\delta}_{\boldsymbol{i+1}}^{(\boldsymbol{i+1})} = \det\left(\bar{\mathbf{H}}_{\boldsymbol{i+1},\tilde{\boldsymbol{\Gamma}}}^{(\boldsymbol{i+1})}\ \bar{\mathbf{H}}_{\boldsymbol{i+1},\tilde{\boldsymbol{\Gamma}}}^{(\boldsymbol{i+1})*}\right)$
    for $\boldsymbol{n} = \boldsymbol{1} : \boldsymbol{i}$ **do**
        Update $\mathbf{F}_{\boldsymbol{n}}^{(\boldsymbol{i+1})} = \mathbf{F}_{\boldsymbol{n}}^{(\boldsymbol{i})} \times \boldsymbol{\mathcal{N}}\left(\mathbf{H}_{\boldsymbol{i+1}}\mathbf{F}_{\boldsymbol{n}}^{(\boldsymbol{i})}\right)$
        $\boldsymbol{\Lambda}_{\boldsymbol{n}}^{(\boldsymbol{i})} = \text{row}\left(\mathbf{H}_{\boldsymbol{n}}\mathbf{F}_{\boldsymbol{n}}^{(\boldsymbol{i})}\right)$
        $\mathbf{G}_{\boldsymbol{n}}^{(\boldsymbol{i+1})} = \boldsymbol{\mathcal{N}}\left(\mathbf{H}_{\boldsymbol{i+1}}\mathbf{F}_{\boldsymbol{n}}^{(\boldsymbol{i})}\right)$
        $\boldsymbol{\delta}_{\boldsymbol{n}}^{(\boldsymbol{i+1})} = \boldsymbol{\delta}_{\boldsymbol{n}}^{(\boldsymbol{i})}\det\left(\boldsymbol{\Lambda}_{\boldsymbol{n}}^{(\boldsymbol{i})*}\mathbf{G}_{\boldsymbol{n}}^{(\boldsymbol{i+1})}\mathbf{G}_{\boldsymbol{n}}^{(\boldsymbol{i+1})*}\boldsymbol{\Lambda}_{\boldsymbol{n}}^{(\boldsymbol{i})}\right)$
    end for
    $\boldsymbol{i} = \boldsymbol{i} + \boldsymbol{1}$
    until $\boldsymbol{i} = \boldsymbol{K}$
    Calculate $\boldsymbol{\alpha_m} = \prod_{\boldsymbol{k}\in\boldsymbol{\Delta}} \boldsymbol{\delta}_{\boldsymbol{k}}^{(\boldsymbol{i})}$
end for
$\boldsymbol{m_{deactivated}} = \arg\max_{\boldsymbol{m}\in\boldsymbol{\Gamma}}\ \boldsymbol{\alpha_m}$
Update $\boldsymbol{\Gamma} = \boldsymbol{\Gamma} - \{\boldsymbol{m_{deactivated}}\}$
Update $\boldsymbol{\Upsilon} = \boldsymbol{\Upsilon} + \{\boldsymbol{m_{deactivated}}\}$
Update $\boldsymbol{N_t}$
until $\mid \boldsymbol{\Gamma} \mid = \boldsymbol{N_s}$

3.3.3 Proposed Algorithm

The proposed transmit antenna selection algorithm is designed to greedily select an optimal set of antennas for transmission. At each iteration, the algorithm removes one antenna from the set of remaining antenna in the BS, which can mitigate the performance degradation to the minimum extent. The removed antenna must optimize a specific performance criterion which is the product of eigenvalues of users' effective channels obtained by the remaining set of antennas in each iteration. The following is a brief summary of the metric. Let $\bar{\mathbf{H}}_{\boldsymbol{k}}^{(\boldsymbol{i})}$ denotes the effective channel matrix for user $\boldsymbol{k}$ at the $\boldsymbol{i}$-th iteration. The $\boldsymbol{l}$-th eigenvalues of matrix $\bar{\mathbf{H}}_{\boldsymbol{k}}^{(\boldsymbol{i})}\bar{\mathbf{H}}_{\boldsymbol{k}}^{(\boldsymbol{i})\boldsymbol{H}}$ are denoted as $\boldsymbol{\lambda}_{\boldsymbol{k},\boldsymbol{p}}^{(\boldsymbol{i})}$, where $\boldsymbol{p} = \mathbf{1}, ..., \boldsymbol{N_r}$. Hence, the product of eigenvalues of matrix $\bar{\mathbf{H}}_{\boldsymbol{k}}^{(\boldsymbol{i})}\bar{\mathbf{H}}_{\boldsymbol{k}}^{(\boldsymbol{i})\boldsymbol{H}}$ can be obtained as

$$\begin{aligned}\boldsymbol{\delta}_{\boldsymbol{k}}^{(\boldsymbol{i})} &= \prod_{\boldsymbol{p}=\mathbf{1}}^{\boldsymbol{N_r}} \boldsymbol{\lambda}_{\boldsymbol{k},\boldsymbol{p}}^{(\boldsymbol{i})} \\ &= \mathbf{det}\left(\bar{\mathbf{H}}_{\boldsymbol{k}}^{(\boldsymbol{i})}\bar{\mathbf{H}}_{\boldsymbol{k}}^{(\boldsymbol{i})\boldsymbol{H}}\right)\end{aligned} \tag{3.25}$$

where $\boldsymbol{\delta}_{\boldsymbol{k}}^{(\boldsymbol{i})}$ denotes the product of $\boldsymbol{\lambda}_{\boldsymbol{k},\boldsymbol{p}}^{(\boldsymbol{i})}$'s. Using equation (3.24), it is possible to calculate the eigenvalues of each user's effective channel from that of the prior iteration as [35]

$$\begin{aligned}\boldsymbol{\delta}_{\boldsymbol{k}}^{(\boldsymbol{i})} &= \boldsymbol{\delta}_{\boldsymbol{k}}^{(\boldsymbol{i}-\mathbf{1})}\det\left(\boldsymbol{\Lambda}_{\boldsymbol{k}}^{(\boldsymbol{i}-\mathbf{1})\boldsymbol{H}}\mathbf{G}_{\boldsymbol{k}}^{(\boldsymbol{i})}\mathbf{G}_{\boldsymbol{k}}^{(\boldsymbol{i})\boldsymbol{H}}\boldsymbol{\Lambda}_{\boldsymbol{k}}^{(\boldsymbol{i}-\mathbf{1})}\right) \\ &= \boldsymbol{\delta}_{\boldsymbol{k}}^{(\boldsymbol{i}-\mathbf{1})}\,\mathbf{cos}^{\mathbf{2}}\,\boldsymbol{\theta}_{\boldsymbol{k}}\end{aligned} \tag{3.26}$$

where $\boldsymbol{\delta}_{\boldsymbol{k}}^{(\boldsymbol{i}-\mathbf{1})}$ denotes the product of eigenvalues of the $\boldsymbol{k}$th user's effective channel at $(\boldsymbol{i}-\mathbf{1})$th iteration. Moreover, $\boldsymbol{\theta}_{\boldsymbol{k}}$ denotes the product angles between $\boldsymbol{\mathcal{R}}\left(\mathbf{H}_{\boldsymbol{k}}\mathbf{F}_{\boldsymbol{k}}^{(\boldsymbol{i}-\mathbf{1})}\right)$ and $\boldsymbol{\mathcal{N}}\left(\mathbf{H}_{\boldsymbol{u_i}}\mathbf{F}_{\boldsymbol{k}}^{(\boldsymbol{i}-\mathbf{1})}\right)$, where $\boldsymbol{u_i}$ denotes the selected user at the $\boldsymbol{i}$-th iteration. The main steps to implement TAS by using product of eigenvalues of effective channels are summarized in **Algorithm 1**, where $\boldsymbol{\Delta}$ is the set of users, $\boldsymbol{\Gamma}$ and $\boldsymbol{\Upsilon}$ are the sets of active antennas and deactivated antennas, respectively. In the beginning, we assume that all transmit antennas are avctive, we collect $\mathbf{H}_{\boldsymbol{k}}\ \forall \boldsymbol{k} \in \boldsymbol{\Delta}$.

Table 3.1: search size comparison of different TAS algorithms.

Algorithm	Search size
exhaustive search	$\boldsymbol{C_{N_t}^{N_s}}$
norm-based [97]	$\boldsymbol{(N_t + N_s + 1)\left(\frac{N_t - N_s}{2}\right)}$
proposed	$\boldsymbol{K\,(N_t + N_s + 1)\left(\frac{N_t - N_s}{2}\right)}$

The main loop of the algorithm starts by, temporarily, deactivating antenna $\boldsymbol{m}$ for every $\boldsymbol{m} \in \boldsymbol{\Gamma}$. Hence, the temporal set of antennas $\tilde{\boldsymbol{\Gamma}}$ at BS has $\boldsymbol{N_t = N_t - 1}$ total transmit antennas. Lines 8-17 iteratively calculate:

- users' channel precoders using iterative precoding method explained earlier (line 9 and line 13);
- the product of eigenvalues of each user's effective channel using (3.26) (line 11 and line 16).

The product of eigenvalues of users' effective channels $\boldsymbol{\alpha}$ is calculated in line 20 for every $\tilde{\boldsymbol{\Gamma}}$. Then, the antenna $\boldsymbol{m}$ that maximize $\boldsymbol{\alpha}$ is selected and removed from the set of transmit antennas $\boldsymbol{\Gamma}$ ($\boldsymbol{m_{deactivated}}$ in line 22). Finally, we update $\boldsymbol{\Gamma}$, $\boldsymbol{\Upsilon}$ and $\boldsymbol{N_t}$. The main loop stops when the number of active transmit antennas reaches $\boldsymbol{N_s}$. The search size of this algorithm is

$$\text{search size} = \boldsymbol{K\,(N_t + N_s + 1)\left(\frac{N_t - N_s}{2}\right)} \tag{3.27}$$

Comparisons of search size of different transmit antenna selection algorithms is listed in Table I.

3.4 Simulation Results

To evaluate the performance of the proposed transmit antenna selection algorithm, we compare it with the following algorithms:

- Exhaustive search algorithm (optimum method)
- Norm-based algorithm (suboptimal method [97])

The algorithm in [97] has been chosen for comparison for two reasons. First, the selection metric in this algorithm depends on the Frobenius norm which can provide a considerable indication about the performance due to close relation between Frobinius norm and the eigenvalues of users' effective channels calculated after precoding stage. Second, the Frobenius norm provides a robust lower bound on the average sum capacity [75]

$$\begin{aligned} \boldsymbol{C} &= \sum_{\boldsymbol{k=1}}^{\boldsymbol{K}} \mathbf{log\,det}\left(\mathbf{I} + \frac{\mathbf{1}}{\boldsymbol{N_o}}\mathbf{H}_{\boldsymbol{k}}\mathbf{W}_{\boldsymbol{k}}\mathbf{Q}_{\boldsymbol{k}}\mathbf{W}_{\boldsymbol{k}}^{\boldsymbol{H}}\mathbf{H}_{\boldsymbol{k}}^{\boldsymbol{H}}\right) \\ &\geq \sum_{\boldsymbol{k=1}}^{\boldsymbol{K}} \mathbf{log}\left(\mathbf{1} + \frac{\boldsymbol{P}}{\boldsymbol{K N_r N_o}}\|\mathbf{H}_{\boldsymbol{k}}\mathbf{W}_{\boldsymbol{k}}\|_{\boldsymbol{F}}^{\mathbf{2}}\right) \\ &> \mathbf{log}\left(\mathbf{1} + \sum_{\boldsymbol{k=1}}^{\boldsymbol{K}} \frac{\boldsymbol{P}}{\boldsymbol{K N_r N_o}}\|\boldsymbol{H_k W_k}\|_{\boldsymbol{F}}^{\mathbf{2}}\right) \end{aligned} \tag{3.28}$$

As seen, maximizing the sum Frobenius norm of users leads to maximize the aggregate capacity lower bound, Equation 3.28. All results are averaged over (1000-2000) i.i.d. Rayleigh channel realizations.

In Figure 3.2, the sum rate capacity of the exhaustive search algorithm, norm-based algorithm and the proposed algorithm is compared for different values of SNR, with 2 users, 2 receive antennas per each user. We assumed the total number of transmit antennas at the base station is 4 and the number of selected antennas is 4, i.e., $\boldsymbol{N_t = 4}$, $\boldsymbol{N_s = 4}$, respectively. We increased $\boldsymbol{N_t}$ while $\boldsymbol{N_s}$ is constant, i.e., $\boldsymbol{N_t = 4, 6, 8, 10, 14}$, while $\boldsymbol{N_s = 4}$. Clearly, the proposed algorithm outperforms the norm-based algorithm and achieves very close to the exhaustive search method.

Similarly, results in Figure 3.3, where in this case there are 2 users and 4 receive antennas per each user, are clearly identical with those in the previous Figure. We also notice that the average sum rate has increased , which is normal because the number of receive antennas of each user has increased as well, i.e., $\boldsymbol{N_r = 4}$ in this case. In another case, which is shown in Figure 3.4, the number of users has increased to 3 users, and each user is equipped with two receive antennas. In this case also, the proposed algorithm achieves the same performance obtained in previous two Figures. Moreover, Figure 3.5 shows the average sum rate comparison with a constant selection ratio, where the ratio of selected antennas to the total number of transmit antennas is assumed fixed and equal to $\mathbf{50\%}$. Clearly, results obtained with constant selection ratio with those of previous Figures demonstrate that the proposed algorithm has constant performance regardless of the number of selected antennas. In addition, these four Figures show that selecting antennas in descending order can achieve almost the same performance obtained by the exhaustive search algorithm, after taking in account the performance metric used in the selection process. This can be explained by noting that the selection process takes into consideration the whole correlations among the columns of the original matrix channel before selecting the first transmit antenna to deactivate.

Figures 3.6 and 3.7 show another significant comparison of the exhaustive, norm-based, and proposed algorithms where the average bit error rate (BER) is calculated for two users with two and four receive antennas per user, respectively. The importance of this comparison is to show how reliable is the proposed algorithm with compared to the brute search algorithm and norm-based algorithm. In both Figures, we have used the zero-forcing detection at the receiver. Unlike the norm-based algorithm, it is quite clear that the proposed algorithm provides a high degree of link reliability which is very close to the exhaustive search algorithm. Moreover, we notice that the average BER has increased in Fig 3.7 than in Fig 3.6 for the same number of additional antennas for both users. This is normal since more information has to be detected at each user, i.e., $\boldsymbol{N_r = 4}$ in this case.

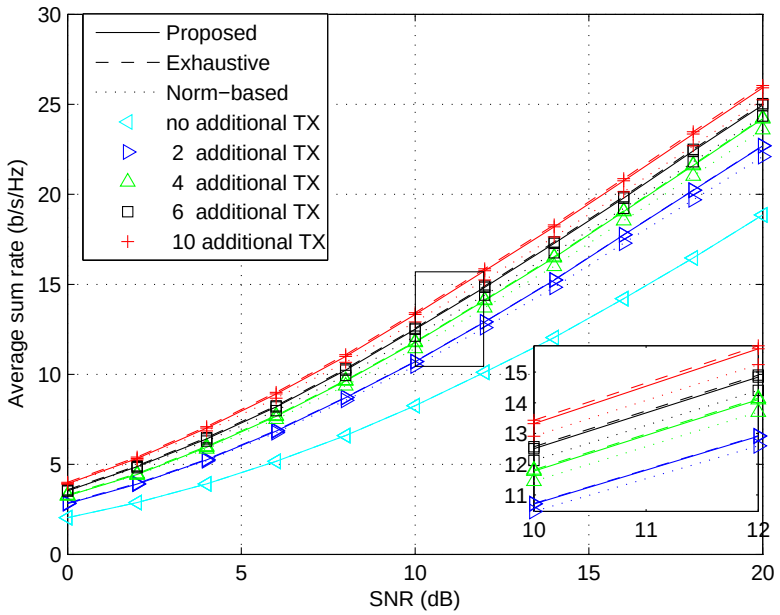

Figure 3.2: Sum rate capacity of proposed, exhaustive, and norm-based transmit antenna selection algorithms with 2 users, 2 receive antennas per user.

In Figures 3.8 and 3.9, the elapsed CPU time of the proposed algorithm, norm-based algorithm, and exhaustive search algorithm is plotted against the number of additional transmit antennas for two users, with two receive antennas and four receive antennas, respectively. These results were attained by 3.4 GHz Core i7 CPU pc. As noted in both figures, the CPU runtime of the proposed algorithm outperforms the exhaustive search and achieves close to the norm-based algorithm which has the shortest runtime. Clearly, these two figures demonstrate the search size comparison presented in Table 3.1 in which we have proved that the proposed algorithm differs from the norm-based algorithm by only a factor of $\boldsymbol{K}$. In summary, the proposed algorithm outperforms the norm-based and achieves very close to the exhaustive search with acceptable limit of complexity.

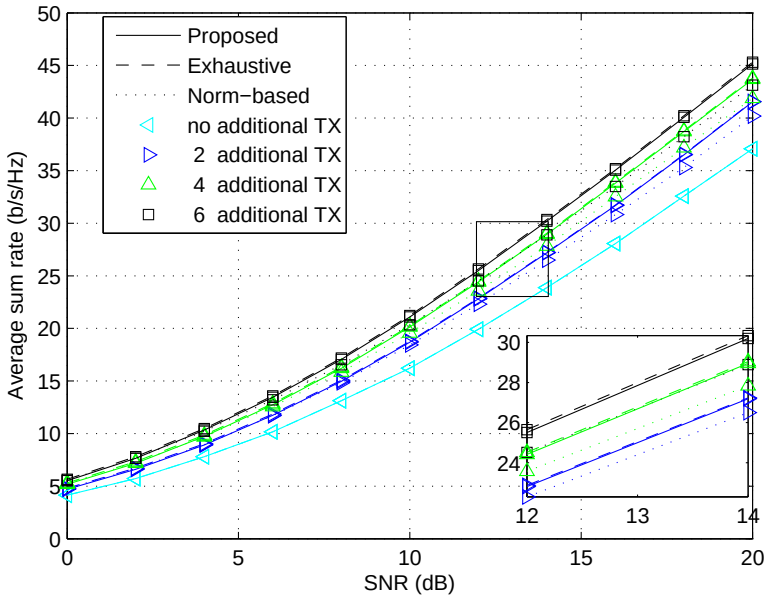

Figure 3.3: Sum rate capacity of proposed, exhaustive, and norm-based transmit antenna selection algorithms with 2 users, 4 receive antennas per user.

3.5 Summary

In this Chapter, we have studied the transmit antenna selection technique for multiuser MIMO downlink systems. Our objective is to design an algorithm of TAS which can almost achieve the same throughput obtained by the exhaustive search algorithm with lower complexity. As a prior stage of the selection process, we used the iterative precoder design to obtain the precoders necessary to precancel interuser interference. Also, we studied the principal angles, which represent the angles between subspaces, and their relation to the eigenvalues. This relation could be exploited in order to obtain the eigenvalues of a specific subspace iteratively from a prior stages using the concept of intersection of null spaces. Simulation results show that the proposed algorithm achieves very close to the optimum search algorithm with a considerable reduction in complexity.

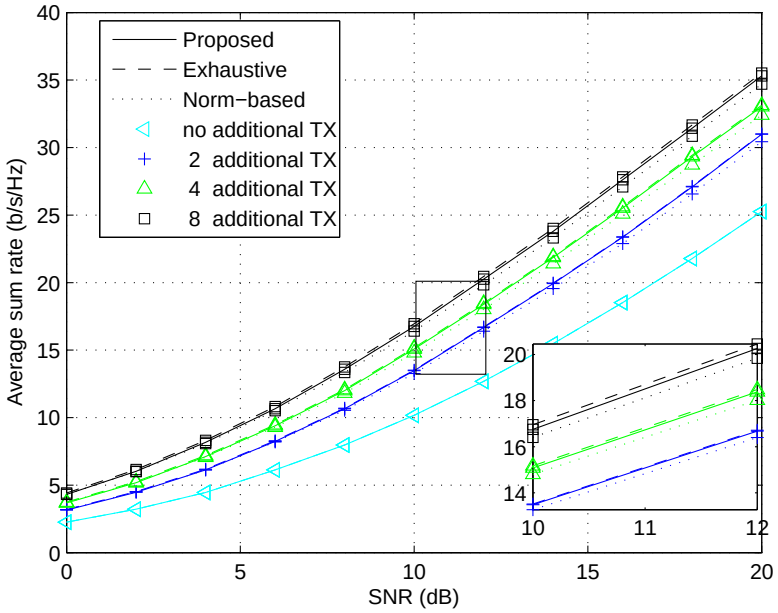

Figure 3.4: Sum rate capacity of proposed, exhaustive, and norm-based transmit antenna selection algorithms with 3 users, 2 receive antennas per user.

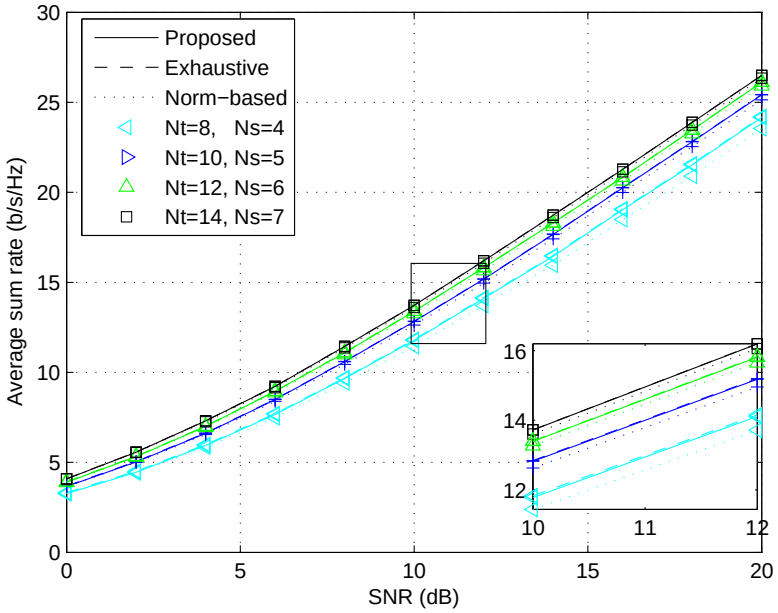

Figure 3.5: Sum rate capacity of proposed, exhaustive, and norm-based transmit antenna selection algorithms with 2 users, 2 receive antennas per user, and with constant selection ratio.

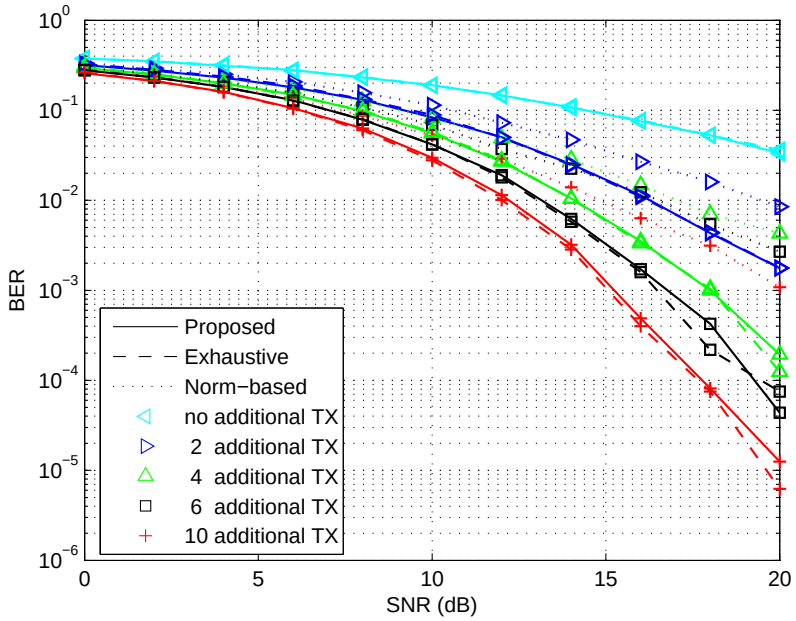

Figure 3.6: BER performance of proposed, norm-based, and exhaustive search transmit antenna selection algorithms with 2 users, 2 receive antennas and 2 data substreams per user, using QPSK modulation and zero-forcing detection at the receiver.

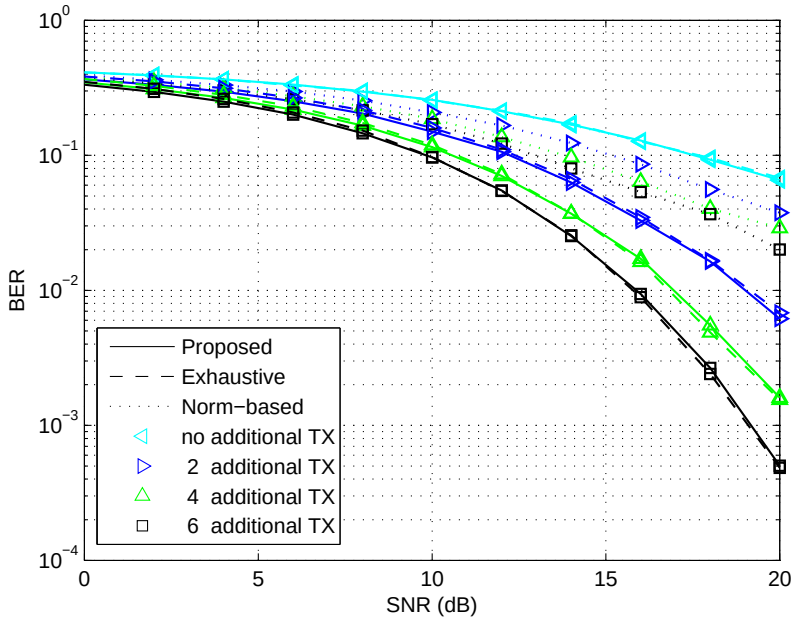

Figure 3.7: BER performance of proposed, norm-based, and exhaustive search transmit antenna selection algorithms with 2 users, 4 receive antennas and 4 data substreams per user, using QPSK modulation and zero-forcing detection at the receiver.

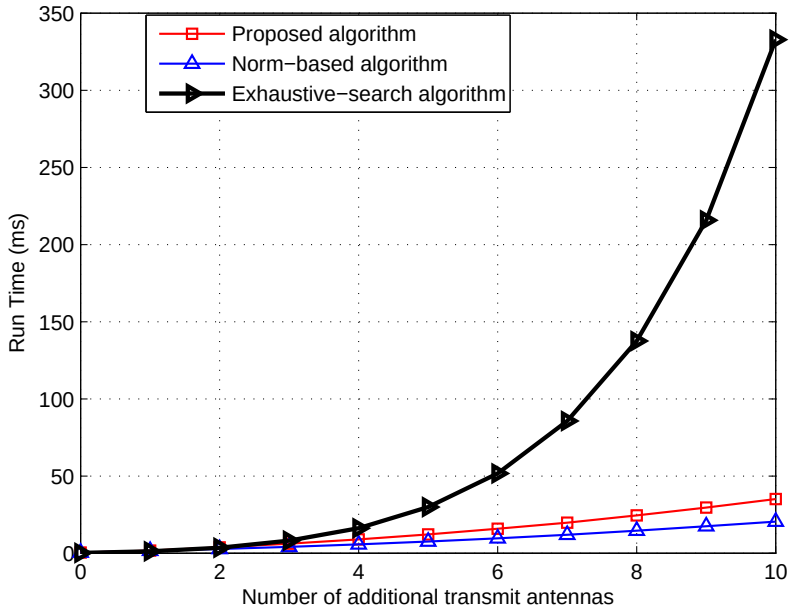

Figure 3.8: Run time comparison of proposed, norm-based, and exhaustive search algorithms with 2 users, 2 receive antennas per user.

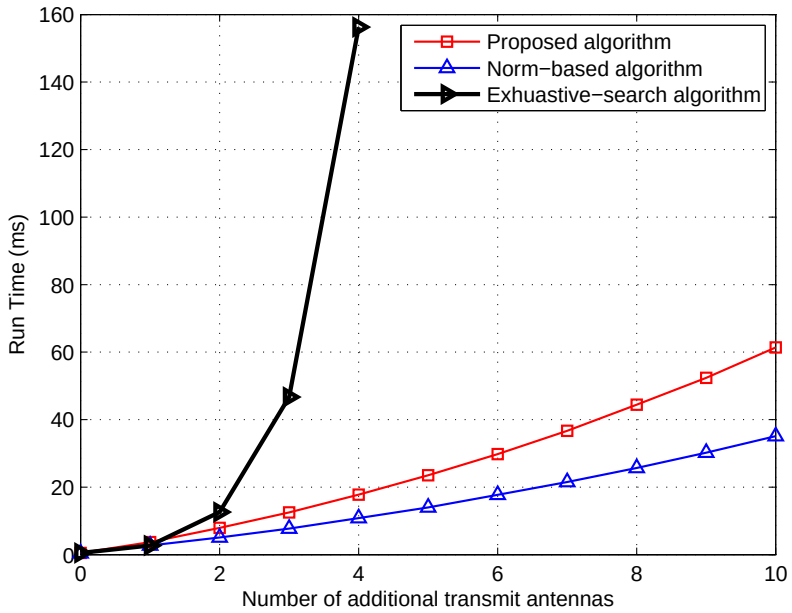

Figure 3.9: Run time comparison of proposed, norm-based, and exhaustive search algorithms with 2 users, 4 receive antennas per user.

Chapter 4

A User Selection Algorithm for MU-MIMO Systems Using Product of Singular Values of Users' Effective Channels

In this chapter, a suboptimal greedy user selection algorithm for downlink MU-MIMO systems is proposed. In each iteration, the user that maximizes the product of singular values of users' effective channels is selected from a pool of users. Moreover, the algorithm designs its precoders using the Gram-Schmidt Orthogonalization operation in order to precancel the interuser interference. The simulation results show that the proposed algorithm achieves the throughput performance of the capacity-based algorithm with significant reduction in complexity.

4.1 Introduction

In modern wireless communications, significant attention has been directed toward multiuser multiple-input multiple-output (MU-MIMO) systems due to their capability of improving system throughput [24][25]. In the case that channel state information (CSI) is available at the base station (BS), interuser interference (IUI) can be precancelled using several efficient methods. Dirty paper coding (DPC) provides optimal IUI cancellation, but its high complexity during coding and decoding makes its application to large multiple antenna systems unrealistic [26] [27]. For practical implementation, zero-forcing beamforming (ZF-BM) and block diagonalization (BD) techniques are proposed instead of DPC as suboptimal preprocessing techniques for MU-MIMO systems [28]. In ZF-BM, where each user has one receive antenna, the transmitted signal is multiplied by a precoding matrix which represents the pseudo-inverse of other users' channels [29]. On the other hand, for users with multiple receive antennas, BD designs each user's precoding matrix to be in the null space of other users' channels. Consequently, BD preeliminates IUI from users and breaks down the overall MU-MIMO channel into several independent parallel single user MIMO (SU-MIMO) downlink channels [30].

The nullspace-based precoding matrix imposes the constraint that a BS must communicate with concurrent users which have a total number of receive antennas less than that of transmit antennas for that BS. When there is a large number of users, the BS may select a subset for communication in order to increase the total sum rate capacity of the system. Optimum users are obtained by exhaustively searching over all possible users combinations, which thus involves high complexity, in particular, when there is a large number of users.

To reduce the complexity of user selection under the BD technique, considerable research effort has been devoted to reducing the complexity of precoding stage. Regarding which, the conventional precoding design method which applies the singular value decomposition (SVD) iteratively to cancel IUI requires high computational burden. Alternatively, an iterative precoder design method is introduced by [31] to

alleviate the computational demand caused by repeated SVD. For user selection, one strategy is to design a greedy suboptimal algorithm, whereby one user that maximizes a specific performance metric is selected at each iteration. Many greedy suboptimal user selection algorithms are proposed, which are based on various selection metrics. A capacity-based algorithm (c-algorithm) is proposed in [32], which selects a user to maximize the average sum rate of the system at each iteration. Despite the high level of performance that the c-algorithm can provide, it requires high complexity due to frequent use of SVD. Another approach to user selection under BD is proposed by [33], which utilizes both backward and forward projection in order to select the most orthogonal user channels optimally. This approach needs to find null space and spatial correlation among users at each iteration, which raises the complexity of selection for large number of users. Moreover, [34] proposes a low-complexity algorithm that greedily selects users to maximize the channel volume which can be found by calculating the product of diagonal elements of the upper triangular matrix R produced by performing QR factorization to the channel matrix. Another low complexity algorithm which is based on the product of squared row norms of effective channels is proposed by [31] to select an optimal set of users for BD systems. However, these low complexity user selection algorithms have a low burden of computation, but performance degradation is unavoidable. Under a high SNR regime, [35] proposes a user selection algorithm based on the product of the eigenvalues of effective channels and the idea of principle angles between subspaces. This algorithm provides good performance, but its complexity depends on the maximum number of users that can be simultaneously served by BS and total number of users in the system.

In this chapter, we propose a greedy suboptimal user selection algorithm for MU-MIMO downlink systems and under high SNR regime. The proposed algorithm utilizes the product of singular values of users' effective channels as a selection metric. The objective behind the proposed algorithm is to reach the performance achieved by the capacity-based algorithm (c-algorithm) as well as to reduce the computational load during the user selection process. To achieve high performance, we have designed our selection metric to express the capacity of BD in a high SNR regime. In terms of complexity, the QR decomposition (QRD) has been used to obtain the product of

the singular values instead of SVD so as to reduce the computational effort at each selection step. Further, to cancel IUI, the proposed algorithm applies Gram-Schmidt Orthogonalization (GSO) operation in order to design the precoders. This precoding scheme has been efficiently used in [32] and doesn't require the use of SVD operation that leads to reduction in computation burden.

4.2 MU-MIMO system with Block Diagonalization

4.2.1 System Model

Consider a single-cell downlink MU-MIMO system with $\boldsymbol{N_t}$ transmit antennas at the base station BS and $\boldsymbol{K}$ users which have an equal number of receive antennas $\boldsymbol{N_r}$. The channels are assumed to be independent and identically distributed (i.i.d) flat fading channels. The channel propagation from BS to the $\boldsymbol{k}$th user is given as $\mathbf{H_k} \in \mathbb{C}^{\boldsymbol{N_r} \times \boldsymbol{N_t}}$, under the assumption of perfect channel information at the transmitter by using either time-division duplexing (TDD) or frequency-division duplexing (FDD) communication mode. Each user's channel $\mathbf{H_k}$ is assumed to be independent of other users' channels and has full rank, i.e.,

$$\text{rank}(\mathbf{H_k}) = \min(\boldsymbol{N_r}, \boldsymbol{N_t}) \ , \quad \boldsymbol{N_t} > \boldsymbol{N_r} \tag{4.1}$$

Consequently, the overall system channel will ascertain a full rank matrix, i.e.,

$$\mathbf{H} = [\mathbf{H_1^H H_2^H ... H_K^H}]^{\boldsymbol{H}} \tag{4.2}$$

Let $\boldsymbol{S} \subset \boldsymbol{\{1, 2, ..., K\}}$ denotes a set of users which can be served simultaneously by the BS. For the $\boldsymbol{k}$th user, a symbol vector $\mathbf{x_k} \in \mathbb{C}^{\boldsymbol{N_r} \times \mathbf{1}}$ is transmitted with an

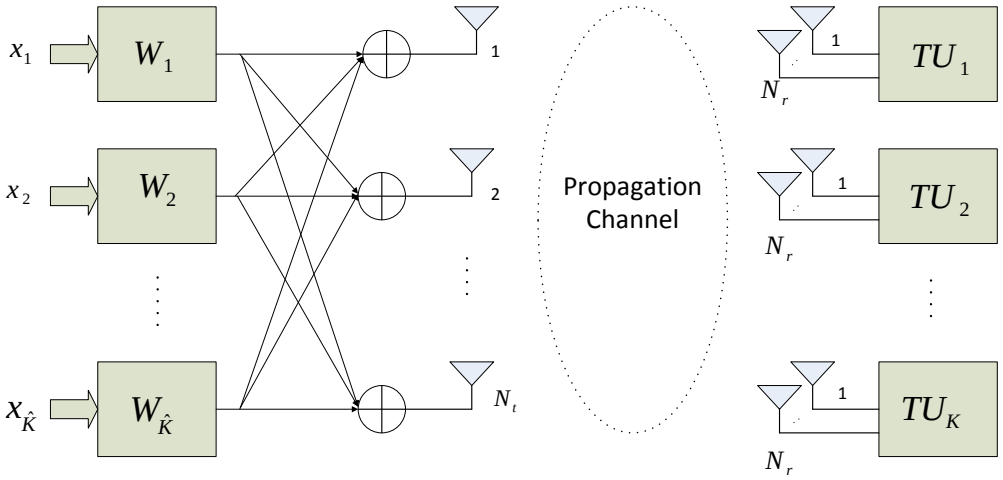

Figure 4.1: Proposed model for a MU-MIMO system with BD precoding technique.

input covariance matrix given as

$$\boldsymbol{Q_k} = \mathbb{E}\{\boldsymbol{x_k x_k^H}\} \tag{4.3}$$

The total transmit power is written as

$$\boldsymbol{P} = \sum_{\boldsymbol{k=1}}^{\boldsymbol{K}} \text{trace}(\boldsymbol{Q_k}) \tag{4.4}$$

Then, the transmitted signal is multiplied by a precoding matrix $\mathbf{W_k} \in \mathbb{C}^{\boldsymbol{N_t \times N_r}}$ and transmitted to users. Thus, the $\boldsymbol{k}$th user receives [36]:

$$\mathbf{y_k} = \mathbf{H_k W_k x_k} + \sum_{\boldsymbol{j=1, j\neq k}}^{\boldsymbol{|S|}} \mathbf{H_k W_j x_j} + \mathbf{z_k} \tag{4.5}$$

where $\boldsymbol{z_k} \in \mathbb{C}^{\boldsymbol{N_r \times 1}}$ denotes the Additive White Gaussian Noise (AWGN) with $\boldsymbol{(0, \sigma^2)}$.

4.2.2 Precoders Design

Block diagonalization serves to cancel the IUI of a MU-MIMO channel and decompose it into parallel SU-MIMO channels. For user $\boldsymbol{k}$, the precoder matrix has to satisfy the condition

$$\mathbf{H}_{\boldsymbol{j}}\mathbf{W}_{\boldsymbol{k}} = \mathbf{0}, \quad \forall \boldsymbol{j} \neq \boldsymbol{k} \tag{4.6}$$

The matrix $\mathbf{W}_{\boldsymbol{k}}$ must be a unitary matrix so as to satisfy the total transmitted power, i.e.,

$$\mathbf{W}_{\boldsymbol{k}} \in \mathbb{U}\left(\boldsymbol{N_t}, \boldsymbol{N_r}\right) \tag{4.7}$$

Moreover, $\mathbf{W}_{\boldsymbol{k}}$ can be broken down into two matrices $\mathbf{F}$ and $\mathbf{\Lambda}$. Hence, the matrix $\mathbf{W}_{\boldsymbol{k}}$ can be written as

$$\mathbf{W}_{\boldsymbol{k}} = \mathbf{F}_{\boldsymbol{k}}\mathbf{\Lambda}_{\boldsymbol{k}} \tag{4.8}$$

where $\mathbf{F}_{\boldsymbol{k}}$ is designed to nullify the IUI and $\mathbf{\Lambda}_{\boldsymbol{k}}$ in order to optimize the data rate [37]. Therefore, $\mathbf{F}_{\boldsymbol{k}}$ is designed to lie in the intersection of all other users' nullspaces except user $\boldsymbol{k}$, i.e., $\boldsymbol{\mathcal{N}}(\tilde{\mathbf{H}}_{\boldsymbol{k}})$, where

$$\tilde{\mathbf{H}}_{\boldsymbol{k}} = \left[\mathbf{H}_{\mathbf{1}}^{\boldsymbol{H}}, ..., \mathbf{H}_{\boldsymbol{k-1}}^{\boldsymbol{H}}, \mathbf{H}_{\boldsymbol{k+1}}^{\boldsymbol{H}}, ..., \mathbf{H}_{\boldsymbol{|S|}}^{\boldsymbol{H}}\right]^{\boldsymbol{H}} \tag{4.9}$$

To ensure nullity of $\tilde{\mathbf{H}}_{\boldsymbol{k}}$, the number of transmit antennas must be larger than the total number of receive antennas of users that are simultaneously communicating with BS, that is

$$\boldsymbol{N_t} > \sum_{\boldsymbol{k=1}}^{\boldsymbol{|S|}} \boldsymbol{N_{r,k}} \tag{4.10}$$

where $\boldsymbol{N_{r,k}}$ denotes the number of receive antennas of user $\boldsymbol{k}$.

In order to obtain the null space of the channel matrix, we utilize the method used by [32] which depends on Gram Schmidt Orthogonalization (GSO) procedure. To clarify the method, assume $\mathbf{H_1} \in \mathbb{C}^{\boldsymbol{p\times q}}$ with $\boldsymbol{p} < \boldsymbol{q}$. Then, the null space $\breve{\mathbf{H}}_{\mathbf{1}} \in \mathbb{C}^{\boldsymbol{q\times q}}$ of matrix $\mathbf{H_1}$ can be obtained as follows

1. Find the transpose of matrix $\mathbf{H_1}$, i.e., $\mathbf{H_1^T} = \text{transpose}(\mathbf{H_1})$

2. Apply GSO procedure on matrix $\mathbf{H_1^T}$ to find $\grave{\mathbf{H}}_\mathbf{1}$

3. The null space $\breve{\mathbf{H}}_\mathbf{1}$ can be obtained as

$$\breve{\mathbf{H}}_\mathbf{1} = \mathbf{I} - \left(\grave{\mathbf{H}}_\mathbf{1}^{\boldsymbol{H}} \grave{\mathbf{H}}_\mathbf{1}\right) \tag{4.11}$$

   where $\mathbf{I}$, $\grave{\mathbf{H}}_\mathbf{1}^{\boldsymbol{H}}$ are $\boldsymbol{q} \times \boldsymbol{q}$ identity matrix and the hermitian matrix of $\grave{\mathbf{H}}_\mathbf{1}$, respectively.

When the total number of users $\boldsymbol{K}$ is larger than the number of simultaneously supportable users, $\hat{\boldsymbol{K}}$, i.e., $\boldsymbol{K} > \hat{\boldsymbol{K}}$, we need to find the set of users $\boldsymbol{S} \subset \boldsymbol{\{1, 2, ..., K\}}$ that can maximize the total throughput of the system. The optimal subset of users can be obtained by exhaustively searching for all possible user combinations, i.e.,

$$\mid \boldsymbol{S} \mid = \boldsymbol{C}_{\boldsymbol{K}}^{\hat{\boldsymbol{K}}} \tag{4.12}$$

where $\boldsymbol{C}$ denotes the combination operation. The exhaustive search becomes prohibitive when the number of users is large, i.e.,

$$\boldsymbol{K} \gg \hat{\boldsymbol{K}} \tag{4.13}$$

Conceptually, it is necessary to find suboptimal user selection methods for realistic use with acceptable efficiency.

4.3 Proposed User Selection Algorithm

In this section, we propose a greedy user selection algorithm, where the product of the singular values of the effective channel matrices is considered as our selection metric. For low complexity, the singular values can be obtained efficiently using QR decomposition rather than SVD. In each iteration, the effective channels of selected

users are updated recursively using the $(n-1)$th previous effective channels to eliminate the interference induced by the new selected user.

4.3.1 Extracting the singular values using QR Decomposition

The singular values of a matrix can be computed using the conventional SVD method. The key weakness of SVD is that it is considered data dependent and hence, it requires expensive calculations to obtain the diagonal elements of the singular values. In contrast, QRD can be used efficiently to extract the product of the singular values instead of SVD and with lower complexity. Without loss of generality, assume matrix $\mathbf{A} \in \mathbb{C}^{p \times q}$ with $p < q$, then $\mathbf{A}$ can be written as

$$\mathbf{A}^{H} = \mathbf{Q} \begin{bmatrix} \mathbf{R_1} \\ \mathbf{0} \end{bmatrix} \tag{4.14}$$

where $\mathbf{Q} \in \mathbb{C}^{q \times q}$ has orthonormal column vectors, and $\mathbf{R_1} \in \mathbb{C}^{p \times p}$ is the upper triangular matrix. Note that in order to get the actual product of the singular values for matrix $\mathbf{A}$, we have used the hermitian matrix $\mathbf{A}^{H}$ instead of $\mathbf{A}$ in (4.14). Then, it is possible to obtain the product of the singular values, $\boldsymbol{\delta}$, as

$$\begin{aligned} \boldsymbol{\delta} &= \left| \prod_{i=1}^{p} r_{ii} \right| \\ &= \prod_{i=1}^{p} \sigma_i \end{aligned} \tag{4.15}$$

where r_{ii} are the entries of the diagonal of $\mathbf{R_1}$, and σ_i represent the singular values of matrix $\mathbf{A}$.

4.3.2 Proposed Algorithm

In this subsection we briefly summarize the proposed algorithm of user selection, where **Algorithm 2** outlines the main operations of the proposed algorithm. The sets of remaining and selected users are denoted by $\boldsymbol{\Psi}$ and $\boldsymbol{\Upsilon}$, respectively. Let $\mathbf{F}_{\boldsymbol{j}}^{(\boldsymbol{n})}$ denote the precoding matrix of the $\boldsymbol{j}$th selected user at the $\boldsymbol{n}$th iteration. $\mathbf{Z}$ denotes the orthonormal basis of the null space of the rows of previously selected users, which can be obtained by applying th Gram-Schmidt Orthogonalization (GCO) procedure on the null space of the rows of earlier selected channel matrices. Initially, the algorithm selects the first user that maximises the product of the singular values $\boldsymbol{\delta}(\mathbf{H}_{\boldsymbol{k}})$ for $\boldsymbol{k} \in \boldsymbol{\Psi}$, $\boldsymbol{k} = \boldsymbol{\{1, 2, ..., K\}}$. We set the initial precoding matrix of the first selected user to be the identity matrix and at the $\boldsymbol{n}$th iteration, the algorithm selects a new user as

$$\boldsymbol{u_n} = \underset{\boldsymbol{j}\in\boldsymbol{\Psi}}{\arg\max} \left(\underbrace{\boldsymbol{\delta}(\bar{\mathbf{H}}_{\boldsymbol{j}})}_{\boldsymbol{term1}} \underbrace{\prod_{\boldsymbol{k}\in\boldsymbol{\Upsilon}} \boldsymbol{\delta}(\bar{\mathbf{H}}_{\boldsymbol{k}})}_{\boldsymbol{term2}} \right) \tag{4.16}$$

where,

- $\boldsymbol{term1}$: constitutes the product of the singular values for the effective channel of the user currently under investigation. (step 8)
- $\boldsymbol{term2}$: constitutes the product of the singular values for the updated effective channels of all previously selected users. (step 11)

More specifically, when there is a new user under investigation, the algorithm takes into consideration the following. It calculates the precoding matrix of this investigated user and its effective channel (line 7 and line 8 in Algorithm 1, respectively). Next, the algorithm temporarily updates first the precoder matrix of each of the previously selected users so as to cancel the interference caused by the investigated user and then their effective channels (lines 9-12 in Algorithm 1). After that, according

to (4.16), a user that yields the maximum product of the singular values of effective channels is selected from set $\mathbf{\Psi}$ (line 13 in Algorithm 2). After a new user is selected, $\mathbf{Z}$ and $\mathbf{F}_{\boldsymbol{k}}^{(\boldsymbol{n})}$ must be updated accordingly. The selection process repeats until the required number of users $\hat{\boldsymbol{K}}$ is obtained.

- **The Physical Meaning of Matrix Z** in **Algorithm 2**:
  In Figure 4.2, we provide a simple example to describe the matrix $\mathbf{Z}$ in **Algorithm 2** which is an orthonormal basis of all rows vectors of previously selected users' channels. Assume we have four users' channel matrices $\mathbf{H_1} \in \mathbb{C}^{\boldsymbol{N_r} \times \boldsymbol{N_t}}$, $\mathbf{H_2} \in \mathbb{C}^{\boldsymbol{N_r} \times \boldsymbol{N_t}}$, $\mathbf{H_3} \in \mathbb{C}^{\boldsymbol{N_r} \times \boldsymbol{N_t}}$, and $\mathbf{H_4} \in \mathbb{C}^{\boldsymbol{N_r} \times \boldsymbol{N_t}}$, as shown in Figure 4.2. In Figure 4.2(a), user 1 has already been selected according to a specific performance metric; we apply GSO operation on $\mathbf{H_1}$ to obtain matrix $\mathbf{\Xi_1}$. Then, the orthonormal basis of the rows of previously selected channel matrices is given as

$$\mathbf{Z} = \mathbf{\Xi_1} \tag{4.17}$$

  The matrix which is perpendicular on $\mathbf{Z}$ can be obtained as

$$\mathbf{Z}_{\perp} = \mathbf{I}_{\boldsymbol{N_t}} - \mathbf{Z}^{\boldsymbol{H}}\, \mathbf{Z} \tag{4.18}$$

  where $\mathbf{I}_{\boldsymbol{N_t}}$ is $\boldsymbol{N_t} \times \boldsymbol{N_t}$ identity matrix. Next, we select user 3 as it has the largest projection on $\mathbf{Z}_{\perp}$ among other users, i.e., $\mathbf{H_2}$ and $\mathbf{H_4}$. We denote the projection of $\mathbf{H_3}$ onto $\mathbf{Z}_{\perp}$ as $\mathbf{L_1}$.
  We repeat the procedure by applying GSO operation on $\mathbf{L_1}$ to obtain $\mathbf{\Xi_2}$. Next, we update the orthonormal basis of all rows vectors of previously selected matrices as

$$\begin{aligned} \mathbf{Z} &= [\mathbf{Z}\ ;\ \mathbf{\Xi_2}] \\ &= [\mathbf{\Xi_1}\ ;\ \mathbf{\Xi_2}] \end{aligned} \tag{4.19}$$

  where the brackets $[;]$ denote matrix concatenation. The matrix $\mathbf{Z}_{\perp}$ can be

updated as

$$\mathbf{Z}_{\perp} = \mathbf{I}_{\boldsymbol{N_t}} - \mathbf{Z}^{\boldsymbol{H}}\ \mathbf{Z} \tag{4.20}$$

In Figure 4.2(b), we note that $\mathbf{Z}_{\perp}$ is now perpendicular onto both $\mathbf{H_1}$ and $\mathbf{H_3}$ since the dot product between $\mathbf{Z}_{\perp}$ and $\mathbf{H_1}$ or $\mathbf{H_3}$ is zero. The matrix $\mathbf{Z}_{\perp}$ is also known as the orthogonal basis of the intersection of null spaces of previously selected users' channel matrices. This procedure is repeated in order to update the matrices $\mathbf{Z}$ and $\mathbf{Z}_{\perp}$ after selecting new users.

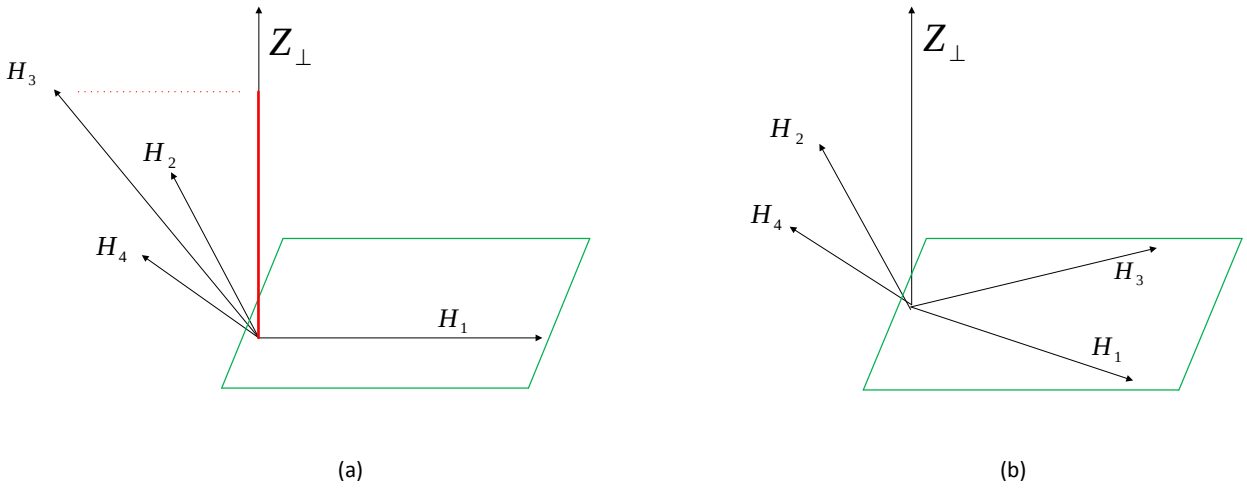

Figure 4.2: Intersection of null spaces of users' channel matrices (a) $\mathbf{H_1}$ is already selected (b) $\mathbf{H_3}$ has been selected and added to $\mathbf{H_1}$.

Algorithm 2 User selection using the product of the singular values.

1: $\boldsymbol{\Psi = \{1, 2, ..., K\}}$, $\boldsymbol{\Upsilon = \varnothing}$
2: Select the first user $\boldsymbol{u_1 = \arg\max_{k \in \Psi} \delta(\mathbf{H}_k)}$
3: Set the precoding matrix of $\boldsymbol{u_1}$: $\mathbf{F}_{u_1}^{(1)} = \mathbf{I}_{N_t}$
4: Let $\mathbf{Z}$ =null($\mathbf{H}_{u_1}$)
5: Update $\boldsymbol{\Psi = \Psi - u_1}$, $\boldsymbol{\Upsilon = \Upsilon + u_1}$, $\boldsymbol{n = 2}$
6: **for** $\boldsymbol{j \in \Psi}$ **do**
7: Set $\mathbf{F}_j = \mathbf{Z}$
8: Calculate the effective channel matrix $\bar{\mathbf{H}}_j^{(n)} = \mathbf{H}_j \mathbf{F}_j$
9: **for** $\boldsymbol{k \in \Upsilon}$ **do**
10: Find the precoder $\mathbf{F}_{temp,k}$
11: Update the effective channel matrices: $\bar{\mathbf{H}}_k^{(n)} = \mathbf{H}_k \mathbf{F}_{temp,k}$
12: **end for**
13: Select the new user as: $\boldsymbol{u_n = \arg\max_{j \in \Psi} \left(\delta(\bar{\mathbf{H}}_j^{(n)}) \prod_{k \in \Upsilon} \delta(\bar{\mathbf{H}}_k^{(n)}) \right)}$
14: Update the orthonormal basis of the null spaces matrices of all previously selected users $\mathbf{Z}$
15: **for** $\boldsymbol{k \in \Upsilon}$ **do**
16: Update $\mathbf{F}_k^{(n)}$
17: **end for**
18: Update:$\boldsymbol{\Psi = \Psi - u_n;\ \Upsilon = \Upsilon + u_n;\ n = n + 1}$
19: **end for**

Table 4.1: Comparison of the complexity order for different user selection algorithms.

Algorithm	Complexity order
c-algorithm [32]	$\mathcal{O}\left(K\hat{K}^2N_t^3\right)$
psrn-algorithm [31]	$\mathcal{O}\left(K\hat{K}N_t^3\right)$
pe-algorithm [35]	$\mathcal{O}\left(K\hat{K}N_t^3\right)$
v-algorithm [34]	$\mathcal{O}\left(\frac{K}{4}\hat{K}N_t^3\right)$
proposed algorithm	$\mathcal{O}\left(K\hat{K}N_t^3\right)$

4.3.3 Computational Complexity Analysis

In this subsection, we investigate the computational complexity of Algorithm 1 and compare it with that of various suboptimal user selection algorithms. This complexity is calculated by the number of flops as in [32] and a flop is defined as a real floating point operation. For example, real addition, multiplication, or division is calculated as one flop. For complex numbers, an addition and a multiplication operation involve two and six flops, respectively. Multiplication of the two matrices $\mathbf{A} \in \mathbb{C}^{p\times a}$ and $\mathbf{B} \in \mathbb{C}^{a\times q}$ requires $8paq$ flops. Moreover, the complexity of the QRD operation for a matrix $\mathbf{H} \in \mathbb{C}^{p\times q}$ is approximated by $4q^2(3p-q)$, as in [31].

Specifically, the proposed algorithm of user selection has the following complexity analysis:

- To select the first user, we need $4KN_r^2(3N_t - N_r)$ flops.
- To find the null space of the first user via GSO operation, we require $8N_r^2N_t - 2N_rN_t$ flops [35].
- For each $j \in \Psi$, $n \geq 2$, we need
  - $8N_rN_t(N_t-(n-1)N_r)$ flops for $\bar{\mathbf{H}}_j^{(n)}$;
  - $16N_rN_t(N_t-(n-2)N_r)+4N_r^2(3N_t-(n-1)N_r)$ flops for $\mathbf{F}_{temp}$;
  - $8N_r(N_t-(n-1)N_r)(N_t-(n-2)N_r)$ flops for $\bar{\mathbf{H}}_k^{(n)}$;

- To select a new user, we need $4nN_r^2(3(N_t-(n-1)N_r)-N_r)$ flops.
- To update the null space $\boldsymbol{Z}$, we need $16N_rN_t(N_t-(n-2)N_r)+4N_r^2(3N_t-(n-1)N_r)$ flops.
- Finally, for each $k \in \Upsilon$, we need $16N_rN_t(N_t-(n-2)N_r)+4N_r^2(3N_t-(n-1)N_r)$ flops to update the precoder $\boldsymbol{F}_k^{(n)}$.

The total number of flops, ψ, of the proposed algorithm becomes

$$\begin{aligned}
\psi \quad & \approx 4KN_r^2(3N_t-N_r)+8N_r^2N_t-2N_rN_t+ \\
& \sum_{n=2}^{\hat{K}} \times\{8N_rN_t(N_t-(n-1)N_r) \\
& +(n-1)[16N_rN_t(N_t-(n-2)N_r) \\
& +4N_r^2(3N_t-(n-1)N_r) \\
& +8N_r(N_t-(n-1)N_r)(N_t-(n-2)N_r)] \\
& +4nN_r^2(3(N_t-(n-1)N_r)-N_r)\} \\
& +16N_rN_t(N_t-(n-2)N_r) \\
& +4N_r^2(3N_t-(n-1)N_r) \\
& +(n-1)[16N_rN_t(N_t-(n-2)N_r) \\
& +4N_r^2(3N_t-(n-1)N_r)] \\
& \approx \mathcal{O}\left(K\hat{K}N_t^3\right)
\end{aligned} \tag{4.21}$$

Note that to simplify the above equation, we have assumed $\hat{K}N_r \approx N_t$. A comparison of the complexity order for different user selection algorithms is listed in Table 4.1. Evidently, the proposed algorithm has a complexity order less than the c-algorithm and the same as the psrn-algorithm and pe-algorithm, while the v-algorithm has the lowest complexity order.

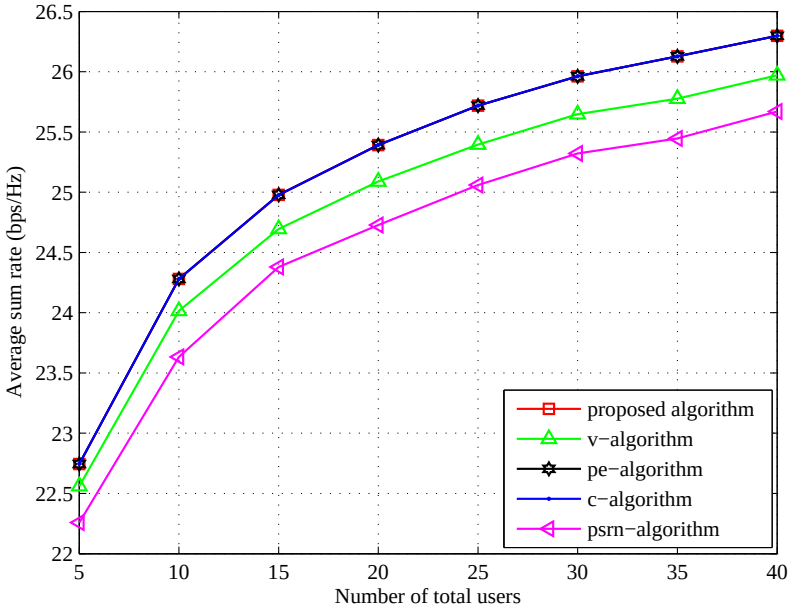

(a)

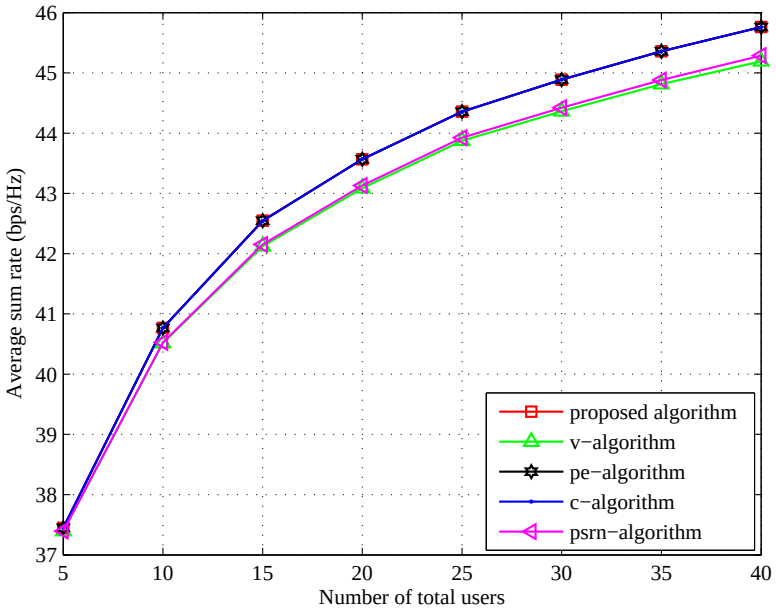

(b)

Figure 4.3: Average sum rate of different user selection algorithms when SNR=20 dB, $\boldsymbol{\rho = 0}$. (a) $\boldsymbol{N_t = 4, N_r = 2,}$ (b) $\boldsymbol{N_t = 8, N_r = 2}$.

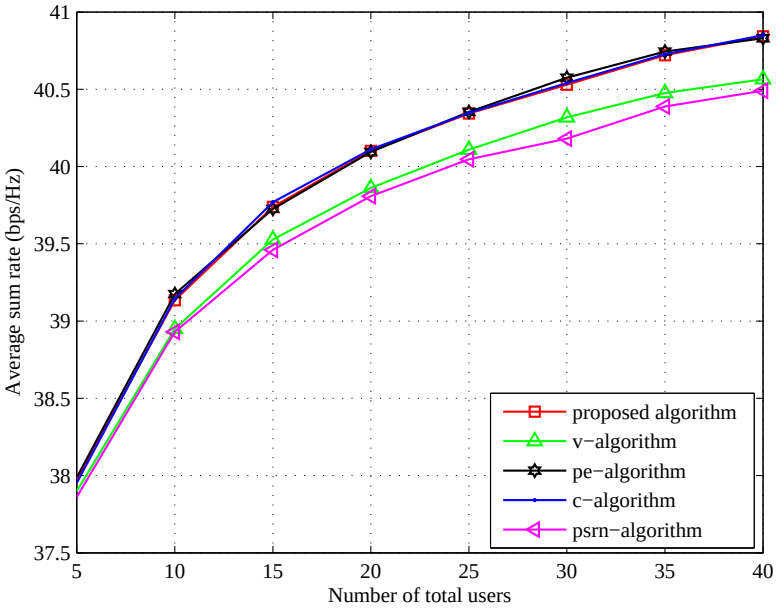

(a)

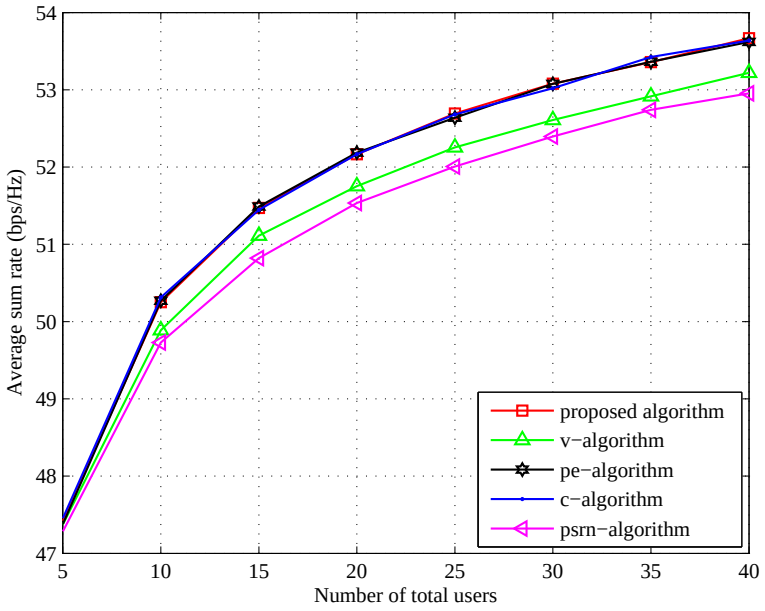

(b)

Figure 4.4: Average sum rate of different user selection algorithms when SNR=20 dB, $\boldsymbol{\rho = 0}$. (a) $\boldsymbol{N_t = 8, N_r = 3,}$ (b) $\boldsymbol{N_t = 10, N_r = 3}$.

4.4 Simulation Results

To evaluate the performance of the proposed user selection algorithm, we compare it with the following algorithms:

- Capacity-based algorithm (c-algorithm) [32];
- Product of the squared row norms of the effective channel matrices-based algorithm (psrn-algorithm) [31];
- Volume-based algorithm (v-algorithm) [34];
- Product of the eigenvalues of effective channel matrices from the angle between subspaces (pe-algorithm) [35];

The numerical results have been averaged over 5,000 independent quasi-static fading channel realizations. Further, the simulation assumed both uncorrelated and correlated channels.

In Figure 4.3 the average sum rate of different user selection algorithms is plotted against the number of total users $\boldsymbol{K}$ for $\boldsymbol{\rho} = \mathbf{0}$ (uncorrelated channels), and SNR =20 dB. It can be seen that for two different antenna scenarios, the proposed algorithm outperforms the v-algorithm and the psrn-algorithm and has the same result as the c-algorithm and pe-algorithm. More specifically, the c-algorithm achieves high performance over other suboptimal user selection algorithms, because its selection metric corresponds directly to the sum rate capacity of the BD channel. Similarly, at high SNR, the throughput of an individual user is an increasing function of the product of the eigenvalues of the effective channels [32]. Hence, taking in consideration the relation between SVD and the eigendecomposition, the proposed selection metric can achieve almost similar performance to the c-algorithm under a high SNR regime. Also, we observe that the psrn-algorithm achieves better performance in Figure 4.3(b), which is because the number of effective transmit antennas has increased

that lead to increase the product of squared row norms of the effective channels [31].

In Figure 4.4, the previous procedure of Figure 4.3 has been repeated except that we increased the number of receive antennas of each user, i.e., $\boldsymbol{N_r = 3}$. We note that the proposed algorithm maintains the previous performance with respect to c-algorithm and pe-algorithm. As seen in both Figures 4.4(a) and 4.4(b) that average sum rate has increased with respect to Figure 4.3, which is due the increase in the number of receive antennas of each user.

In Fig 4.5, we validate the performance results of different user selection algorithms under a highly correlated MIMO channel ($\boldsymbol{\rho = 0.95}$) and at high SNR. We model the MIMO channel matrix according to the Kronecker model as [92]-[95]

$$\boldsymbol{H_k = \Omega_{k,r}^{\frac{1}{2}} H_{k,iid} \Omega_{k,t}^{\frac{1}{2}}} \tag{4.22}$$

where $\boldsymbol{H_{k,iid}}$ is an independent and identically distributed complex Gaussian distribution with zero mean and unit variance and $\boldsymbol{\Omega_{k,t}^{\frac{1}{2}}}$ denotes $\boldsymbol{N_t \times N_t}$ transmit covariance matrix, i.e., [38]

$$\boldsymbol{\Omega_{k,t} = \Omega_{k,t}^{\frac{1}{2}} \Omega_{k,t}^{\frac{H}{2}}} \tag{4.23}$$

The correlation matrix for the receive antennas is denoted by $\boldsymbol{\Omega_{k,r}^{\frac{1}{2}}}$ and here is assumed as the identity matrix (i.e., the receive antennas elements are uncorrelated) [39]. Under this assumption, the MIMO channel has a transmit correlation only and the above model can be written as

$$\boldsymbol{H_k = H_{k,iid} \Omega_{k,t}^{\frac{1}{2}}} \tag{4.24}$$

Simulation results are generated using the exponential correlation model which is given as [96]

$$\boldsymbol{[\Omega_{k,t}]_{i,j} = \rho_k^{|i-j|}} \tag{4.25}$$

where $\boldsymbol{[\ ]_{i,j}}$ is the entry of matrix $\boldsymbol{\Omega_{k,t}}$ with index $\boldsymbol{(i,j)}$, and $\boldsymbol{\rho_k}$ is the correlation coefficient for user $\boldsymbol{k}$ defined as

$$\boldsymbol{\rho_k = \rho e^{j\phi_k}} \tag{4.26}$$

where $\boldsymbol{\phi_k}$ is i.i.d. and uniformly distributed over $\mathbf{[0, 2\pi]}$ [40] [41]. Clearly, the results shown in Fig 4.5 indicate that the proposed algorithm outperforms the v-algorithm and the psrn-algorithm, with almost similar performance to the c-algorithm and the pe-algorithm. In addition, we notice that the proposed algorithm is less affected by channel correlation than the psrn-algorithm and the volume-algorithm for the same number of transmit antennas, which is expected since the proposed performance metric corresponds directly to the data rate of BD in high SNR scenario. However, as the channel correlation increases, the instantaneous channels of the users tend to be more dependent (i.e., quasi-identical) and, as a result, the sum rate is reduced due to loss in the spatial degrees of freedom. [42]–[44].

Figure 4.6 plots a comparison of the elapsed CPU time of various user selection algorithms versus the number of total users for $\boldsymbol{\rho = 0}$ (uncorrelated channels), and SNR =20 dB. These results are attained by 3.4 GHz Core i7 CPU PC. In the first scenario[Fig. 4.6(a)], where the maximum number of users that can be supported by BS is two, the simulation time results show that the proposed algorithm needs less run time than that of the pe-algorithm. In contrast, Fig. 4.6(b) presents the run time comparison when $\boldsymbol{N_t = 8, N_r = 2}$. In this scenario, we observe that the running time of the proposed algorithm starts to be greater than that of the pe-algorithm when the number of total users exceeds a particular limit (in this case $\boldsymbol{K = 15}$). In either way the proposed algorithm has less run time than the c-algorithmn, while the volume-based has the shortest run time. This difference in running time comes although the proposed algorithm has the same complexity order with some other algorithms. This is because the complexity order is usually derived using approximate calculations, as shown in section 4.3.3. In summary, the proposed algorithm gives the same performance as the c-algorithm and pe-algorithm in high SNR as seen in Fig 4.3 and 4.5. In terms of complexity, the proposed algorithm has a shorter run time than the c-algorithm and pe-algorithm when the maximum number of simultaneously supportable users, $\hat{\boldsymbol{K}}$, is two, but it becomes more dependant on the total number of users, $\boldsymbol{K}$, to whom data is transmitted by BS as seen in Fig. 4.6.

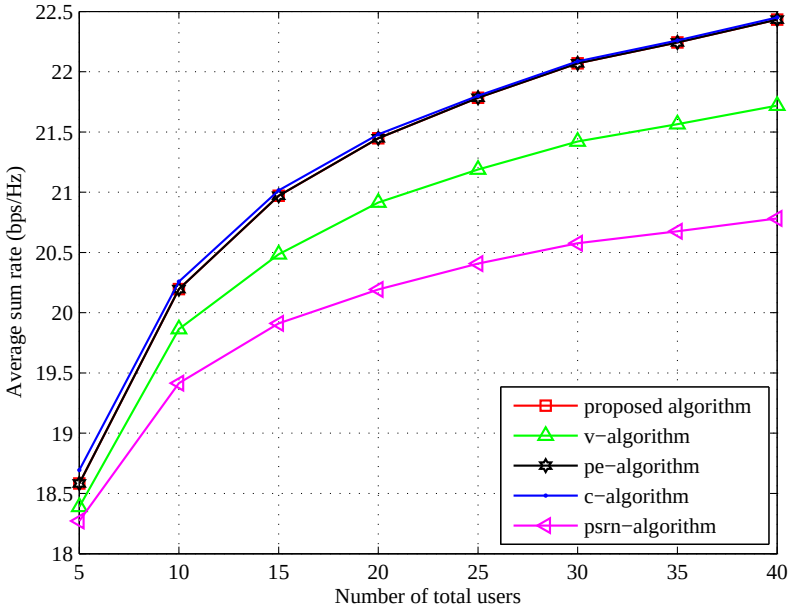

(a)

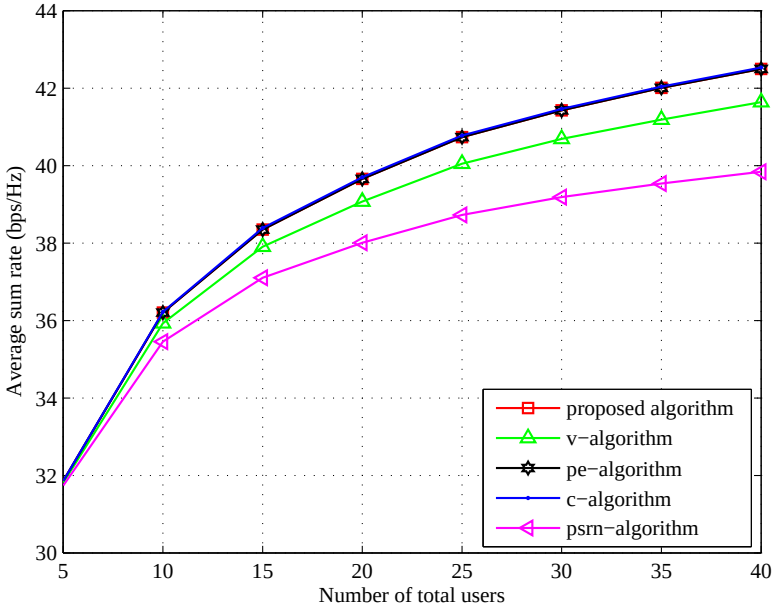

(b)

Figure 4.5: Average sum rate of different user selection algorithms when SNR=20 dB, $\boldsymbol{\rho = 0.95}$. (a) $\boldsymbol{N_t = 4, N_r = 2,}$ (b) $\boldsymbol{N_t = 8, N_r = 2}$.

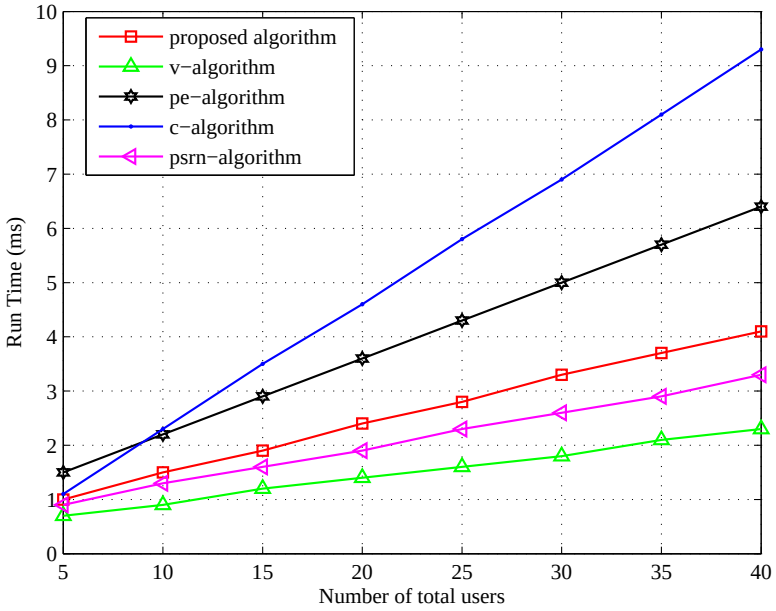

(a)

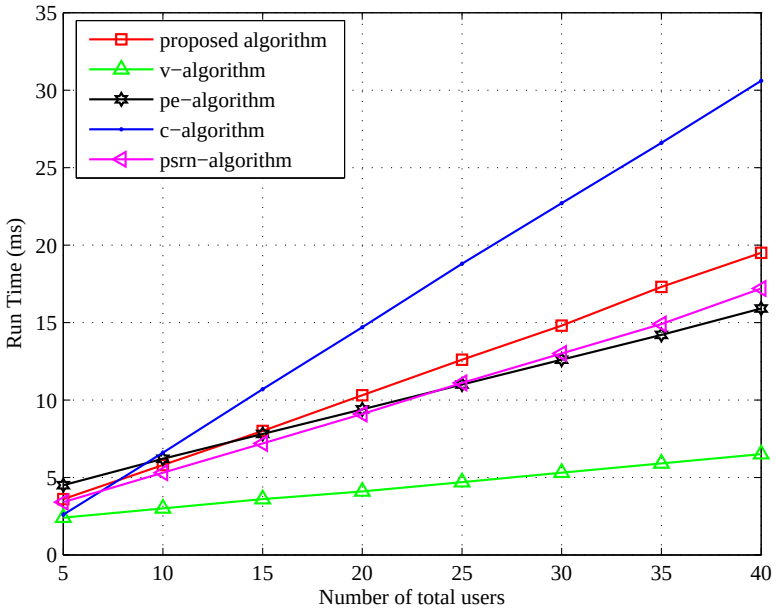

(b)

Figure 4.6: Run time of different user selection algorithms when SNR=20 dB, $\boldsymbol{\rho = 0}$. (a) $\boldsymbol{N_t = 4, N_r = 2}$ (b) $\boldsymbol{N_t = 8, N_r = 2}$.

4.5 Summary

In this chapter, we have studied user selection technology for multiuser MIMO systems. In the case that channel information is available at the transmitter side, it is possible to precancel interuser interference before applying user selection technique. In this correspondence, we designed the precoders of the proposed algorithm depending on the procedure of Gram-Schmidt Orthogonalization, by which IUI can be completely removed.

As seen in the chapter, user selection algorithms may vary in their performance and complexity according to the selection metric they adopt. Under high SNR regime, we have proposed a suboptimal user selection algorithm which utilizes the product of the singular values of users' effective channel as a performance metric. The singular values can be obtained using the QR decomposition operation. Simulation results have been taken over correlated and uncorrelated channels. The results show that the proposed algorithm achieve the same throughput performance of the c-algorithm with lower complexity.

Chapter 5

Proportional Fairness Scheduling For Multiuser MIMO Downlink Systems

In this chapter, we propose a proportional fairness (PF) scheduling algorithm for multiuser MIMO (MU-MIMO) downlink system. Two selection metrics have been proposed to achieve the scheduling process. Both metrics are designed using the upper triangular matrix obtained by applying the QRD on the users' effective channel matrices. The first proposed selection metric adopts the maximum entry of the upper triangular matrix in order to achieve the selection process. On the other hand, the second metric uses the ratio between the maximum and minimum entries of the upper triangular matrix multiplied by the product of singular values of users' effective channels in order to achieve the PF scheduling. Simulation results have been compared to the results achieved by the algorithm proposed by [35] and they show considerable degree of fairness.

5.1 Introduction

With the availability of full CSI at the transmitter, increasing the number of simultaneous users, which have independent faded paths with base station, will increase the probability to find one user with good channel condition at any time. By allocating most of the shared channel resource to that user, the total throughput of the system is significantly maximized [59] [68]-[72]. Hence, increasing the system throughput is considered the main objective behind *multiuser diversity* technique.

The technique of multiuser diversity can be applied in a real system after taking into account two matters: fairness and delay [68]. In the case of similar fading statistics of users (ideal situation), communicating with the user whose channel condition is the best will maximize the total throughput of the system as well as the individual throughput of users. In real applications, users' statistics can not be symmetric; some users can be closer to BS which will enhance their average SNR and make it better; there are some other users are stationary and others are moving; other users may move in a scattering medium and others have no scatterers surrounding them. Moreover, the multiuser strategy concerns only with the long term average throughput; In reality the latency requirements are an important issue to be considered in practice. In other words, the average throughput taken over the delay time scale is considered the metric of interest to evaluate the system performance. In this chapter, we aim to handle these two issues in order to significantly exploit the multiuser diversity gain in multiuser MIMO downlink system with independent and fluctuating channel conditions.

5.2 Proportional Fairness Scheduling

The two constraints, fairness and delay, mentioned above can be meet by the use of *proportional fairness* (PF) scheduler which allows, in the same time, to utilize muliuser diversity. Based on the requested rates of users sent to the base station at

each time slot, the scheduler selects a set of users to transmit information to. In the same time, the scheduler repeatedly updates the average throughput $\bar{R}_k(t)$ of each user over a window of length t_c. Let $R_k(t)$ denotes the requested (instantaneous) rate of user k at time slot t, where $k = 1, ..., K$. Hence, the base station receives the instantaneous rates from all active users in the system. As a result, the scheduling algorithm decides to transmit to user $k^\star$ who has the largest [59]

$$\frac{R_k(t)}{\bar{R}_k(t)} \tag{5.1}$$

among all simultaneous users supported by the base station. The average throughput $\bar{R}_k(t)$ of each user can be repeatedly updated by using an exponentially weighted low pass filter as follows [68]

$$\bar{R}_k(t+1) = \begin{cases} \left(1 - \frac{1}{t_c}\right) \bar{R}_k(t) + \frac{1}{t_c} R_k(t), & k = k^\star \\ \\ \left(1 - \frac{1}{t_c}\right) \bar{R}_k(t), & k \neq k^\star \end{cases} \tag{5.2}$$

Figures 5.1 and 5.2 are simple example about how this algorithm works. For two users, the instantaneous data rates are plotted as a function of time slots, where each sample path is taken over 240 time slots. In Figure 5.1, the two users experience identical channel fading statistics. As a result, the average throughput $\bar{R}_k(t)$ of each user will converge to similar values [59]. Consequently, the scheduling process is reduced to always selecting the user whose requested rate is the highest among other users. In other words, the algorithm picks the user with good channel conditions and at the same time leads to fairness in scheduling process in the long-term.

In Figure 5.2, the channel of one of the users (the blue one) is stronger than the other (the red one) on average, although both users are fluctuating due to multipath fading. This perhaps caused by the difference in users' distances from the base station, i.e., the user in blue colour is closer to the base station than of the red colour. Hence, selecting the user which has the highest instantaneous rate means allocating

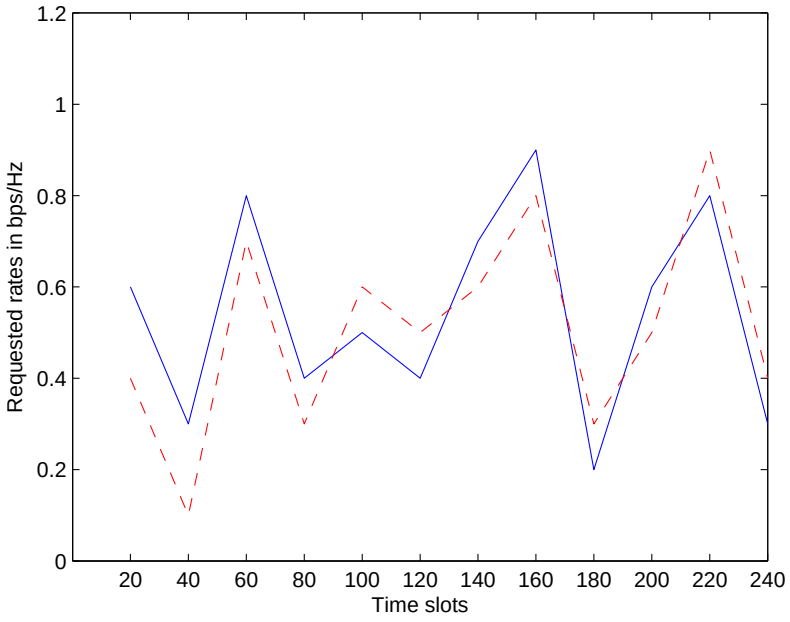

Figure 5.1: The two users have symmetric channel statistics. The scheduler reduces to picking the user with the largest instantaneous rate. (Extracted from [59])

the whole system resources to the user with statistically stronger channel condition and causes significant unfairness. On the contrary, adopting the previously described scheduling algorithm will bring fairness among all users because the system resources are allocated depending on requested rates of the users normalized by their average throughput. More specifically, the average throughput $\bar{R}_k(t)$ of the kth user with statistically poor channel conditions in previous time slots is low; then this user will have better chance to be scheduled in the next time slots. Hence, the scheduling algorithm picks a user when the quality of its channel is high with respect to its average channel condition through a specific time-scale, i.e., t_c.

The parameter t_c corresponds to the latency time-scale. In the case of large latency time-scale, then the average throughput is taken over a longer time-scale and the scheduler can give more tolerance in time and wait longer before a user being scheduled when the peak of its channel is high.

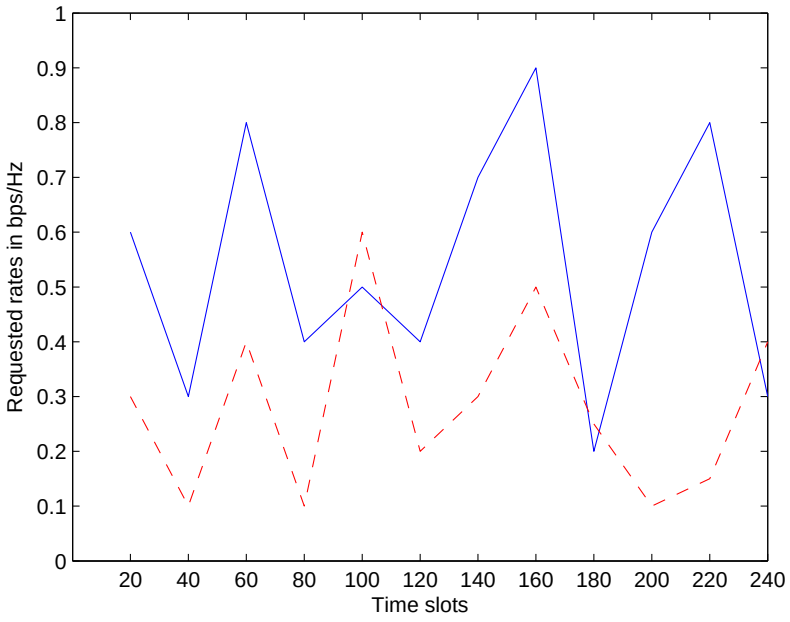

Figure 5.2: The two users have asymmetric channel statistics. In this case, the scheduler picks a user when its channel reaches high peak. (Extracted from [59])

5.3 User Selection and Multiuser Diversity

In multiuser MIMO downlink system and when the number of total simultaneous users $\boldsymbol{K}$ is very large, the base station can select a set of users with good channel quality to communicate with in order to improve overall system throughput [82]. That means the multiuser diversity has been exploited to improve the whole throughput of the system through user selection technique [84] [87]-[91].

Many suboptimal user selection algorithms have been proposed which adopts various selection metrics such as matrix determinant, Frobenius norm, chordal-distance, and etc. Although these algorithms are designed to reduce the computation burden of selection process, degradation in performance is inevitable. Moreover, these low complexity user selection algorithms cannot be applied to provide proportional fairness because the performance metrics they adopt are not directly related to data rate [85]. The product of eigenvalues of effective channels matrices calculated by using

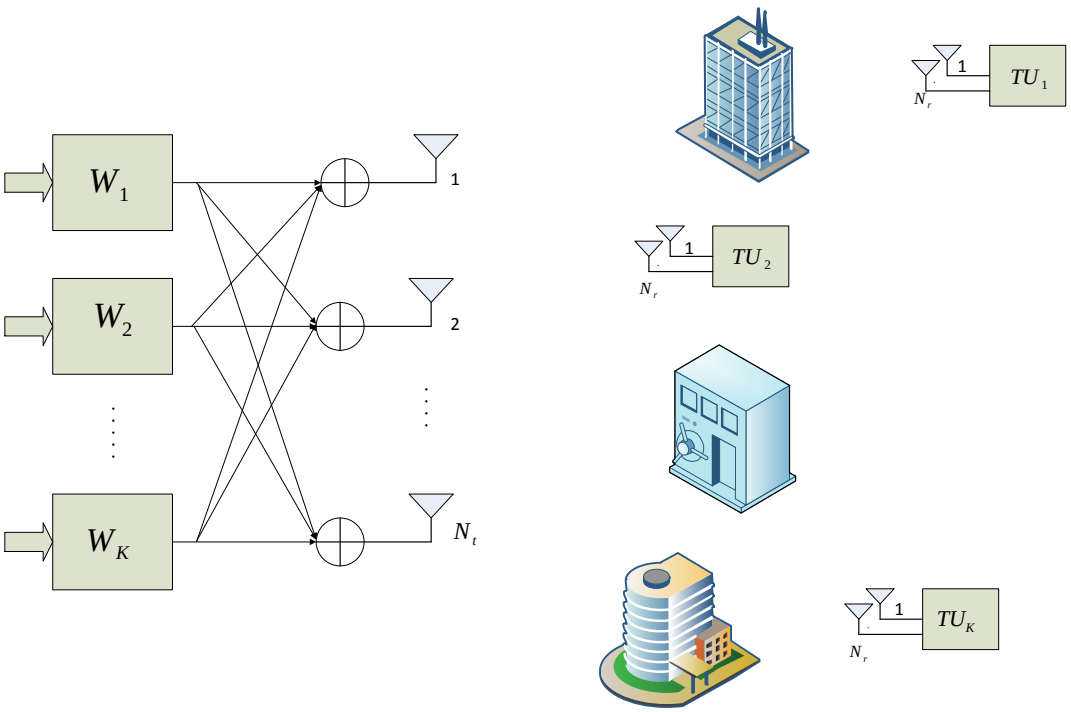

Figure 5.3: The base station transmits to a total of $\boldsymbol{K}$ simultaneous users and the channel quality of these users are different. This may happen for many reasons such as the difference in distance from BS, availability of rich scatters environment, moving or not, and etc.

angle between subspaces is proposed by [35] as a selection metric. The proposed algorithm can achieve the same performance as that of the capacity-based algorithm and with lower complexity, as shown in chapter four. In addition, the algorithm can be modified to achieve PF scheduling through number of steps. In [31], the authors have proposed the product of squared row norms of the effective channels matrices as a user selection metric. The scheduling algorithm can provide a trade off between complexity and performance, and can be modified to achieve PF scheduling.

5.4 System Model

5.4.1 Multiuser MIMO System

Let us consider a multiuser MIMO downlink system which has a single base station equipped with $\boldsymbol{N_t}$ transmit antennas . The base station communicates with $\boldsymbol{K}$ mobile users simultaneously, and each $\boldsymbol{k}$th user is equipped with $\boldsymbol{N_{r,k}}$ receive antennas, $\boldsymbol{k = 1, 2, ..., K}$, as shown in Figure 5.3.

The sub-channels of the system are assumed to be independent and identically distributed (i.i.d) flat fading channels. Hence, the channel propagation from BS to the $\boldsymbol{k}$th user is given as

$$\mathbf{H}_{\boldsymbol{k}} \in \mathbb{C}^{\boldsymbol{N_{r,k}} \times \boldsymbol{N_t}} \tag{5.3}$$

where perfect channel state information (CSI) at the receiver and transmitter is assumed. Each user's channel $\mathbf{H}_{\boldsymbol{k}}$ is assumed to be independent of other users' channels and has full rank, i.e.,

$$\text{rank}(\mathbf{H}_{\boldsymbol{k}}) = \min(\boldsymbol{N_{r,k}}, \boldsymbol{N_t}) \tag{5.4}$$

Then, the overall system channel is given as

$$\mathbf{H} = [\mathbf{H}_{\mathbf{1}}^{\boldsymbol{H}} \mathbf{H}_{\mathbf{2}}^{\boldsymbol{H}} ... \mathbf{H}_{\boldsymbol{K}}^{\boldsymbol{H}}]^{\boldsymbol{H}} \tag{5.5}$$

which ascertains a full rank matrix.

Let $\boldsymbol{S} \subset \boldsymbol{\{1, 2, ..., K\}}$ denotes a set of users which can be served simultaneously by the BS. For the $\boldsymbol{k}$th user, a symbol vector $\mathbf{x}_{\boldsymbol{k}} \in \mathbb{C}^{\boldsymbol{N_{r,k}} \times \mathbf{1}}$ is transmitted with an input covariance matrix given as

$$\boldsymbol{Q_k} = \mathbb{E}\{\boldsymbol{x_k x_k^H}\} \tag{5.6}$$

and a total transmit power as

$$\boldsymbol{P} = \sum_{\boldsymbol{k=1}}^{\boldsymbol{K}} \text{trace}(\boldsymbol{Q_k}) \tag{5.7}$$

where $\boldsymbol{P}$ denotes the total transmit power in the system. Then, the transmitted signal to user $\boldsymbol{k}$ is multiplied by a precoding matrix $\mathbf{W}_{\boldsymbol{k}} \in \mathbb{C}^{\boldsymbol{N_t} \times \boldsymbol{N_{r,k}}}$ before being transmitted. Thus, the $\boldsymbol{k}$th user receives [36]:

$$\mathbf{y}_{\boldsymbol{k}} = \mathbf{H}_{\boldsymbol{k}}\mathbf{W}_{\boldsymbol{k}}\mathbf{x}_{\boldsymbol{k}} + \sum_{\boldsymbol{j=1, j\neq k}}^{\boldsymbol{|S|}} \mathbf{H}_{\boldsymbol{k}}\mathbf{W}_{\boldsymbol{j}}\mathbf{x}_{\boldsymbol{j}} + \mathbf{n}_{\boldsymbol{k}} \tag{5.8}$$

where $\boldsymbol{n_k} \in \mathbb{C}^{\boldsymbol{N_r} \times \boldsymbol{1}}$ denotes the Additive White Gaussian Noise (AWGN) with $\boldsymbol{(0, \sigma^2)}$.

5.4.2 Gram-Schmidt Orthogonalization

Block diagonalization serves to cancel the IUI of a MU-MIMO channel and decompose it into parallel SU-MIMO channels. For user $\boldsymbol{k}$, the precoder matrix has to satisfy the condition

$$\mathbf{H}_{\boldsymbol{j}}\mathbf{W}_{\boldsymbol{k}} = \mathbf{0}, \quad \forall \boldsymbol{j \neq k} \tag{5.9}$$

The matrix $\mathbf{W}_{\boldsymbol{k}}$ must be a unitary matrix so as to satisfy the total transmitted power, i.e.,

$$\mathbf{W}_{\boldsymbol{k}} \in \mathbb{U}\left(\boldsymbol{N_t}, \boldsymbol{N_r}\right) \tag{5.10}$$

Moreover, $\mathbf{W}_{\boldsymbol{k}}$ can be broken down into two matrices $\mathbf{F}$ and $\mathbf{\Lambda}$. Hence, the matrix $\mathbf{W}_{\boldsymbol{k}}$ can be written as

$$\mathbf{W}_{\boldsymbol{k}} = \mathbf{F}_{\boldsymbol{k}}\mathbf{\Lambda}_{\boldsymbol{k}} \tag{5.11}$$

where $\mathbf{F}_{\boldsymbol{k}}$ is designed to nullify the IUI and $\mathbf{\Lambda}_{\boldsymbol{k}}$ in order to optimize the data rate [37]. Therefore, $\mathbf{F}_{\boldsymbol{k}}$ is designed to lie in the intersection of all other users' nullspaces

except user $\boldsymbol{k}$, i.e., $\boldsymbol{\mathcal{N}(\tilde{\mathbf{H}}_k)}$, where

$$\tilde{\mathbf{H}}_{\boldsymbol{k}} = \left[\mathbf{H}_{\mathbf{1}}^{\boldsymbol{H}}, ..., \mathbf{H}_{\boldsymbol{k-1}}^{\boldsymbol{H}}, \mathbf{H}_{\boldsymbol{k+1}}^{\boldsymbol{H}}, ..., \mathbf{H}_{\boldsymbol{|S|}}^{\boldsymbol{H}}\right]^{\boldsymbol{H}} \tag{5.12}$$

To ensure nullity of $\tilde{\mathbf{H}}_{\boldsymbol{k}}$, the number of transmit antennas must be larger than the total number of receive antennas of users that are simultaneously communicating with BS, that is

$$\boldsymbol{N_t} > \sum_{\boldsymbol{k=1}}^{\boldsymbol{|S|}} \boldsymbol{N_{r,k}} \tag{5.13}$$

where $\boldsymbol{N_{r,k}}$ denotes the number of receive antennas of user $\boldsymbol{k}$.

In order to obtain the null space of the channel matrix, we utilize the method used by [32] which depends on Gram Schmidt Orthogonalization (GSO) procedure. To clarify the method, assume $\mathbf{H_1} \in \mathbb{C}^{\boldsymbol{p \times q}}$ with $\boldsymbol{p < q}$. Then, the null space $\breve{\mathbf{H}}_{\mathbf{1}} \in \mathbb{C}^{\boldsymbol{q \times q}}$ of matrix $\mathbf{H_1}$ can be obtained as follows

1. Find the transpose of matrix $\mathbf{H_1}$, i.e., $\mathbf{H}_{\mathbf{1}}^{\boldsymbol{T}} = \text{transpose}(\mathbf{H_1})$
2. Apply GSO procedure on matrix $\mathbf{H}_{\mathbf{1}}^{\boldsymbol{T}}$ to find $\grave{\mathbf{H}}_{\mathbf{1}}$
3. The null space $\breve{\mathbf{H}}_{\mathbf{1}}$ can be obtained as

$$\breve{\mathbf{H}}_{\mathbf{1}} = \mathbf{I} - \left(\grave{\mathbf{H}}_{\mathbf{1}}^{\boldsymbol{H}}\ \grave{\mathbf{H}}_{\mathbf{1}}\right) \tag{5.14}$$

   where $\mathbf{I}$, $\grave{\mathbf{H}}_{\mathbf{1}}^{\boldsymbol{H}}$ are $\boldsymbol{q \times q}$ identity matrix and the hermitian matrix of $\grave{\mathbf{H}}_{\mathbf{1}}$, respectively.

When the total number of users $\boldsymbol{K}$ is larger than the number of simultaneously supportable users, $\hat{\boldsymbol{K}}$, i.e., $\boldsymbol{K > \hat{K}}$, we need to find the set of users $\boldsymbol{S \subset \{1, 2, ..., K\}}$ that can maximize the total throughput of the system. The optimal subset of users can be obtained by exhaustively searching for all possible user combinations, i.e.,

$$\boldsymbol{\mid S \mid = C_K^{\hat{K}}} \tag{5.15}$$

where $\boldsymbol{C}$ denotes the combination operation.

5.5 Proposed PF Scheduling Algorithm

In this section, we propose a PF scheduler depending on the user selection algorithm proposed in chapter four. The product of singular values can be obtained using QR decomposition (QRD) and, then, utilized to design the selection metric of the proposed user selection algorithm as seen in chapter four. Further, the decomposition process has been used to design the performance metric of the proposed PF scheduler with tradeoff between complexity and performance as shown next.

5.5.1 Extracting the singular values using QR Decomposition

QR Decomposition (QRD) can be used efficiently to extract the product of the singular values for a particular matrix. Without loss of generality, assume matrix $\mathbf{A} \in \mathbb{C}^{\boldsymbol{p}\times\boldsymbol{q}}$ with $\boldsymbol{p} < \boldsymbol{q}$, then $\mathbf{A}$ can be written as

$$\mathbf{A}^{\boldsymbol{H}} = \mathbf{Q}\begin{bmatrix}\mathbf{R_1}\\ \mathbf{0}\end{bmatrix} \tag{5.16}$$

where $\mathbf{Q} \in \mathbb{C}^{\boldsymbol{q}\times\boldsymbol{q}}$ has orthonormal column vectors, and $\mathbf{R_1} \in \mathbb{C}^{\boldsymbol{p}\times\boldsymbol{p}}$ is the upper triangular matrix. Note that in order to get the actual product of the singular values for matrix $\mathbf{A}$, we have used the hermitian matrix $\mathbf{A}^{\boldsymbol{H}}$ instead of $\mathbf{A}$ in (4.14). Then, it is possible to obtain the product of the singular values, $\boldsymbol{\delta}$, as

$$\begin{aligned}\boldsymbol{\delta} &= \left|\prod_{\boldsymbol{i}=\boldsymbol{1}}^{\boldsymbol{p}} \boldsymbol{r_{ii}}\right| \\ &= \prod_{\boldsymbol{i}=\boldsymbol{1}}^{\boldsymbol{p}} \boldsymbol{\sigma_i}\end{aligned} \tag{5.17}$$

where r_{ii} are the entries of the diagonal of $\mathbf{R_1}$, and σ_i represent the singular values of matrix $\mathbf{A}$. Then, we can define the following two quantities

$$r_{max} = \max_{R_1} r_{ii} \ , \quad i = 1, ..., p \tag{5.18}$$

$$r_{min} = \min_{R_1} r_{ii} \ , \quad i = 1, ..., p \tag{5.19}$$

where r_{max}, r_{min} denote the maximum and minimum diagonal entries of matrix $\mathbf{R_1}$, respectively. These two quantities have been efficiently utilized to design the selection metric of the proposed PF scheduler.

5.5.2 Proposed Algorithm

In cellular network, users experience different channel conditions due to variation in distance between them and base station. Moreover, some users may move in a scattering medium and others have no scatterers surrounding them. Fair scheduling tries to ensure fairness in throughput among users. In this section, we adapt the proposed algorithm of user selection to tackle this problem. The optimal proportional fairness (PF) of scheduling can be expressed [85] [118]

$$\Re_{PF} = \max_{S \subset \{1,2,...,K\}} \sum_{k \in S} \frac{R_k(t)}{\bar{R}_k(t)} \tag{5.20}$$

with constraint

$$|S| \leq \hat{K} \tag{5.21}$$

where K, $\hat{K}$ are the number of total users in the system and the number of selected users, respectively. The set S contains the indexes of selected users. Under high SNR regime, the scenario of equal power allocation can be considered nearly optimal [86].

Let $\boldsymbol{\Psi}$,$\boldsymbol{\Upsilon}$ denote the sets of unselected and selected users, then

$$\boldsymbol{R_k^{(j)} \approx \sum_{i=1}^{N_r} \log_2 \left(1 + \frac{P}{jN_r} \lambda_{k,i}^{(j)}\right)} \tag{5.22}$$

where $\boldsymbol{R_k^{(j)}}$ denotes the instantaneous data rate of user $\boldsymbol{k}$ at the $\boldsymbol{j}$th iteration. Here, we have assumed that each user is equipped with equal number of receive antennas, i.e.,

$$\boldsymbol{N_r = N_{r,k}} \tag{5.23}$$

For each $\boldsymbol{k \in \Upsilon}$, $\boldsymbol{\lambda_{k,i}^{(j)}}$ denotes the $\boldsymbol{i}$th eigenvalue of the effective channel matrix of that user at the $\boldsymbol{j}$th iteration. The average throughput of user $\boldsymbol{k}$ can be repeatedly updated as

$$\boldsymbol{\bar{R}_k(t+1) = \begin{cases} \left(1 - \frac{1}{t_c}\right) \bar{R}_k(t) + \frac{1}{t_c} R_k(t), & k \in \Upsilon \\ \left(1 - \frac{1}{t_c}\right) \bar{R}_k(t), & k \notin \Upsilon \end{cases}} \tag{5.24}$$

1. **First selection metric**: we use Equation 5.18 to design the first selection metric of the proposed PF scheduling algorithm. It has been noted that for a set of users $\boldsymbol{\Psi}$, the value of $\boldsymbol{r_{max,k}}$ for each $\boldsymbol{k \in \Psi}$ can be utilized to provide general comparison among users regarding to their instantaneous data rate. More specifically, by substituting Equation 5.18 in Equation 5.22 we obtain

$$\boldsymbol{R_{comp1,k}^{(j)} = \log_2 \left(1 + \frac{P}{jN_r}\, r_{max,k}^{(j)}\right)} \tag{5.25}$$

   where $\boldsymbol{R_{comp1,k}^{(j)}}$ is a general indication about the instantaneous rate of user $\boldsymbol{k}$ and it can be used for comparison between users. Here, $\boldsymbol{r_{max,k}}$ denotes the maximum diagonal entry of matrix $\boldsymbol{R_1}$ for user $\boldsymbol{k}$. We note that the proposed Equation 5.25 has lower complexity than Equation 5.22 because we skipped the summation and the process is approximately similar to finding the best receive antenna (or mode) of user $\boldsymbol{k}$. Then, the first proposed selection metric is given

as

$$\boldsymbol{u_{sel1,j}} = \arg\max_{m \in \Psi} \frac{\boldsymbol{R^{(j)}_{comp1,m}}}{\bar{\boldsymbol{R}}_{\boldsymbol{m}}} + \sum_{k \in \Upsilon} \frac{\boldsymbol{R^{(j)}_{comp1,k}}}{\bar{\boldsymbol{R}}_{\boldsymbol{k}}} \tag{5.26}$$

where $\boldsymbol{u_{sel1,j}}$ denotes the selected user at the $\boldsymbol{j}$th iteration.

2. **Second selection metric:** The second proposed selection metric for the PF scheduling algorithm is given as

$$\boldsymbol{\varpi^{(j)}_k} = \frac{\boldsymbol{r^{(j)}_{max,k}}}{\boldsymbol{r^{(j)}_{min,k}}} \, \boldsymbol{\delta^{(j)}_k} \tag{5.27}$$

where $\boldsymbol{r^{(j)}_{max,k}}$,$\boldsymbol{r^{(j)}_{min,k}}$ can be obtained from Equations 5.18 and 5.19 at the $\boldsymbol{j}$th iteration, respectively. $\boldsymbol{\delta^{(j)}_k}$ is the product of singular values of the effective channel matrices of user $\boldsymbol{k}$ at the $\boldsymbol{j}$th iteration, which can be obtained using Equations 5.16 and 5.17. Then, by substituting $\boldsymbol{\varpi^{(j)}_k}$ in Equation 5.22 we obtain

$$\boldsymbol{R^{(j)}_{comp2,k}} = \log_2 \left(1 + \frac{\boldsymbol{P}}{\boldsymbol{j N_r}} \, \boldsymbol{\varpi^{(j)}_k} \right) \tag{5.28}$$

Similar to $\boldsymbol{R^{(j)}_{comp1,k}}$, the value of $\boldsymbol{R^{(j)}_{comp2,k}}$ represents an indication which can be used for comparison between users. Again, we have skipped the summation process that leads to reduce the complexity of scheduling. Then, the second proposed selection metric is given as

$$\boldsymbol{u_{sel2,j}} = \arg\max_{m \in \Psi} \frac{\boldsymbol{R^{(j)}_{comp2,m}}}{\bar{\boldsymbol{R}}_{\boldsymbol{m}}} + \sum_{k \in \Upsilon} \frac{\boldsymbol{R^{(j)}_{comp2,k}}}{\bar{\boldsymbol{R}}_{\boldsymbol{k}}} \tag{5.29}$$

where $\boldsymbol{u_{sel2,j}}$ denotes the selected user at the $\boldsymbol{j}$th iteration.

It is important to mention here that Equations 5.25 and 5.28 don't provide the exact instantaneous rate but a general indication about the rate of that user which can be utilized for comparison with other users in the system.

Algorithm 3 and **Algorithm 4** outline the main operations of the proposed PF scheduling algorithm.

Algorithm 3 The proposed PF scheduling algorithm

1: $\boldsymbol{\Psi = \{1, 2, ..., K\}}$, $\boldsymbol{\Upsilon = \varnothing}$
2: Calculate $\boldsymbol{\delta_k}$ $\forall \boldsymbol{k \in \Psi}$
3: Select the first user as $\boldsymbol{u_1 = \arg\max_{k \in \Psi} \left(R_k(t) / \bar{R}_k(t) \right)}$
4: Set the precoding matrix of $\boldsymbol{u_1}$: $\mathbf{F}_{u_1}^{(1)} = \mathbf{I}_{N_t}$
5: Let $\mathbf{Z}$ =null($\mathbf{H}_{u_1}$)
6: Update $\boldsymbol{\Psi = \Psi - u_1}$, $\boldsymbol{\Upsilon = \Upsilon + u_1}$, $\boldsymbol{n = 2}$
7: **for** $\boldsymbol{j \in \Psi}$ **do**
8: Set $\mathbf{F}_j = \mathbf{Z}$
9: Calculate the effective channel matrix $\bar{\mathbf{H}}_j^{(n)} = \mathbf{H}_j \mathbf{F}_j$
10: **for** $\boldsymbol{k \in \Upsilon}$ **do**
11: Set $\mathbf{F}_{temp} = \mathbf{F}_k^{(n-1)} \times$ null($\mathbf{H}_j \mathbf{F}_k^{(n-1)}$)
12: Update the effective channel matrices: $\bar{\mathbf{H}}_k^{(n)} = \mathbf{H}_k \mathbf{F}_{temp}$
13: **end for**
14: Select a new user by using either Equation 5.26 or Equation 5.29
15: Update the intersection of the null spaces of all previously selected users: $\mathbf{Z} = \mathbf{Z} \times$ null($\mathbf{H}_{u_n} \mathbf{Z}$)
16: **for** $\boldsymbol{k \in \Upsilon}$ **do**
17: Update $\mathbf{F}_k^{(n)} = \mathbf{F}_k^{(n-1)} \times$ null($\mathbf{H}_{u_n} \mathbf{F}_k^{(n-1)}$)
18: **end for**
19: Update:$\boldsymbol{\Psi = \Psi - u_n}$; $\boldsymbol{\Upsilon = \Upsilon + u_n}$; $\boldsymbol{n = n + 1}$
20: **end for**

Algorithm 4 obtaining the average throughput of each user after PF scheduling process

Initiate the time window $\boldsymbol{T}$
Initiate the time-scale parameter $\boldsymbol{t_c}$
Initiate the average throughput $\bar{\boldsymbol{R}}_{\boldsymbol{j}}(\boldsymbol{t})$ for each $\boldsymbol{j} \in \boldsymbol{\Psi}$
for $\boldsymbol{t = 1 : T}$ **do**
    Obtain users' channels
    Use **Algorithm 3** to select users
    Calculate the precoders of the selected users using block diagonalization method explained earlier.
    Calculate the effective channel matrices of the selected users
    for $\boldsymbol{k} \in \boldsymbol{\Upsilon}$ **do**
        Calculate the instantaneous date rate $\boldsymbol{R_k(t)}$
    end for
    for $\boldsymbol{j} \in \boldsymbol{\Psi}$ **do**
        update average throughput $\bar{\boldsymbol{R}}_{\boldsymbol{j}}(\boldsymbol{t})$ using Equation 5.24
    end for
end for
for $\boldsymbol{j} \in \boldsymbol{\Psi}$ **do**
    Calculate the average data rate $\boldsymbol{R_j(t)}$ over the time window $\boldsymbol{T}$
end for

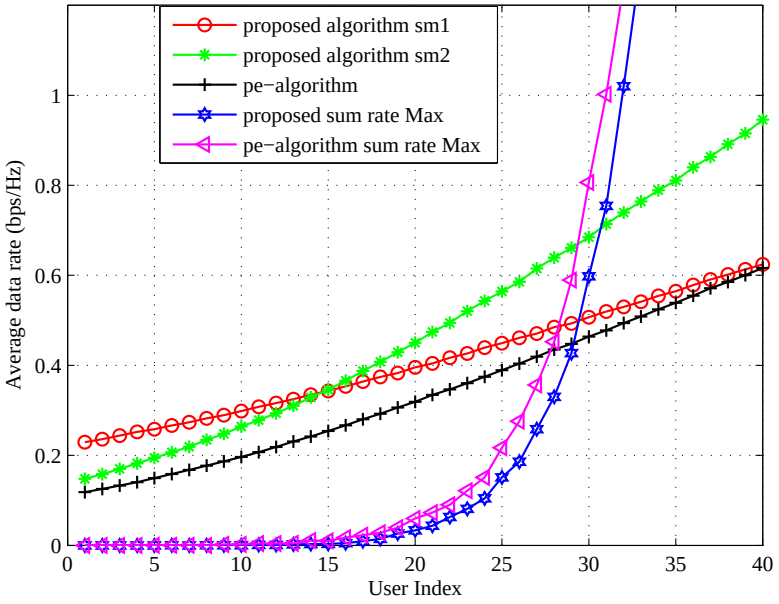

Figure 5.4: Average data rage of individual users with $\boldsymbol{N_t = 8}$,$\boldsymbol{N_r = 2}$. The maximum number of selected users is 4.

5.6 Simulation Results

To evaluate the performance of the proposed PF scheduling algorithm, we compare it with the algorithm proposed in [35] (pe-algorithm), in which the product of the eigenvalues of effective channel matrices from the angle between subspaces is adopted as a selection metric. We compare the proposed algorithm to this algorithm due to the high performance it achieves. The numerical results have been averaged over 10,000 independent quasi-static fading channel realizations.

To obtain the performance of the proposed algorithm, we assume asymmetric SNRs for the total users in the system before the start of selection process. More specifically, Let the number of total users be $\boldsymbol{K = 40}$. These users receive varying values of SNRs that are according to the loglinear scale [31] [33] [82]. To perform that, we have expressed the channel matrix for user $\boldsymbol{k}$ as

$$\mathbf{H}_{\boldsymbol{k}} = \sqrt{\boldsymbol{\vartheta}_{\boldsymbol{k}}}\mathbf{H}_{\boldsymbol{k},\boldsymbol{iid}} \tag{5.30}$$

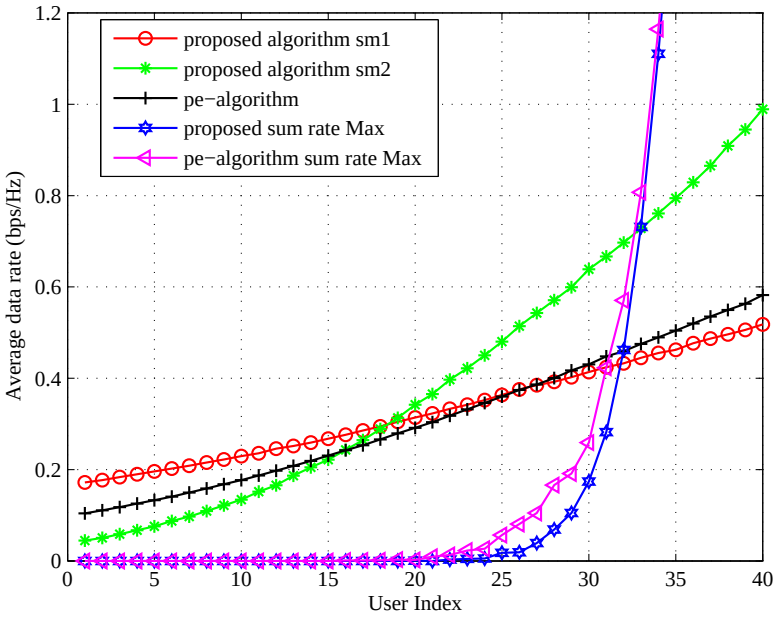

Figure 5.5: Average data rage of individual users with $\boldsymbol{N_t = 8}$,$\boldsymbol{N_r = 3}$. The maximum number of selected users is 4.

where $\mathbf{H}_{\boldsymbol{k,iid}}$ is a matrix of independent and identically distributed complex Gaussian entries with zero mean and unit variance. For each user $\boldsymbol{k} \in \boldsymbol{\Psi}$, the weighting factor $\boldsymbol{\vartheta_k}$ can be obtained from the loglinear scale from $\mathrm{SNR}_{\min} = \mathbf{0}$ dB to $\mathrm{SNR}_{\max} = \mathbf{20}$ dB, i.e.,

$$\mathbf{log_{10}}\left(\boldsymbol{\vartheta_{k+1}}\right) = \frac{\mathrm{SNR}_{\max} - \mathrm{SNR}_{\min}}{\boldsymbol{K-1}}\,\boldsymbol{k} + \mathrm{SNR}_{\min} \tag{5.31}$$

$$\text{for} \quad \boldsymbol{k = 0, 1, ..., K-1}$$

Further, the values of $\boldsymbol{\vartheta_k}$ are normalized as

$$\boldsymbol{\vartheta_k} = \frac{\boldsymbol{\vartheta_k}}{\boldsymbol{\vartheta_{max}}}\ ,\ \forall \boldsymbol{k} \in \boldsymbol{\Psi} \tag{5.32}$$

where $\boldsymbol{\vartheta_{max}}$ is the maximum value of $\boldsymbol{\vartheta_k}$'s in the set $\boldsymbol{\Psi}$.

All plotted figures have fix number of $\boldsymbol{K}$, i.e., $\boldsymbol{K = 40}$. In Figure 5.4, the average data rate of individual users is plotted against users' index. In this Figure, we put

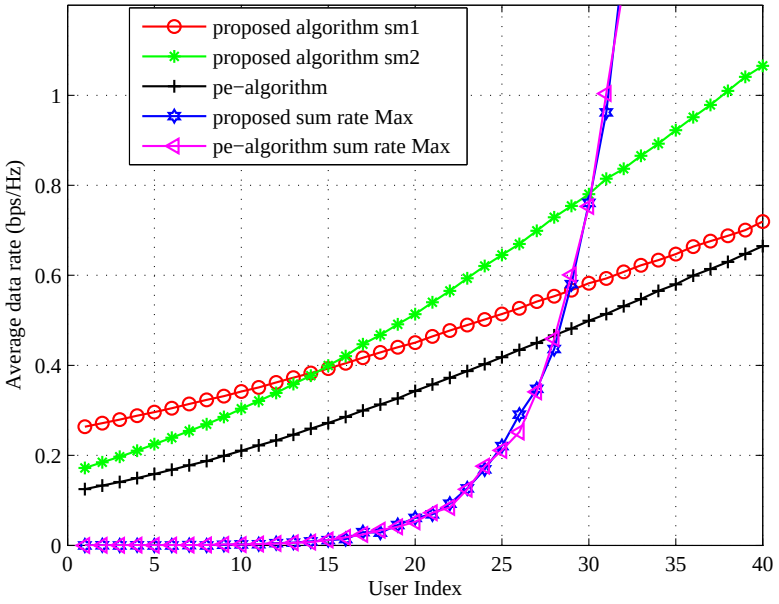

Figure 5.6: Average data rage of individual users with $\boldsymbol{N_t = 10}$,$\boldsymbol{N_r = 2}$. The maximum number of selected users is 5.

$\boldsymbol{N_t = 8}$ and $\boldsymbol{N_r = 2}$, hence the maximum number of selected users that can be simultaneously supported by the base station is 4. As seen, the maximum sum rate algorithms which are without PF scheduling, i.e., the blue and the magenta colours, support the users with high SNR. More specifically, users 20 through 40 share most of the throughput, while users 1 through 15 don't receive data at all. By comparing the proposed PF scheduling algorithm with the first selection metric, i.e., the red one, to the PF pe-algorithm, we notice that both algorithms have almost similar degree of fairness for users with high SNR, and they differ in that the proposed algorithm gives some form of priority to users with lower SNR. In contrast, the proposed PF algorithm with the second selection metric, i.e., the green colour, has almost the same degree of fairness with the PF pe-algorithm for users with low SNR. The priority of selection of the proposed PF scheduler with the second selection metric increases for users with higher SNR.

In Figure 5.5, we have increased the number of receive antennas of each user, i.e., $\boldsymbol{N_r = 3}$, while we fixed the number of transmit antennas, i.e., $\boldsymbol{N_t = 8}$. In this

case, the maximum number of selected users which are simultaneously supported by the base station is 3. All algorithms almost follow the same pattern except that the average sum rate is lower. This is normal since the number of selected users now is less than that in Figure 5.4.

In Figure 5.6, we have increased the total number of transmit antennas $\boldsymbol{N_t = 10}$, while we fixed the number of receive antennas of each user, i.e., $\boldsymbol{N_r = 2}$. In this case, the maximum number of selected users that can be simultaneously supported by the base station is 5. We notice that all algorithms have almost the same previous pattern except that the total throughput have increased. This is because the number of selected users which are simultaneously supported by the base station has increased.

5.7 Summary

In this chapter, we have studied the proportional fairness scheduling. We have seen that multiuser diversity can be exploited to improve the system throughput through user selection technology. The selection process may experience an important constraint which is fairness among users when applying selection. We have proposed a PF scheduling algorithm with two selection metrics. Further, we studied the block diagonalization method of precoding which can be used as an alternative of the iterative precoding design in order to cancel the interuser interference in multiuser MIMO downlink systems. By comparing the proposed algorithm to the algorithm which adopts the product of eigenvalues of users' effective channel matrices, we noticed that a considerable degree of fairness has been achieved when applying the proposed two selection metrics of PF scheduler.

Chapter 6

Conclusion and Future Work

Due to rapid development of smartphone devices and their widespread integration in everyday life, the demand of high data traffic is becoming more and more important in wireless communications. Multiuser MIMO comes as one of the prime technologies for increasing data rate transmission and improving link reliability in wireless systems. This can be achieved by exploiting the degrees of freedom offered by deploying antenna elements on both the transmitter and receiver sides and without the need of additional power or bandwidth.

Transmit antena selection, user selection and proportional fairness scheduling technologies play essential role in reducing the complexity of MU-MIMO systems as well as improving the total system throughput. In this thesis, MU-MIMO has been studied according to these perspectives.

In this chapter, we summarise the main findings of the thesis and provide suggestions for future research.

6.1 Summary of Results

In chapter 3, we have studied transmit antenna selection technology for MU-MIMO downlink systems. In this context, a greedy TAS algorithm is proposed. The proposed algorithm selects an optimal set of antennas out of the total antennas deployed in the base station for transmission. The selection process is achieved in a descending order, where in each iteration the antenna which maximizes the product of eigenvalues of users' effective channels is deactivated. The iterative precoding design method is used to cancel the interuser interference that has to be done before starting selection. Simulation results demonstrate that the proposed algorithm achieves very close performance to the exhaustive search algorithm with much lower complexity and has high link reliability which is almost similar to that of the exhaustive search.

In chapter 4, we have investigated user selection technology for MU-MIMO systems. In this correspondence, a greedy suboptimal user selection algorithm is proposed. The key idea is that, for each iteration, the algorithm selects a user to maximize the product of the singular values of the effective channels from a set of unselected users. To evaluate its performance and complexity, the algorithm is compared to four other algorithms. In terms of complexity, we demonstrated that the proposed scheme is approximately equivalent to the psrn-algorithm and pe-algorithm and has less complexity than that of the c-algorithm. More specifically, the algorithm has a shorter run time than the pe-algorithm and is close to the psrn-algorithm if the maximum number of users that can be simultaneously supported is two, but it becomes more dependant on the total number of users in the system when this figure is greater than two. In either case, the proposed algorithm has less run time than the c-algorithm. Furthermore, simulation results show that the proposed algorithm outperforms the psrn-algorithm and v-algorithm as well as providing performance that is the same as that of the c-algorithm and pe-algorithm under a high SNR regime, for both correlated and uncorrelated channels.

In chapter 5, we have proposed a proportional fairness scheduling algorithm and two

selection metrics. Both metrics are designed by utilizing the upper triangular matrix obtained by applying the QR decomposition on the users' effective channel matrices. The first metric is designed using the maximum entry of the upper triangular matrix, while the second metric is designed using the ratio between the maximum and minimum entries of the triangular matrix multiplied by the product of singular values of effective channels. Simulation results demonstrate that a considerable degree of fairness is achieved when applying any of the proposed two metrics. However, compared to PF pe-algorithm, the first metric gives some form of priority to users with lower SNR. On the other hand, we noticed that the second metric provides slightly more priority to users with high SNR compared to the PF pe-algorithm.

6.2 Future Work

In the context of transmit antenna selection, the thesis has assumed single cell MU-MIMO downlink system. However, the issue can be extended into two other cases:

1. Multi-cell MU-MIMO networks, by which network capacity can be maximized by using efficient methods of interference mitigation. In this case, nullifying inter-cell interference (ICI) as well as IUI must be taken into consideration.

2. Massive MIMO systems, in which the BSs are equipped with a large number of antenna elements. For such systems, selecting an optimal group of antennas for transmission is considered a challenging task. This is because the search process is achieved on a large number of antennas in order to select the required subset among them. Hence, it is essential to find more practical algorithms of antenna selection which can deal with such large number of antennas with more flexibility and in the same time keep the diversity advantages of MIMO systems.

For user selection, possible work can be done to more alleviate the complexity of the proposed algorithm. One idea to achieve that is by passing channel matrices into a coarse filter before starting the selection process. For instance, subspace collinearity

can be applied to obtain the dependency between any two subspaces (channels). The preprocessing of channel matrices will help to find channels which are less correlated to each other. Then, the remaining users after collinearity process will enter the selection operation in order to find the final optimal group of users.

Another important issue which should be considered in future MU-MIMO systems is the channel state information feedback. By scaling up MIMO systems, the need of limited feedback becomes more crucial in order to reduce the computational burden on user terminals. Hence, investigating both technologies of antenna selection and user scheduling for massive MU-MIMO systems with limited channel state information is considered a pioneering research work for massive MU-MIMO systems.

Bibliography

[1] A. Gorokhov, D. A. Gore, and A. J. Paulraj, "Receive antenna selection for MIMO spatial multiplexing: theory and algorithms," *IEEE Trans. Signal Process.*, vol. 51, no. 11, pp. 2796-2807, Nov. 2003.

[2] A. F. Molisch, and M.Z. Win, "MIMO systems with antenna selection," *IEEE Microw. Mag.*, vol. 5, no. 1, pp. 46-56, Mar. 2004.

[3] S. Sanayei, and A. Nosratinia, "Antenna selection in MIMO systems," *IEEE Commun. Mag.*, vol. 42, no. 10, pp. 68-73, Oct. 2004.

[4] J-K. Lain, "Joint transmit/receive antenna selection for MIMO systems: a real-valued genetic approach," *IEEE commun. Lett.*, vol. 15, no. 1, pp. 58-60, Jan. 2011.

[5] A. F. Molisch, M. Z. Win, and J. H. Winters, "Reduced-complexity transmit/receive-diversity systems," *IEEE Trans. Signal. Process.*, vol. 51, no. 11, pp. 2729-2738, Nov. 2003.

[6] K. Dong, N. Prasad, X. Wang, and S. Zhu, "Adaptive antenna selection and Tx/Rx beamforming for large-scale MIMO systems in 60GHz channels," in *Proc. EURASIP J. Wireless Commun. Netw.*, Aug. 2011.

[7] P. Zhang, S. Chen, C. Dong, and L. Li, "Norm-based joint transmit/receive antenna selection aided and two-tier channel estimation assisted STSK systems," in *Proc. Int. Conf. Communications (ICC) 2014*, Sydney, Australia, pp. 5049-5054.

[8] A. Gorokhov, D. A. Gore, and A. J. Paulraj, "Receive antenna selection for MIMO flat-fading channels: Theory and algorithms," *IEEE Trans. Inf. Theory*, vol. 49, no. 10, pp. 2687-2696, Oct. 2003.

[9] A. F. Molisch, M. Z. Win, Y.-S. Choi, and J. H. Winters, "Capacity of MIMO systems with antenna selection," *IEEE Trans. Wireless Commun.*, vol. 4, no. 4, pp. 1759-1772, Jul. 2005.

[10] L. Zhou, and M. Shimizu, "Fast recursive algorithm for efficient transmit antenna selection i spatial multiplexing systems," in *Proc. IEEE VTC Fall*, Anchorage, AK, USA, pp. 1-5, Sept. 2009.

[11] C. Chen, "A computationally efficient near-optimal algorithm for capacity-maximization based joint transmit and receive antenna selection," *IEEE commun. Lett.*, vol. 14, no. 5, pp. 402-405, May 2010.

[12] R. Vaze, and H. Ganapathy, "Sub-modularity and antenna selection in MIMO systms," *IEEE commun. Lett.,* vol. 16, no. 9, pp. 1446-1449, Sept. 2012.

[13] R. Chen, R.W. Heath, and J.G. Andrews, "Transmit selection diversity for unitary precoded multiuser spatial multiplexing systems with linear receivers," *IEEE Trans. Signal Process.*, vol. 55, no. 3, pp. 1159-1171, Mar. 2007.

[14] R. W. Heath, and D. J. Love, "Transmit antenna selection for decision feedback detection in MIMO fading channels," *IEEE Trans. Signal Process.*, vol. 53, no. 8, pp. 3042-3056, Aug. 2005.

[15] H. A. Saleh, and W. Hamouda, "Multimode antenna selection for spatial multiplexing systems with linear receivers," *IEEE Trans. Wireless Commun.*, vol. 8, no. 9, pp. 4440-4444, Sept. 2009.

[16] M. Gkizeli, and G. N. Karystinos, "Maximum-SNR antenna selection among a large number of transmit antennas," *IEEE J. Sel. Topics Signal Process.*, vol. 8, no. 5, pp. 891-901, Oct. 2014.

[17] H. Li, L. Song, and M. Debbah, "Energy efficiency of large-scale multiple antenna systems with transmit antenna selection," *IEEE Trans. Commun.*, vol. 62, no. 2, pp. 638-647, Feb. 2014.

[18] S. Nam, J. Kim, and Y. Han, "A user selection algorithm using angle between subspaces for downlink MU-MIMO Systems," *IEEE Trans. Commun.*, vol. 62, no. 2, pp. 616-624, Feb. 2014.

[19] G.H. Golub, and C. F. V. Loan, *Matrix Computations,* 3rd ed. The John Hopkins Univ. Press, 1996.

[20] Y. Cho, J. Kim, W. Yang, and C. Kang, *MIMO-OFDM wireless communications with MATLAB*, 1st edition, Singapore: WILEY press, 2010.

[21] A. Bjorck, and G. H. Golub, "Numerical methods for computing angles between linear subspaces," *Math. Comput.,* vol. 27, no. 123, pp. 579-594, July 1973.

[22] I. B. Risteski, and K. G. Trencevski, "Principal values and principal subspaces of two subspaces of vector spaces with inner product," *Beitrage Algebra Geom,* vol. 42, pp. 289-300, 2001.

[23] W. S.-B. Hendra Gunawan, O. Neswan, "A formula for angles between subspaces of inner product spaces," vol. 46, pp. 311-320, 2005.

[24] L. Lu, G. Lee, A. Swindlehurst, A. Ashikhmin, and R. Zhang, "An overview of massive MIMO: benefits and challenges," *IEEE J. Sel. Topics Signal Process.*, vol. 8, no. 5, pp. 742-758, Oct. 2014.

[25] T. Khomyat, P. Uthansakul, M. Uthansakul, and S. Hee, "On the performance of the zero-forcing-space-time block coding multiple-input-multiple-output receiver with channel estimation error and error propagation," *IET Commun.*, vol. 8, no. 18, pp. 3381-3392, 2014.

[26] M. Costa, "Writing on dirty paper," *IEEE Trans. Inf. Theory*, vol. 29, no. 3, pp. 439-441, May 1983.

[27] L. Donghun, "Performance analysis of zero-forcing-precoded scheduling system with adaptive modulation for multiuser-multiple input multiple output transmission," *IET Commun.*, vol. 9, no. 16, pp. 2007 - 2012, 2015.

[28] D. H. N. Nguyen, H. Nguyen-Le, and T. Le-Ngoc, " Block-diagonalization precoding in a multiuser multicell MIMO System: competition and coordination," *IEEE Trans. Wireless Commun.*, vol. 60, no. 8, pp. 968 - 981, Feb. 2014.

[29] G. Caire and S. Shamai, "On the achievable throughput of a multiantenna Gaussian broadcast channel," *IEEE Trans. Inf. Theory*, vol. 49, no. 7, pp. 1691-1706, July 2003.

[30] Q. Spencer, A. Swindlehurst, and M. Haardt, "Zero-forcing methods for downlink spatial multiplexing in multiuser MIMO channels," *IEEE J. Sel. Topics Signal Process.*, vol. 52, no. 2, pp. 461-471, Feb. 20004.

[31] L-N Tran, M. Bengtsson, and B. Ottersten, "Iterative precoder design and user scheduling for block-diagonalized systems," *IEEE Trans. Signal Process.*, vol. 60, no. 7, pp. 3762-3739, July 2012.

[32] Z. Shen, R. Chen, J. Andrews, R. W. Heath, and B. L. Evans, "Low complexity user selection algorithms for multiuser MIMO systems with block diagonalization," *IEEE Trans. Signal Process.*, vol. 54, no. 9, pp. 3658-3663, Sept. 2006.

[33] S. Sigdel and W. A. Krzymien, "Simplified fair scheduling and antenna selection algorithms for multiuser MIMO orthogonal space-division multiplexing downlink," *IEEE Trans. Veh. Technol.*, vol. 58, no. 3, pp. 1329-1344, March 2009.

[34] L. Jin, X. Gu, and Z. Hu, "Low-complexity scheduling strategy for wireless multiuser multiple-input multiple-output downlink system," *IET Commun.*, vol. 5, no. 7, pp. 990-995, 2011.

[35] S. Nam, J. Kim, and Y. Han, "A user selection algorithm using angle between

subspaces for downlink MU-MIMO Systems," *IEEE Trans. Commun.*, vol. 62, no. 2, pp. 616-624, Feb. 2014.

[36] Y. Cho, J. Kim, W. Yang, and C. Kang, *MIMO-OFDM wireless communications with MATLAB* Singapore: WILEY Press, 1st edn. 2010.

[37] M. Fuchs, G. D. Galdo, and M. Haardt, "Low-complexity space-time-frequency scheduling for MIMO systems with SDMA," *IEEE Trans. Veh. Technol.*, vol. 56, no. 5, pp. 2775-2784, Sept. 2007.

[38] J. P. Kermoal, L. Schumacher, K. I. Pedersen, and P. E. Moqensen, "A stochastic MIMO radio channel model with experimental validation," *IEEE J. Sel. Areas Commun.*, vol. 20, no. 6, pp. 1211-1226, Aug. 2002.

[39] M. Kang and M. S. Alouini, "Capacity of correlated MIMO rayleigh channels," *IEEE Trans. Wireless commun.*, vol. 5, no. 1, pp. 143-155, Jan. 2006.

[40] S. L. Loyka, "Channel capacity of MIMO architecture using the exponential correlation matrix," *IEEE Commun. Lett.*, vol. 5, no. 9, pp. 369-371, Oct. 2001.

[41] K. Yu, M. Bengtsson, B. Ottersten, D. McNamara, P. Karlsson, and M. Beach, "Second order statistics of NLOS indoor MIMO channels based on 5.2 GHz measurements," *Proc. IEEE GLOBECOM*, vol. 1 pp. 156-160, Nov. 2001.

[42] J. Akhtar and D. Gesbert, "Spatial multiplexing over correlated MIMO channels with closed-form precoder," *IEEE Trans. Wireless Commun.*, vol. 4, no. 5, pp. 2400-2409, Sept. 2005.

[43] C-N. Chuah, D. N. C. Tse, J. M. Kahn, and R. A. Valenzuela, "Capacity scaling in MIMO wireless systems under correlated fading," *IEEE Trans. Inf. Theory*, vol. 48, no. 3, pp. 637-650, Mar. 2002.

[44] M. A. Girnyk, M. Vehkapera, and L. K. Rasmussen, "Large-system analysis of correlated MIMO multiple access channels with arbitrary signaling in the presence

of interference," *IEEE Trans. Wireless commun.*, vol. 13, no. 4, pp. 2060-2073, Apr. 2014.

[45] V. Tarokh, H. Jafarkhani, and A. R. Calderbank, "Space-time block codes from orthogonal desing," *IEEE Trans. on Info. Theory*, vol. 45, no. 5, pp. 1456-1467, July 1999.

[46] V. Tarokh, N. Seshadri, and A. R. Calderbank, "Space-time codes for high data rate wireless communication: performance criterion and code construction," *IEEE Trans. on Info. Theory*, vol. 44, no. 2, pp. 744-765, Mar. 1998.

[47] S. M. Alamouti, "A simple transmit diversity technique for wireless communications," *IEEE Journal on Sel. Areas in Communications,*, vol. 16, no. 8, pp. 1451-1458, Oct. 1998.

[48] G. J. Foschini, "Layered space-time architecture for wireless communication in a fading environment when using multiple antennas," *Bell Labs Technical Journal*, vol. 1, no. 2, pp. 41-59, Autumn 1996.

[49] M. El-hajjar, L. Hanzo,"Multifunctional MIMO systems: a combined diversity and multiplexing design perspective," *IEEE Wireless Communications*, vol. 17, no. 2, pp. 1456-1467, Apr. 2010.

[50] L. Garcia-Ordonez, A. Pages-Zamora, and J. R. Fonollosa,"Diversity and multiplexing tradeoff of spatial multiplexing MIMO systems with CSI," *IEEE Trans. on Info. Theory*, vol. 54, no. 7, pp. 2959-2975, July 2008.

[51] L. Zheng and D. Tse, "Diversity and Multiplexing: A fundamental tradeoff in multiple antenna channels," *IEEE Trans. on Info. Theory*, vol. 49, no. 5, pp. 1073-1096, May 2003.

[52] R. W. Heath, Jr. and A. J. Paulraj, "Switching between diversity and multiplexing in MIMO systems," *IEEE Trans. on Communications,*, vol. 53, no. 6, pp. 962-968, June 2005.

[53] R. W. Heath, Jr., and D. J. Love, "Multimode precoding for MIMO wireless systems: Part II," *IEEE Trans. on Signal Processing,*, vol. 53, no. 8, pp. 4042-3056, Aug. 2005.

[54] E. Biglieri, R. Calderbank, A. Constantinides, A. Goldsmith, A. Paulraj, and H. Vincent Poor, *MIMO wireless communicaitons.* Cambridge: Cambridge University Press, 2007.

[55] M. A. Khalighi, J-M. Brossier, G. Jourdain, and K. Raoof, "Water filling capacity of rayleigh MIMO Channels," in *Proc. IEEE 12th Int. Symp. Personal, Indoor, and Mobile Radio Communications,* vol. 1, San Diego, CA, Sept. 2001, pp. 155-158.

[56] D. Wübben, R. Böhnke, V. Kühn, and K. D. Kammeyer, "MMSE extension of V-BLAST based on sorted QR decomposition," in *Proc. IEEE Vehicular Technol. Conf. (VTC),* Orlando, FL, USA, Oct. 2003, pp. 508-512.

[57] R. Böhnke, D. Wübben, V. Kühn, and K. D. Kammeyer, "Reduced complexity MMSE detection for BLAST architectures," in *Proc. IEEE Globecom,* San Francisco, California, USA, Dec. 2003, pp. 2258-2262.

[58] D. Wübben, R. Böhnke, V. Kühn, and K. D. Kammeyer, "Near-maximum-likelihood detection of MIMO systems using MMSE-based lattice-reduction," in *Proc. IEEE Int. Conf. Commun. (ICC'04),* Paris, France, June 2004, pp. 798-802.

[59] D. Tse and P. Viswanath, *Fundamentals of wireless communication.* Cambridge: Cambridge University Press, 2005.

[60] A. Lozano and N. Jindal, " Transmit diversity vs. spatial multiplexing in modern MIMO systems," *IEEE Trans. Wireless Commun.*, vol. 9, no. 1, pp. 186-197, Jan. 2010

[61] L. Zheng and D. N. C. Tse, " Diversity and multiplexing: a fundamental tradeoff in multiple-antenna channels," *IEEE Trans. Inf. Theory*, vol. 49, no. 5, pp. 1073-1096, May 2003.

[62] F. D. Flaviis, L. Jofri, J. Romeu, and A. Grau, *Multiantenna systems for MIMO communications.* Arizona, USA: Morgan & Claypool, 2008.

[63] H. Jafarkhani, *Space-time coding: theory and practice.*, 1st ed., Cambridge: Cambridge University Press, 2005.

[64] D-S Shiu, G. J. Foschini, M. J. Gans, and J. M. Kahn, " Fading correlation and its effect on the capacity of multielement antenna systems," *IEEE Trans. Commun.*, vol. 48, no. 3, pp. 502-513, Mar. 2000.

[65] K. Yu, M. Bengtsson, B. Ottersten, D. McNamara, P. Karlsson, and M. Beach, "A wideband statistical model for NLOS indoor MIMO channels," in *Proc. IEEE Veh. Technol. Conf.—Spring,* 2002, pp. 370-374.

[66] S. A. Jafar and A. Goldsmith, " Transmitter optimization and optimality of beamforming for multiple antenna systems," *EEE Trans. Wireless Commun.*, vol. 3, no. 4, pp. 1165-1175, July 2004.

[67] K. Yu, M. Bengtsson, B. Ottersten, P. Karlsson, D. McNamara, and M. Beach, "Measurement analysis of NLOS indoor MIMO channels," in *Proc. IST Mobile Communications Summit Barcelona Spain,* Sept. 2002, pp. 277-282.

[68] P. Viswanath, D. N. C. Tse, and R. Laroia " Opportunistic beamforming using dumb antennas," *IEEE Trans. Inf. Theory*, vol. 48, no. 6, pp. 1277-1294, June 2002.

[69] D. Gesbert, M. Kountouris, R.W. Heath Jr., C.-B. Chae, T. Salzer," Shifting the MIMO paradigm: From single-user to multiuser com- munications," *IEEE Signal Process. Mag.*, vol. 24, no. 5, pp. 36-46, Sept. 2007.

[70] K. K. J. Chung, C.-S. Hwang, and Y. K. Kim, " A random beamforming technique in MIMO systems exploiting multiuser diversity," *IEEE J. Sel. Areas Commun.*, vol. 21, no. 5, pp. 848-855, June 2003.

[71] I. R. Baran and B. F. Uchoa-Filho,"A modified opportunistic beamforming for

time-Correlated fading channels," *IEEE Trans. Wireless Commun.*, vol. 7, no. 11, pp. 4082-4087, Nov. 2008.

[72] H. Yang, P. Lu, H. Sung, and Y. Ko, "Exact sum-rate analysis of MIMO broadcast channels with random unitary beamforming," *IEEE Trans. Commun.*, vol. 59, no. 11, pp.2982-2986, June 2011.

[73] R. Chen, Z. Shen, J. G. Andrews, and R. W. Heath, "Multimode transmission for multiuser MIMO systems with block diagonalization," *IEEE Trans. Signal Process.*, vol. 56, no. 7, pp.3294-3302, July 2008.

[74] O. Oyman, R. U. Nabar, H. Bolcskei, and A. J. Paulraj,"Characterizing the statistical properties of mutual information in MIMO channels: insights into diversity-multiplexing tradeoff ," in *Proc. Asilomar Conf. Signals, Sys., Comput.,* Nov. 2002, pp. 521-525.

[75] O. Oyman, R. U. Nabar, H. Bolcskei, and A. J. Paulraj, "Characterizing the statistical properties of mutual information in MIMO channels," *IEEE Trans. Signal Process.*, vol. 51, no. 11, pp.1159-1171, Nov. 2003.

[76] R. Chen, R. W. Heath, and J. G. Andrews, "Transmit selection diversity for unitary precoded multiuser spatial multiplexing systems with linear receivers," *IEEE Trans. Signal Process.*, vol. 55, no. 3, pp.2784-2795, Mar. 2007.

[77] A. E. Forooshani, A. A. Lotfi-Neyestanak, and D. G. Michelson, "Optimization of antenna placement in distributed MIMO systems for underground mines," *IEEE Trans. Wireless Commun.*, vol. 13, no. 9, pp.2784-2795, Sept. 2014.

[78] H. Sampath, S. Talwar, J. Tellado, V. Erceg, and A. J. Paulraj, "A fourth generation MIMO-OFDM broadband wireless system: Design, performance, field trial results," *IEEE Commun. Mag.*, vol. 40, no. 9, pp.143-149, Sept. 2002.

[79] E. Björnson and E. Jorswieck, "Optimal resource allocation in coordinated multi-cell systems," *Found. Trends in Commun. Inf. Theory*, vol. 9, no. 2-3, pp. 113-381, Jan. 2013.

[80] G. Dimic and N. D. Sidiropoulos, "On downlink beamforming with greedy user selection: performance analysis and a simple new algorithm," *Found. Trends in Commun. Inf. Theory*, vol. 53, no. 10, pp. 3857 - 3868, Oct. 2005.

[81] J. Wang, D. J. Love, and D. Zoltowski, "User selection with zero-forcing beamforming achieves the asymptotically optimal sum rate," *IEEE Trans. Signal Process.*, vol. 56, no. 8, pp. 3713 - 3726, Aug. 2008.

[82] T. Yoo and A. Goldsmith, "Optimality of zero-forcing beamforming with multiuser diversity ," in *Proc. IEEE ICC,* May 2005, vol. 1, pp.542–546.

[83] T. Yoo and A. Goldsmith, "On the optimality of multiantenna broadcast scheduling using zero-forcing beamforming," *IEEE Trans. Signal Process.*, vol. 24, no. 3, pp. 528 - 541 , Mar. 2006.

[84] A. Bayesteh and A. K. Khandani, "On the User Selection for MIMO Broadcast Channels," *IEEE Trans. Inf. Theory*, vol. 54, no. 3, pp. 1086 - 1107 , Mar. 2008.

[85] S. Nam, J. Kim, and Y. Han, "A PF scheduling with low complexity for downlink multi-user MIMO systems," in *Proc. IEEE Vehicular Technol. Conf. (VTC),* Las Vegas, NV, USA, Sept. 2013.

[86] J. Lee and N. Jindal, "High SNR analysis for MIMO broadcast channels: Dirty paper coding versus linear precoding," *IEEE Trans. Inf. Theory*, vol. 53, no. 12, pp. 4787 - 4792, Dec. 2007.

[87] E. S. Lo, P. W. C. Chan, V. K. N. Lau, R. S. Cheng, K. B. Letaief, R. D. Murch, and W. H. Mow, "Adaptive resource allocation and capacity comparison of downlink multiuser MIMO-MC-CDMA and MIMO-OFDMA," *IEEE Trans. Wireless Commun.*, vol. 6, no. 3, pp. 1083 - 1093, Mar. 2007.

[88] C-B. Chae, D. Mazzarese, N. Jindal, and R. W. Heath, "Coordinated beamforming with limited feedback in the MIMO broadcast channel," *IEEE J. Sel. Areas Commun.*, vol. 26, no. 8, pp. 1083 - 1093, Oct. 2008.

[89] J. Choi and F. Adachi, "User selection criteria for multiuser systems with optimal and suboptimal LR based detectors," *IEEE Trans. Signal Process.*, vol. 58, no. 10, pp. 5463 - 5468, Oct. 2010.

[90] J. H. Lee, W. Choi, and B. D. Rao, "Multiuser diversity in interfering broadcast channels: achievable degrees of freedom and user scaling law," *IEEE Trans. Wireless Commun.*, vol. 12, no. 11, pp. 5837 - 5849, Nov. 2013.

[91] Y. Huang, F. Al-Qahtani, C. Zhong, Q. Wu, J. Wang, and H. Alnuweiri, "Performance analysis of multiuser multiple antenna relaying networks with co-channel interference and feedback delay," *IEEE Trans. Commun.*, vol. 62, no. 1, pp. 59 - 73, Jan. 2014.

[92] B. E. Godana and T. Ekman, "Parametrization based limited feedback design for correlated MIMO channels using new statistical models," *IEEE Trans. Wireless Commun.*, vol. 12, no. 10, pp. 5172 - 5184, Oct. 2013.

[93] W. Zeng, C. Xiao, M. Wang, and J. Lu, "Linear precoding for finite-alphabet inputs over MIMO fading channels with statistical CSI," *IEEE Trans. Signal Process.*, vol. 60, no. 6, pp. 3134 - 3148, June 2012.

[94] M. R. Bhatnagar and and A. Hjorungnes, "Linear Precoding of STBC over Correlated Ricean MIMO Channels," *IEEE Trans. Signal Process.*, vol. 9, no. 6, pp. 1832 - 1836, June 2010.

[95] V. Raghavan, R. W. Heath, and A. M. Sayeed, "Systematic codebook designs for quantized beamforming in correlated MIMO channels," *IEEE J. Sel. Areas Commun.*, vol. 25, no. 7, pp. 1298 - 1310, Sept. 2007.

[96] H. Joung, H-S. Jo, C. Mun, and J-G. Yook, "Capacity loss due to polarization-mismatch and space-correlation on MISO channel," *IEEE Trans. Wireless Commun.*, vol. 13, no. 4, pp. 2124 - 2136, Apr. 2014.

[97] R. Chen, J. Andrews, and R. W. Heath, "Efficient transmit antenna selection

for multiuser MIMO systems with block diagonalization ," in *Proc. IEEE Global Telecommun. Conf.*, Nov. 2007, pp. 3499-3503.

[98] C. Wang and R. D. Murch, "Adaptive downlink multi-user MIMO wireless systems for correlated channels with imperfect CSI," *IEEE Trans. Wireless Commun.*, vol. 5, no. 9, pp. 2435 - 2446, Sept. 2006.

[99] C. Wang and R. D. Murch, "Adaptive downlink multi-user MIMO wireless systems for correlated channels with imperfect CSI," *IEEE Trans. Wireless Commun.*, vol. 5, no. 9, pp. 2435 - 2446, Sept. 2006.

[100] M. S. Sim, J. Park and R. W. Heath , "Compressed channel feedback for correlated massive MIMO systems," *Journal of Communications and Networks*, vol. 18, no. 1, pp. 95 - 104, Mar. 2016.

[101] W. Xiong, A. Mukherjee, and H. M. Kwon, "MIMO cognitive radio user selection with and without primary channel state information," *IEEE Trans. Veh. Technol*, vol. 65, no. 2, pp. 985 - 991, Feb. 2016.

[102] X. Yi and E. K. S. Au, "User scheduling for heterogeneous multiuser MIMO systems: a subspace viewpoint," *IEEE Trans. Veh. Technol.*, vol. 60, no. 8, pp. 4004 - 4013, Oct. 2011.

[103] M. Hanif, H.-C. Yang, G. Boudreau, and E. Sich, "Low complexity antenna subset selection for massive MIMO systems with multi-cell cooperation ," in *Proc. IEEE Globecom Workshops (GC Wkshps)*, San Diego, CA, Dec. 2015.

[104] J. Tang and S. Lambotharan, "Interference alignment techniques for MIMO multi-cell interfering broadcast channels," *IEEE Trans. Commun.*, vol. 61, no. 1, pp. 164 - 175, Jan. 2013.

[105] X. Chen and C. Yuen, "Performance analysis and optimization for interference alignment over MIMO interference channels with limited feedback," *IEEE Trans. Signal Process.*, vol. 62, no. 7, pp. 1785 - 1795, Apr. 2014.

[106] M. Min, Y.-S. Jeon, and G.-H. Im, "Block diagonalization and user selection for MIMO broadcast channels with limited feedback ," in *Proc. IEEE International Conference on Communications(ICC)*, London, June 2015.

[107] J. Hou, N. Yi, and Y. Ma, "Joint space–frequency user scheduling for MIMO random beamforming with limited feedback," *IEEE Trans. Commun.*, vol. 63, no. 6, pp. 2224 - 2236, June 2015.

[108] Y.-W. P. Hong, W.-C. Li, T.-H. Chang, and C.-H. Lee, "Coordinated multicasting with opportunistic user selection in multicell wireless systems," *IEEE Trans. Signal Process.*, vol. 63, no. 13, pp. 3506 - 3521, July 2015.

[109] D. Jaramillo-Ramírez, M. Kountouris, and E. Hardouin, "Coordinated multipoint transmission with imperfect CSI and other-cell interference," *IEEE Trans. Wireless Commun.*, vol. 14, no. 4, pp. 1882 - 1896, Apr. 2015.

[110] M. Razaviyayn, M. Baligh, A. Callard, and Z.-Q. Luo, "Joint user grouping and transceiver design in a MIMO interfering broadcast channel," *IEEE Trans. Signal Process.*, vol. 62, no. 1, pp. 85 - 94, Jan. 2014.

[111] L. Liu, Y.-H. Nam, and J. (Charlie) Zhang, "Proportional fair scheduling for multi-cell multi-user MIMO systems ," in *Proc. IEEE Information Sciences and Systems (CISS)*, Princeton, NJ, Mar. 2010.

[112] M. Torabzadeh and W. Ajib, "Packet scheduling and fairness for multiuser MIMO systems," *IEEE Trans. Veh. Technol.*, vol. 59, no. 3, pp. 1330 - 1340, Mar. 2010.

[113] D. Gesbert, S. Hanly, H. Huang, S. S. Shitz, O. Simeone, and W. Yu, "Multicell MIMO cooperative networks: a new look at interference," *IEEE J. Sel. Areas Commun.*, vol. 28, no. 9, pp. 1380 - 1408, Dec. 2010.

[114] J. Zhang and J. G. Andrews, "Adaptive spatial intercell interference cancellation in multicell wireless networks," *IEEE J. Sel. Areas Commun.*, vol. 28, no. 9, pp. 1455 - 1468, Dec. 2010.

[115] Y. Cheng, V. K. N. Lau, and Y. Long, "A scalable limited feedback design for network MIMO using per-cell product codebook," *IEEE Trans. Wireless Commun.*, vol. 9, no. 10, pp. 3093 - 3099, Oct. 2010.

[116] H. Anton and C. Rorres, *Elementary linear algebra.* Asia: John Wiley & Sons, 2011.

[117] G. Williams, *Linear algebra with applications.* United States of America: Jones and Bartlett Publishers, 2001.

[118] Y. Xin, Y.-H. Nam, Y. Li, and J. (Charlie) Zhang, "Reduced complexity precoding and scheduling algorithms for full-dimension MIMO systems ," in *Proc. IEEE Global Communications Conference*, Austin, TX, Dec. 2014.

Appendix A

A.1 Gram-Schmidt Orthogonalization

It is possible to convert a basis vectors $\{\mathbf{u_1}, \mathbf{u_2}, \ldots, \mathbf{u}_r\}$ into an orthogonal basis $\{\mathbf{v_1}, \mathbf{v_2}, \ldots, \mathbf{v}_r\}$ by performing the following steps of computations: [116] [117]

Step 1. Set $\mathbf{v_1} = \mathbf{u_1}$

Step 2. $\mathbf{v_2} = \mathbf{u_2} - \frac{\langle \mathbf{u_2}, \mathbf{v_1} \rangle}{\|\mathbf{v_1}\|^2} \mathbf{v_1}$

Step 3. $\mathbf{v_3} = \mathbf{u_3} - \frac{\langle \mathbf{u_3}, \mathbf{v_1} \rangle}{\|\mathbf{v_1}\|^2} \mathbf{v_1} - \frac{\langle \mathbf{u_3}, \mathbf{v_2} \rangle}{\|\mathbf{v_2}\|^2} \mathbf{v_2}$

Step 4. $\mathbf{v_4} = \mathbf{u_4} - \frac{\langle \mathbf{u_4}, \mathbf{v_1} \rangle}{\|\mathbf{v_1}\|^2} \mathbf{v_1} - \frac{\langle \mathbf{u_4}, \mathbf{v_2} \rangle}{\|\mathbf{v_2}\|^2} \mathbf{v_2} - \frac{\langle \mathbf{u_4}, \mathbf{v_3} \rangle}{\|\mathbf{v_3}\|^2} \mathbf{v_3}$

$\vdots$

(continue for r steps)

Then, to convert this orthogonal basis into an orthonormal basis $\{\mathbf{x_1}, \mathbf{x_2}, \ldots, \mathbf{x}_r\}$, normalize the orthogonal basis vectors.

Note: the symbol $\langle , \rangle$ refers to the inner product between two vectors.